Optimal Interventions for Epidemic Outbreaks

Ph.D. thesis

Khalil Muqbel

Supervisor:

Prof. Dr. Gergely Röst

Doctoral School of Mathematics
and Computer Science
University of Szeged, Bolyai Institute

Szeged

2020.

Acknowledgements

Firstly, I would like to express my sincere gratitude to my supervisor Prof. Gergely Röst for the continuous support of my Ph.D. study and related research, for his patience, motivation and immense knowledge. His guidance helped me in all the time of research and writing of this thesis.

I am also thankful to Prof. Attila Dénes and Prof. Gabriella Vas, whom we have been working for three years with. They motivated me greatly and taught me a lot about Dynamical systems and Delay Differential equations.

I am also grateful for the support of the Stipendium Hungaricum Foundation, the Bolyai Institute and Doctoral School in Mathematics and Computer Science. My sincere thanks also go to the Dynamical Models in Biology team and the PhD students of Bolyai Institute, who encouraged me to go a long way.

I would like to thank my parents and siblings for their continued support that started from my childhood and has been continuing until this moment. Also, I thank my wife and children for their patient for my long absent.

Last but not least, I would like to thank my extended family and friends for their moral support throughout the writing of this thesis and my life in general.

Contents

List of Figures

1

Introduction

The present dissertation aims to propose the following: First, a family of temporary vaccination strategies in the framework of the SIR model. These strategies are characterized by parameters (k, p) where vaccination starts when the number of infected hosts reaches a threshold level k, and with rate p we continue vaccination until herd immunity is achieved (VUHIA). Second, a family of temporary non-pharmaceutical intervention (NPIs) strategies. For the sake of simplicity, we work in the basic SIR-framework. An intervention strategy will be defined by two parameters (k, u_*) which determine the time interval it is applied as well as the intensity of intervention, where NPIs start when the number of infected hosts reaches a threshold level k, and with rate u_* we continue intervention till herd immunity is reached (ITHIR).

In Chapters 3 and 4 of this thesis, we assign a total cost to each strategy composed of cost of disease burden and cost of intervention, and systematically investigate the dependence of the total cost on the parameters. Our goal in these two chapters is to find out which strategy is the most cost-efficient. In Chapter 5, we construct the final size system for each strategy and investigate the impact of the VUHIA-strategy and ITHIR-strategy on the final epidemic size.

In addition, this thesis aims to propose and analyze a mathematical model for infectious disease dynamics with a discontinuous control function, where the control is activated with some time delay after the density of the infected population reaches a threshold. The model is mathematically formulated as a delayed relay system, and the dynamics are determined by the switching between two vector fields (the so-called free and control systems) with a time delay with respect to a switching manifold. Our results in Chapter 6 provide insight into disease management, by exploring the effect of the interplay of the control efficacy, the triggering threshold and the delay in implementation. This thesis is based on the publications [33] and [34] of the author.

Mathematical models of the transmission dynamics of infectious diseases are useful in gaining insights into the mechanisms of disease spread, in estimating key epidemiological parameters, in making predictions about the expected outcomes, and also in devising, evaluating and comparing intervention strategies.

One of the simplest compartmental models for epidemiology is the SIR model (susceptible, infectious, recovered), which is a special case of the general model introduced by Kermack and McKendrick in 1927. It has been used to study a variety of diseases such as pandemic and seasonal influenza, SARS, and many other disease. Many papers that simulate these epidemics are discussed in the introduction of [26]. The aim of using the SIR model is to simulate the disease outbreak and evaluate the impacts of selected control measures under various determined scenarios.

Depending on the nature of the epidemic, many control measures can be used to contain, mitigate, or prevent epidemic outbreaks. They might be pharmaceutical or non-pharmaceutical interventions. Vaccination is the most successful and cost-effective preventive measure against many infectious diseases [9]. However, for some emerging diseases, the delay in identification of the pathogen (such as the particular strain), the time needed to develop novel vaccinations, and the limited capacity in production, distribution and administration of vaccines may lead to a situation where vaccination programs run parallel in time with the disease outbreak.

During the recent West African Ebola virus epidemic (2013–2016), at the beginning no licensed vaccines for the disease were available. The rVSV-ZEBOV vaccine was developed during the course of the epidemic [32]. Until the vaccine became available, other coordinated public health measures have been implemented [3]. A similar situation occurred also in many developed countries during the 2009 influenza H1N1 outbreak [22]. For instance, in Canada, due to the limited availability of the vaccine at the outset of the outbreak, and the inability to vaccinate the entire population simultaneously, a sequencing strategy has been developed that identified groups of different levels of priority [10]. In some countries a significant portion of the influenza vaccines were administered in the later phase of the epidemics [22], when the number of prevented cases per a unit of administered vaccine drops sharply. This raises the question of cost-effectiveness, and also suggests that the vaccination program should stop at some well defined point of the epidemics.

Emerging coronavirus and influenza threaten the world with more and more pandemics. The ongoing COVID-19 caused by a novel SARS-CoV-2 has infected a confirmed 62,721,869 humans, killing 1,460,894 from January 2020 to November 2020. We have experienced the emergence of the influenza pandemics in the periods $1918 - 1919$,

1957 − 1958, 1968 − 1969, and also a novel H1N1 pandemic influenza strain in 2009 − 2010 that caused substantial morbidity and mortality around the world and has transitioned into a seasonal strain [6]. Every year around 1 billion people worldwide suffer from seasonal influenza, of which $3 - 5$ million of them are classified as serious cases and some $290000 - 650000$ die from chronic respiratory illness associated with influenza [19, 48].

Seasonal epidemics cause an economic burden caused by direct and indirect medical costs such as loss of productivity due to absence from work resulting in infection. These losses are estimated about 0.6% of global income [12]. Reducing the burden of seasonal influenza is a major goal of national and international public health organizations. Integrating non-pharmaceutical interventions (NPIs) into prevention and control programs is one of the key actions of the Global Influenza Strategy of WHO for 2019 − 2030 [48]. NPIs, also known as community mitigation strategies, proven effectiveness in addressed to the $1918 - 1919$ influenza pandemic in the USA, were the only available set of interventions [31]. NPIs may cover a range of measures including social distancing, school closure, hand hygiene, cough etiquette, mask usage and so on. NPIs have different costs and different impacts on the epidemic outcome, hence it is important to develop a framework to determine their cost-effectiveness.

Reducing the final epidemic size of infectious diseases is a major goal for national and international public health organizations. One of the strategic objective of Global Influenza Strategy for 2019 − 2030 of WHO is to expand seasonal influenza prevention and control policies and programs to protect the vulnerable [48]. The tools for the prevention and control of epidemics include non-pharmaceutical interventions (NPIs) to slow down the spread of illness, vaccines to reduce transmission, disease severity and incidence of serious complications and death, and isolation or antiviral drugs to reduce the infection rate and treat the illness and reduce the risk of serious complications [48].

Final epidemic size (FES), the number of individuals of the population who become infected over the course of the epidemic, is an important factor in computing the total cost of intervention strategies for epidemic outbreaks (see for example [20, 26, 33, 39, 51]). Estimating the final size is one of the key questions that arise when emerging infectious diseases appear. A mathematical tool for this estimation is the so-called final size relation.

The final size relation has been derived recently for a variety of compartmental models of mathematical epidemiology to predict the total number of cases during the outbreak when intervention strategies are implemented. For example, the generalized mean-field and pairwise models for non-Markovian epidemics on networks with arbitrary recovery time distributions [38], EVD dynamics, including virus transmission in the community, at hospitals, and at funerals[3], a generalization of pairwise models to non-Markovian epi-

demics on networks [21], a delay differential model for pandemic influenza with antiviral treatment [1], for SEIR models with quarantine and isolation [13].

Switching models have been used recently in the compartmental models of mathematical epidemiology to analyze the impact of control measures on the disease dynamics. For example, it has been observed that if the treatment rate [46] or the incidence function [2] is non-smooth, that may lead to various bifurcations. These sharp changes occur in [2] and [46] when the total population, or the infected population reaches a threshold level. Such a sudden change may even be discontinuous, for example due to the implementation and termination of an intervention policy such as vaccination or school closures.

Mathematically, such situations are described by Filippov systems, when the phase space is divided into two (or more) parts and the system is given by different vector fields in each of those parts. Examples include sudden changes in vaccination [33, 44], hospitalization [47], transmission [49], travel patterns [29], or the combination of several effects [45]. They have been used for vector borne diseases as well [52]. An overview of the basic theory and applications of switching epidemiological models can be found in [30]. Many of the mathematical challenges appear due to the incompatible behaviours of the vector fields at their interfaces, on the so-called switching manifold.

Switching systems typically assume that the change in the vector field occurs immediately whenever the switching manifold is touched, for example, a threshold in a population variable is reached. However, in reality, implementing a policy may have some time lag, hence it is natural to consider the situation when we switch to the new vector field with some delay after the solution intersected the switching manifold. These systems are called delayed relay systems [40], and they are of different mathematical nature than the Filippov systems.

Delayed relay systems have been applied to an SIS model [28], where explicit periodic solutions were constructed for the case of a delayed reduction in the contact rate after the density of infection in the population passed through a threshold value. The dynamics of this discontinuous system was different from its continuous counterpart [27],[24], showing that it is worthwhile to analyse the dynamics of epidemiological systems with delayed switching. The simplistic SIS model of [28] could be reduced to a scalar equation, and here we initiate the study of more realistic and more complex compartmental models in this context.

In particular, in chapter 6 of this thesis our starting point is an SIR model with switching, which has been thoroughly investigated in [49]. The model represents circumstances when intervention measures are taken only when the density of infectious individuals is exceeding a certain threshold value. This is expressed by a discontinuous

incidence rate, more precisely, the intervention causes a drop in the transmission rate. They showed that the solutions ultimately approach one of the two endemic states of the two structures (the free and the control system), or the so-called sliding equilibrium located on the switching surface, depending on the threshold level.

In chapter 6, we introduce the possibility of a time delay in the threshold policy. We prove several global stability theorems for the system with delay. An important difference in the dynamics is that while in the model of [49] the existence of limit cycles was excluded, for our model periodic orbits exist, and we prove that by constructing a Poincaré-type return map on a special subset of the phase space. These periodic solutions oscillate around the threshold level. On the other hand, the sliding mode control in [49] does not appear in our system. Our results contribute to the development of a systematic way of designing simply implementable controls that drive the dynamics towards disease control or mitigation.

2

Mathematical framework

2.1 The basic SIR model

An epidemic is a sudden outbreak of a disease that infects a substantial portion of the population in a region before it disappears. In this thesis, we are interested in the epidemic caused by viral agents and it transmits from individual to individual in a population. So, we assume that the epidemic divide the constant population N, which we normalize to a unity ($N = 1$), into three compartments. Namely, susceptibles (S), infecteds (I), recovereds (R), see Figure 2.1. The new infection occurs with transmission coefficient β and infected individual recover with rate α, upon recovery full immunity is assumed. Hence we consider the following system of differential equations:

$$\begin{aligned} S'(t) &= -\beta S(t)I(t), \\ I'(t) &= \beta S(t)I(t) - \alpha I(t), \\ R'(t) &= \alpha I(t), \end{aligned} \tag{2.1}$$

with the initial data $S(0) = S_0$, $I(0) = I_0$, $R(0) = 0$, where I_0 is relatively small compared to the total population size $N = S + I + R$. The first two equations of (2.1) are independent of the third one. Hence we consider the following system of differential equations

$$\begin{aligned} S'(t) &= -\beta S(t)I(t), \\ I'(t) &= \beta S(t)I(t) - \alpha I(t) \end{aligned} \tag{2.2}$$

with $S(0) = S_0$, $I(0) = I_0$, and we denote its solution by $(S(t), I(t))$. It is known (see [18, Chapter 11] and [7, Chapter 9]) that, from the first equation of (2.2), S is decreasing for all $t \geq 0$, and from the second one we can see that $I'(t) = 0$ if $I = 0$ or $S = \alpha/\beta$. $I' > 0$ if $S > \alpha/\beta$ while $I' < 0$ if $S < \alpha/\beta$. Hence for (S_0, I_0), S decreases

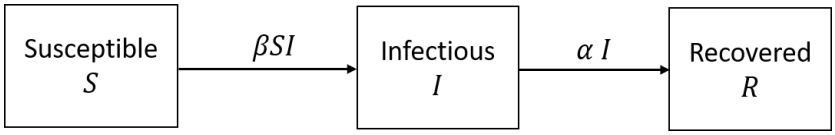

Figure 2.1: **Scheme of Susceptible-Infectious-Recovered (SIR) Model. Boxes represent compartments and arcs represent flux between compartments.**

monotonically, while I at first increases, but eventually reaches a maximum and then start decreases and eventually tends to zero. Epidemic outbreak occurs when $I'(0) > 0$. That is $\beta S(0)/\alpha > 1$. This threshold is called the basic reproduction number, which is the average number of secondary cases per infectious case in a population composed of both susceptible and non-susceptible individuals during the course of an outbreak, i.e.

$$\mathcal{R}_0 = \frac{\beta S_0}{\alpha},$$

however if $I_0 << 1$, we have $S_0 \approx 1$ hence the reproduction number simplifies to $\mathcal{R}_0 = \beta/\alpha$. In other words epidemic outbreak occurs when $\mathcal{R}_0 > 1$.

Division the first equation of (2.2) and integration from 0 to t gives

$$I(t) + S(t) - \mathcal{R}_0^{-1} \log S(t) = 1 - \mathcal{R}_0^{-1} \log S_0. \tag{2.3}$$

This implicit relation between S and I describes the orbits of solutions of (2.2) in the (S, I) plane. Indeed, the function $I + S - \mathcal{R}_0^{-1} \log S$ is constant along solution curves. It then follows that there is a unique solution curve connecting each equilibrium point in the interval $\alpha/\beta < S < 1$ to one in the interval $0 < S < \alpha/\beta$..

Let $I_{\max}$ denotes the peak of the SIR-epidemic in the absence of any intervention. If $I(0) > 0$, then $I'(t_*) = 0$ when $S(t_*) = \alpha/\beta = \mathcal{R}_0^{-1}$. Substitution $I = I_{\max}$ and $S = \mathcal{R}_0^{-1}$ in (2.3) gives

$$I_{\max} = 1 - \mathcal{R}_0^{-1}(1 + \log \mathcal{R}_0), \tag{2.4}$$

the maximum number of infecteds for the SIR model (with $N = 1$).

The sum of the first two equations of (2.1) is

$$(S(t) + I(t))' = -\alpha I(t).$$

It is not difficult to prove that $\lim_{t\to\infty} I(t) = 0$, $\lim_{t\to\infty}(S(t)+I(t)) = \lim_{t\to\infty} S(t) := S_\infty$, and $\alpha \int_0^\infty I(t)dt = 1 - S_\infty$. Division the first equation of (2.1) on $S(t)$ and integration from 0 to ∞ gives

$$\log \frac{S_0}{S_\infty} = \mathcal{R}_0(1 - S_\infty). \tag{2.5}$$

Equation 2.5 is called the final size relation. It gives a relationship between the basic reproduction number and the final size of the epidemic $(1 - S_\infty)$, the total number

of individuals who get infected during the course of the epidemic. The final size relation (2.5) can be generalized to epidemic models with more complicated compartmental structure than the simple SIR model (2.1), including vaccination or non-pharmaceutical interventions. Indeed, this is a one of our interests in this thesis, see Chapter 5.

2.2 Intervention strategies for epidemic outbreaks

A usual way of introducing intervention strategies is to start the control measures when the number of infected reaches a given level and stop the intervention if the number of infected becomes smaller than this level. The problem with this strategy is that if the number of infected starts growing again once the intervention is stopped as shown in Figure 2.2 (left), the intervention policy might become unpopular among the population as it might seem unsuitable to stop the epidemic.

In the control literature ([49], [11], [14], [42], [43]), a threshold policy leads to a variable structure system with two distinct structures with their own equilibrium points, separated by the threshold level. A sliding mode [43, 49] along the threshold level may ensue, if in its vicinity the vector fields of both structures are directed toward each other, see Figure 2.2 (right), which means that the number of infected people should be kept constant for some time, which is not realistic.

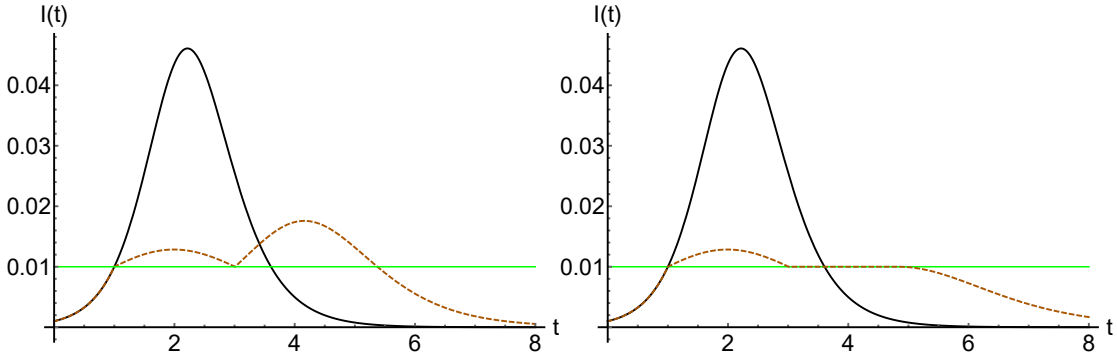

Figure 2.2: The second wave resulting from lifting the control measures (left) and the sliding mode control of outbreaks resulting from the threshold policy. Parameters are $\mathcal{R}_0 = 1.4$, $\alpha = 6$, $\beta = 8.4$.

There has been a number of studies using SIR model with optimal control theory to find a control function that minimizes some (typically linear, quadratic, exponential) cost function (see [20, 26, 39, 51] for examples). However, a continuously changing control function, which is the common output from that approach for nonlinear cost functions, is not feasible to be realized as a public health policy.

Motivated by these problems we aim to define a strategy in a simpler way, and we assume that the control function is a piecewise constant function, taking values of either 0 (control is off), or some positive value (control is on). This means that we propose to apply the interventions with a given rate on some time interval. We assume that the starting point of intervention is when the density of infecteds reaches a threshold value as in [49] and stop the intervention only when herd immunity is achieved. Mathematically, from the second equation of (2.1) $I'(t) < 0$ for every $t > t_*$ if and only if $S(t) < \alpha/\beta = 1/\mathcal{R}_0$. That is the number of infected individuals start decreasing for every $t > t_*$ if and only if the number of susceptible population drops below $1/\mathcal{R}_0$. That is, (with $N = 1$), $1 - 1/\mathcal{R}_0$ of the population recovered from the disease and they are immune. In the literature this threshold is called *herd immunity* (HIT)(see [15]). For example, the herd immunity threshold for seasonal influenza is 21.9% as the basic reproduction number is 1.28 (see [5]).

2.3 Numerical computations

In this section, we describe the code we used in the simulations, which was implemented in Wolfram Mathematica 12. Wolfram Mathematica provides the following commands:

- Table $[\text{expr}, \{i, i_{\min}, i_{\max}, di\}, \{j, j_{\min}, j_{\max}, dj\}]$: gives a nested list of the values of expr when i runs from i_{min} to i_{max} and j runs for every i from j_{min} to j_{max} using steps di and dj;

- NDSolve, $[\text{eqns}, u, \{x, x_{\min}, x_{\max}\}]$: finds a numerical solution to the ordinary differential equations eqns for the function u with the independent variable x in the range $x_{\min}$to $x_{\max}$;

- WhenEvent [event, action]: specifies an action that occurs when the event triggers it for equations in NDSolve and related functions.

- Flatten [list, n]: flattens out nested lists to level n.

- Interpolation $[\{\{\{x_1, y_1, \ldots\}, f_1\}, \{\{x_2, y_2, \ldots\}, f_2\}, \ldots\}]$: constructs an interpolation of multidimensional data.

- ContourPlot $[(f, \{x, x_{\min}, x_{\max}\}, \{y, y_{\min}, y_{\max}\})]$: generates a contour plot of f as a function of x and y.

For example, in Chapter 3 we investigated the dependence of the total (TC) cost of an outbreak on the threshold level k, the starting point of the intervention, and on the

vaccination rate p. The total cost is assessed as follows

$$TC(k,p) \coloneqq C_1\tilde{I} + C_2\tilde{V},$$

where $\tilde{I}(k,p)$ is the total infected people during the course of the epidemic and applying *VUHIA*-strategy of (k,p)-type (see page 15 of this thesis for more details about VUHIA strategy) and $\tilde{V}(k,p)$ is the total vaccinated people, which are defined in (3.4). Indeed, we defined the total cost as a function in two variables. We built this function as follows: First we calculated the maximum number of infecteds ($I_{\max}$) in the absence of any intervention by using (2.4). Second, we used the Table command to generate a nested list of the values of a numerical solution of (3.1), where k runs from I_0 to I_{max} and p runs for every k from $p_{\min}$ to p_{max} using steps k_{step} and p_{step}. The code can be written as Table [NDsolve [System 3.1] , $\{k, I_0, I_{\max}, k_{step}\}, \{p, p_{\min}, p_{\max}, p_{step}\}$]. The WhenEvent command is used while resolving the system to collect and memorize the values of $\tilde{I}(k,p)$ and $\tilde{V}(k,p)$. Then one can interpolate the collected data by using Interpolation and Flatten commands to have the functions $\tilde{I}(k,p)$ and $\tilde{V}(k,p)$. Finally, one can use ContourPlot command to generate a contour plot of TC as a function of k and p, see for example Figure 3.7.

3

Optimal temporary vaccination strategies for epidemic outbreaks

In this chapter, we propose temporary vaccination strategies in the SIR disease outbreak model, where vaccination starts when the infection level reaches a threshold, and continues until susceptibles drop below a level such that the number of infected hosts is decreasing without further intervention. Costs are assigned to vaccination and disease burden, and we investigate which one of this two parameter family of VUHIA (vaccinate until herd immunity achieved) strategies gives the minimal cost. When the cost of vaccination is very small compared to the cost of disease burden, the optimal strategy is to start vaccination as early as possible and as high rate as possible. When vaccination is very expensive, the minimal cost is attained without vaccination. However, when these costs are of similar magnitudes, we uncover some counter-intuitive phenomena, namely the total cost can be a non-monotone function of the vaccination rate and the threshold value. We also show that for different basic reproduction numbers, the corresponding optimal strategies can be very different.

3.1 Specification of the VUHIA-strategy and its total cost

To understand the following discussion, the reader is referred to Figure 3.1. We consider a constant population divided into susceptible ($S(t)$), infected ($I(t)$), and removed ($R(t)$) compartments. New infections occur with transmission coefficient β and infected individuals recover with rate α. Upon recovery, full immunity is assumed. Vaccination of susceptibles is included in the model with time dependent vaccination rate $v(t)$, to be specified later. Vaccination is assumed to be fully protective, thus vaccinated individuals are placed in the R-compartment as well. Hence, we consider the following system of

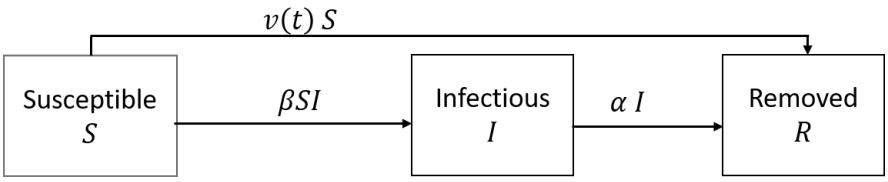

Figure 3.1: **Scheme of Susceptible-Infectious-Removed (SIR) Model of the VUHIA-strategy.** Boxes represent compartments and arcs represent flux between compartments.

differential equations:

$$\begin{aligned} S'(t) &= -\beta S(t)I(t) - v(t)S(t), \\ I'(t) &= \beta S(t)I(t) - \alpha I(t), \\ R'(t) &= \alpha I(t) + v(t)S(t). \end{aligned} \tag{3.1}$$

We are interested in the situation when a small number of infected hosts are introduced into a fully susceptible population, hence we consider initial data $S(0) = S_0$, $I(0) = I_0$, $R(0) = 0$, where I_0 is relatively small compared to the total population size $N = S+I+R$. The basic reproduction number is given by

$$\mathcal{R}_0 = \frac{\beta S_0}{\alpha},$$

however by normalizing the population size at $N = 1$ and with $I_0 << 1$, we have $S_0 \approx 1$ hence the reproduction number simplifies to $\mathcal{R}_0 = \frac{\beta}{\alpha}$. Epidemic outbreak occurs when $\mathcal{R}_0 > 1$.

The total cost (TC) of an outbreak will be assessed by considering two components, the disease burden and the cost of vaccination. Disease burden is calculated as the total number of infections during the course of the outbreak (denoted by $\tilde{I}$) multiplied by the cost C_1 of a single infection. Vaccination cost is calculated as the total number of administered vaccines (denoted by $\tilde{V}$) multiplied by the cost C_2 of a single vaccination. This way, for the total cost we have

$$TC := C_1\tilde{I} + C_2\tilde{V}, \tag{3.2}$$

where

$$\tilde{I} := \int_0^\infty \beta S(t)I(t)dt = \alpha \int_0^\infty I(t)dt, \tag{3.3}$$

$$\tilde{V} := \int_0^\infty v(t)S(t)dt. \tag{3.4}$$

There has been a number of studies using optimal control theory to find the control function $v(t)$ that minimizes some (typically quadratic) cost function (see [50] for an example). However, a continuously changing $v(t)$, which is the common output from that approach, is not feasible to be realized as a public health policy. Hence, we aim to define a strategy $v(t)$ in a simpler way, and we assume that $v(t)$ is a piecewise constant function, taking values of either 0 (control is off), or some $p > 0$ (control is on). This means that we propose to apply vaccination with a given rate on some time interval. It remained to determine when to start and when to finish the intervention. We can not expect in general that the intervention can start immediately, as the epidemic may not have been detected or the resources are not in place at the beginning of the outbreak. A reasonable assumption is that the starting point of interventions is when the number of infected individuals reach a threshold value k, as it has been in [49]. However, in outbreak models using the same threshold to define the end of intervention may not be adequate, given that if k is too large then we finish vaccination too early, while when k is too small then vaccination may go on even when it does not have any significant impact on the epidemic any more. Instead, we propose to stop the vaccination when the number of infections start decreasing, which is the same point when the number of susceptibles becomes so low that herd immunity is reached in the population. We call such an intervention a *VUHIA*-strategy of (k, p)-type, referring to *vaccinate until herd immunity achieved* with parameters (k, p).

In mathematical terms, the *VUHIA*-strategy of (k, p)-type is defined as follows. Let

$$v(t) = \begin{cases} 0, & t \notin J, \\ p, & t \in J, \end{cases} \tag{3.5}$$

where J is the intervention interval $J = [T_{\text{start}}, T_{\text{end}}]$ with

$$T_{\text{start}} = \min\{t \geq 0 : I(t) \geq k\} \tag{3.6}$$

and

$$T_{\text{end}} = \min\{t \geq 0 : \beta S(t) - \alpha \leq 0\}. \tag{3.7}$$

The time T_{start} is well defined as long as $k \in [I_0, I_{\max}]$, where $I_{\max}$ denotes the peak of the SIR-epidemic in the absence of any intervention. It is well known for the SIR model (with $N = 1$) that

$$I_{\max} = 1 - \mathcal{R}_0^{-1}(1 + \ln \mathcal{R}_0).$$

Clearly we have $I'(t_*) = 0$ when $S(t_*) = \alpha/\beta$, and $I'(t) < 0$ for any $t > t_*$ regardless we vaccinate or not at some $t > t_*$. Since the epidemic eventually always dies out, T_{end}

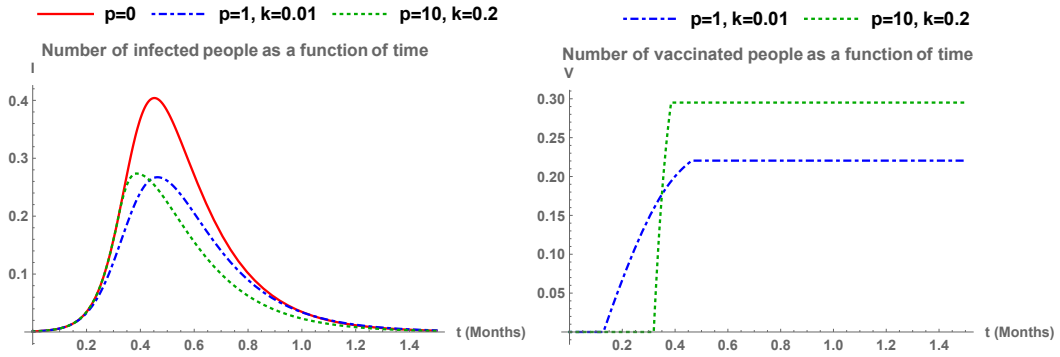

Figure 3.2: The total number of infected (left) and vaccinated (right) people during the epidemic for different strategies. The epidemic parameters are $\mathcal{R}_0 = 4$, $\alpha = 6$, $\beta = 24$. On the left, the red curve is the epidemic curve in the absence of intervention. On the right, we can clearly see when the vaccination starts and stops.

is well defined, and (3.4) becomes

$$\tilde{V} := p \int_{T_{\text{start}}}^{T_{\text{end}}} S(t)dt. \tag{3.8}$$

Figure 3.2 depicts how the epidemic plays out with two different strategies. In one, we start vaccinating early with a low rate; in the other we start vaccinate later but with a higher rate. As Figure 3.2 shows, it is unclear which of these two strategies is better, hence we will systematically explore this in the forthcoming sections by computer simulations.

3.2 The relation between the total cost and the vaccination rate p

To see how the total cost depends on the vaccination rate, we shall consider various fixed k-s and vary p. The change in the total cost then depends on

$$\frac{d}{dp}TC(p,k) = C_1\frac{d}{dp}\tilde{I} + C_2\frac{d}{dp}\tilde{V}.$$

From Figure 3.3 we can see that $\tilde{I}$ decreasing while $\tilde{V}$ decreasing in p, thus the sign of the rate of change of the total cost is determined by the ratio of C_1 and C_2 relative to the rates of change in $\tilde{I}$ and $\tilde{V}$. In the sequel we always normalize the cost of disease burden $C_1 = 100$, and we will vary C_2 to compare different scenarios. What we can see in Figure 3.4 is that when $C_2 \ll C_1$, the total cost is decreasing in p, meaning that when vaccination is relatively cheap, we should vaccinate as high rate as possible. On the

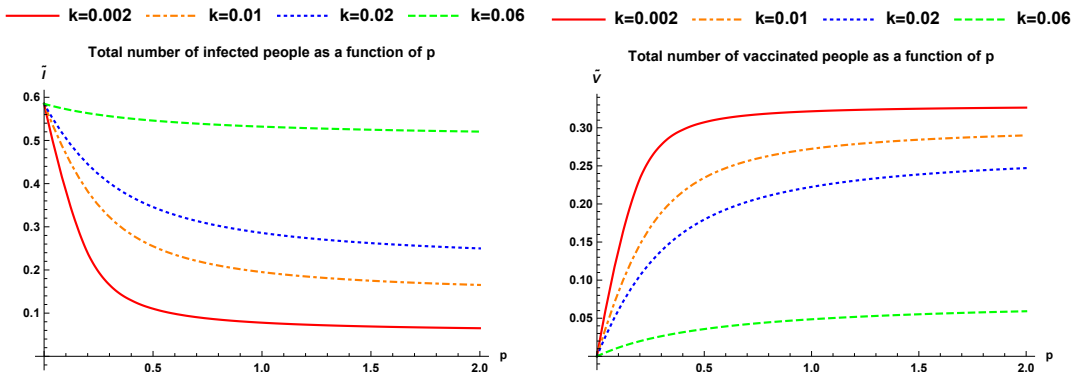

Figure 3.3: The total number of infected (left), and vaccinated (right) people during the epidemic as a function of vaccination rate p. Parameters are $\mathcal{R}_0 = 1.5$, $\alpha = 6$, $\beta = 9$.

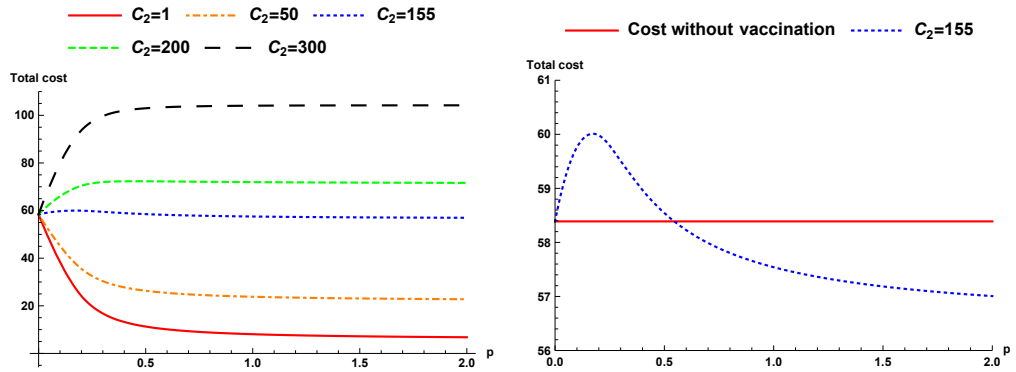

Figure 3.4: The total cost as a function of p, for five different vaccination costs (left). In the right, the case $C_2 = 155$ is highlighted by zooming in. Parameters are $\mathcal{R}_0 = 1.5$, $\alpha = 6$, $\beta = 9$, $k = 0.002$.

other hand, when $C_2 \gg C_1$, the total is increasing in p, meaning that when vaccination is very expensive relative to the disease burden, the strategy that give minimal cost is to not vaccinate at all. We can also see that the total cost is most sensitive to p when the vaccination rate is small. These results are what one would expect, however there is a curious situation when C_1 and C_2 are of similar magnitudes: there is a possibility that the total cost is not monotone in p. This scenario is highlighted in Figure 3.4, right. In this case, vaccination with a small rate yields a higher cost than no vaccination (see the red line), however vaccination with a high rate yields a smaller cost. Let p_* be the value where the cost curve intersects the straight red line corresponding to cost of no vaccination. This means that if we are capable to vaccinate with a sufficiently high rate $p > p_*$, then we should do it, but if with our capacities and resources only a smaller rate $p < p_*$ can be achieved, it is better to not vaccinate at all.

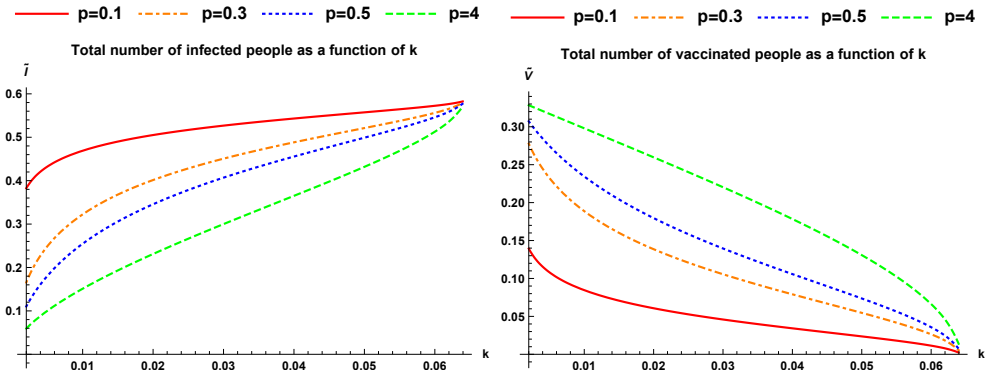

Figure 3.5: The total number of infected (left) and vaccinated (right) people during the epidemic as a function of k. Parameters are $\mathcal{R}_0 = 1.5$, $\alpha = 6$, $\beta = 9$.

3.3 The relation between the total cost and the threshold level k

Next we consider how the total cost changes when we vary k for fixed values of p. Figure 3.5 shows that by increasing k, that is we start vaccinating later, the total number of infections increasing while the total number of vaccinations decreasing. Again, the change in total depends on how $C_1 : C_2$ relates to $\frac{d\tilde{I}}{dk} : \frac{d\tilde{V}}{dk}$. This is depicted in Figure 3.6 (left) for various values of C_2. Similarly as before, we see that if vaccination is relatively cheap, it is better to start early, and when it is very expensive, it is better not to start at all. The graphs of all five curves meet at the right when $k \to I_{\max}$. When similar costs are assigned to disease burden and vaccination, we can see a non-monotone behaviour, which is highlighted in the right of Figure 3.6. The interpretation of this figure is that in the scenario if the blue dotted curve there is a k_*, such that if we are capable to start the intervention earlier that k_*, then we should as soon as possible. But, if for any reason we could not start the intervention before $I(t)$ reached k_*, then it is better not to vaccinate at all. This k_* is given by the intersection of the blue dotted curve with the horizontal red line.

3.4 Conclusions and summary

We have proposed a family of temporary vaccination strategies in the framework of the SIR model. These strategies are characterized by parameters (k, p), where vaccination starts when the number of infected hosts reach the threshold value k, and with rate p we continue vaccination until herd immunity is achieved (*VUHIA*). The advantages of the

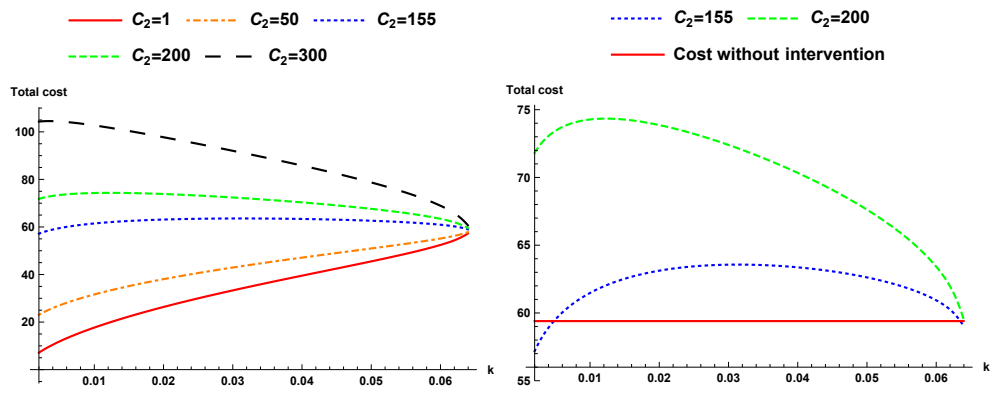

Figure 3.6: The total cost as a function of k for five different vaccination costs (left). The cases $C_2 = 155$ and $C_2 = 200$ are highlighted by zooming in (right). Parameters are $\mathcal{R}_0 = 1.5$, $\alpha = 6$, $\beta = 9$, $p = 1.5$.

VUHIA-strategy are the following. First, it has a clear and meaningful definition: we start vaccinate with rate p when a threshold k is reached in the level of infection, and we start the vaccination then the number of susceptibles drops below $\mathcal{R}_0^{-1}$, that is herd immunity achieved the number of infected will decrease anyway. Second, it is determined only by the parameters (k, p), hence all strategies from this family can be explored in a two dimensional parameter space.

We have assigned a total cost to each strategy composed of cost of disease burden and cost of vaccination, and systematically investigated the dependence of the total cost on the parameters. Essentially, we have found three types of behaviours:

(a) *vaccination cost is very low compared to the cost associated to disease burden*: in this case increasing the vaccination rate and start vaccination earlier reduce the total cost;

(b) *vaccination cost is very high compared to the cost associated to disease burden*: in this case the optimal strategy is to not vaccinate at all;

(c) *vaccination cost and disease burden cost are of similar magnitudes*: there may be non-monotone relationships between the vaccination rate, the starting threshold and the total cost.

These three typical behaviours are plotted into a heatmap in Figure 3.7. In case (c), it may happen that a better strategy is to start earlier but only if we can start sufficiently early, or, it better to increase vaccination rate but only if we can increase it to a sufficiently high level. If we cannot meet those criteria, then the best decision is to not vaccinate. The top plot of Figure 3.7 illustrates these intricate non-monotonicity properties.

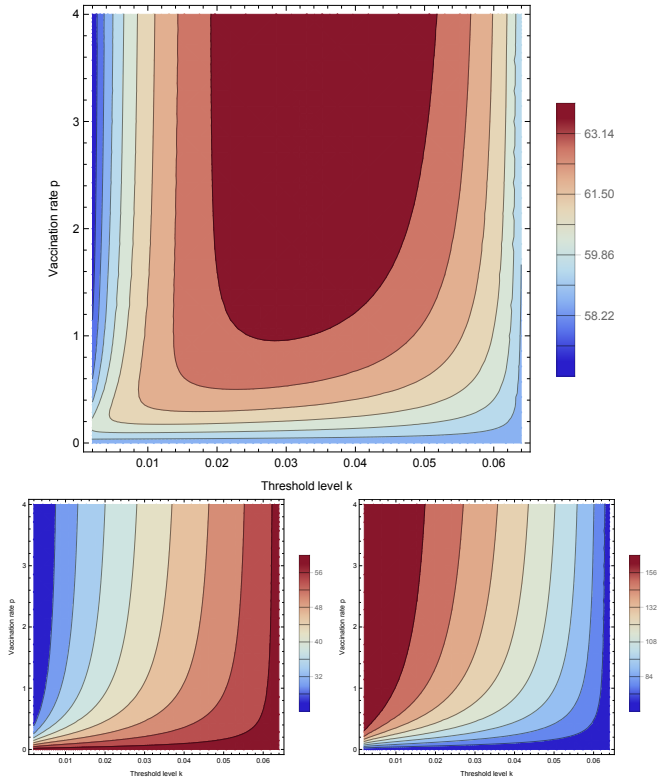

Figure 3.7: Dependence of the total cost on (k, p) in three typical situations: $C_2 = 50 \ll C_1$ (bottom left), $C_2 = 500 \gg C_1$ (bottom right), and $C_2 = 155$ (top). Parameters are $\mathcal{R}_0 = 1.5$, $\alpha = 6$, $\beta = 9$, and $C_2 = 50, 155, 500$ respectively. The bottom plots show monotone cases, while in the top plot we can find non-monotonicity in both k and p.

Depending on the available resources and public health capacities, there may be constraints on the parameters, such as $k \geq k_{\min}$ and $p \leq p_{\max}$. Finding the optimal strategy with such constraints can be found even in these cases from the graphs in Figures 3.4, 3.6, 3.7. It is very easy when the total cost depends monotonically on the parameters, for example with an upper bound on p and in the situation of $C_2 = 50$ in Figure 3.4, the optimal strategy is always $p = p_{\max}$. In contrast, for $C_2 = 155$ (see Figure 3.4 right), $p = p_{\max}$ is the optimal strategy only if $p_* < p_{\max}$, otherwise the optimal strategy is $p = 0$.

Another interesting phenomenon is depicted in Figure 3.8, showing that for a fixed p, the monotonicity of the total cost in k can reverse varying the reproduction number. In that particular situation of Figure 3.8, for a less contagious disease ($\mathcal{R}_0 = 1.2$), to minimize the cost vaccination should start as early as possible ($k \to 0$), while for a more contagious disease ($\mathcal{R}_0 = 4$) the lowest cost comes from not vaccination at all ($k \to I_{\max}$).

Although this SIR vaccination model is certainly too simplistic to apply to any real

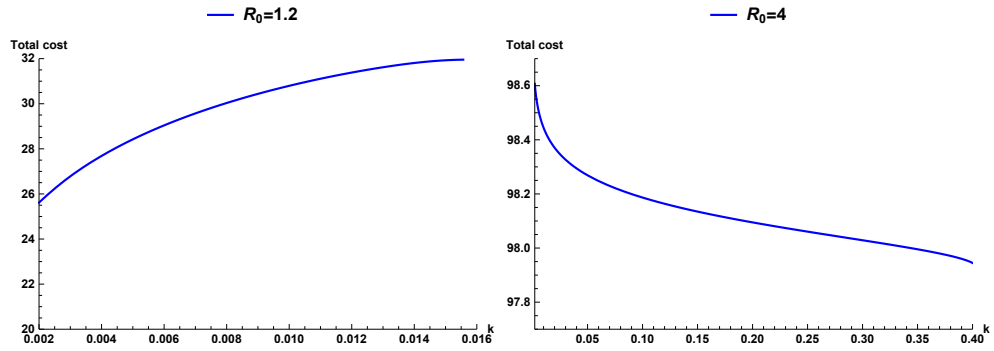

Figure 3.8: Effect of $\mathcal{R}_0$ on the monotonicity of the cost curve. Parameters are $p = 0.25$, $C_2 = 115$, $\alpha = 6$ and $\beta = 7.2$, resp. $\beta = 24$. For $\mathcal{R}_0 = 1.2$, optimal strategy is achieved by vaccinating early, while for $\mathcal{R}_0 = 4$ it is better to not vaccinate at all.

outbreak, this simple epidemiological model already exhibits some surprising and counter-intuitive features, highlighting that in real applications with more complex models, a comprehensive mathematical investigation of the possible intervention strategies is really necessary.

4

Optimal temporary non-pharmaceutical intervention strategies for epidemic outbreaks

Striking a fine balance between protecting public health and minimizing economic disruption is a major goal for authorities during the battle against the COVID-19 pandemic. In addition, reducing the burden of seasonal influenza is a major goal of national and international public health organizations. Integrating non-pharmaceutical interventions (NPIs) into prevention and control programs is one of the key actions of the Global Influenza Strategy of WHO for 2019-2030. In fact, NPIs are key tools to mitigate COVID-19 as well. NPIs may cover a range of measures including social distancing, school closure, hand hygiene, cough etiquette, mask usage and so on. NPIs have different costs and different impacts on the epidemic outcome, hence it is important to develop a framework to determine their cost-effectiveness.

In this chapter, we propose temporary non-pharmaceutical intervention strategies in the SIR disease outbreak model, where NPIs start when the density of infected individuals reaches a threshold level, and continues with the same intensity until the density of susceptibles drops below a critical level such that the infection can not spread any more even without further intervention. Such a strategy is determined by two parameters: the threshold of infection density when the intervention is triggered, and the intensity of the intervention efforts. Costs are assigned to NPIs and to disease burden, and we investigate which member of this two-parameter family of ITHIR (intervene till herd immunity reached) strategies gives the minimal cost. We systematically investigate and compare a variety of possible cost functions.

We identified a parameter region where the herd immunity will never be reached, in which case the intervention is not feasible as its cost exceeds any given bound. Consid-

ering the feasible region of limited costs, when the cost of NPIs is very small compared to the cost of disease burden, we maximized the allowed length of intervention, and we could find the optimal strategy with such restriction. When the NPI is very expensive, the minimal cost is attained without any intervention. However, when these costs are of similar magnitudes, we uncover some counter-intuitive phenomena, namely that the total cost can be a non-monotone function of the control intensity and the threshold value, and in this case we can determine which strategy gives the minimal total cost. We also demonstrated that the corresponding optimal strategies can be very different for pandemic and for seasonal influenza.

We systematically investigated the cost-effectiveness of a newly proposed family of temporary NPIs. We uncovered the impact of various cost functions, and provided valuable insights to develop effective control strategies for seasonal and pandemic influenza.

4.1 Modelling framework

We consider a constant population N divided into three compartments: susceptible ($S(t)$), infected ($I(t)$), and recovered ($R(t)$), see Figure 4.1. At the beginning, an outbreak runs its natural course, hence new infections occur with transmission coefficient $\beta > 0$. However, if the number of infected individuals reaches a threshold level k, then the authorities impose certain non-pharmaceutical interventions (NPIs) with control intensity $u_* \in (0, 1)$, resulting in a reduction in the transmission coefficient. This reduction is included in the model with time dependent NPIs intensity rate $u(t)$, to be specified later. Infected individuals recovered with rate α. Upon recovery, full immunity is assumed. Hence we consider the following system of differential equations:

$$\begin{aligned} S'(t) &= -[1-u(t)]\beta S(t)I(t), \\ I'(t) &= [1-u(t)]\beta S(t)I(t) - \alpha I(t), \\ R'(t) &= \alpha I(t). \end{aligned} \tag{4.1}$$

We are interested in the situation when a small number of infected hosts are introduced into a fully susceptible population, hence we consider initial data $S(0) = S_0$, $I(0) = I_0$, $R(0) = 0$, where I_0 is relatively small compared to the total population size $N = S+I+R$. The basic reproduction number is given by

$$\mathcal{R}_0 = \frac{\beta S_0}{\alpha},$$

however by normalizing the population size at $N = 1$ and with $I_0 << 1$, we have $S_0 \approx 1$ hence the reproduction number simplifies to $\mathcal{R}_0 = \beta/\alpha$. Epidemic outbreak occurs when $\mathcal{R}_0 > 1$.

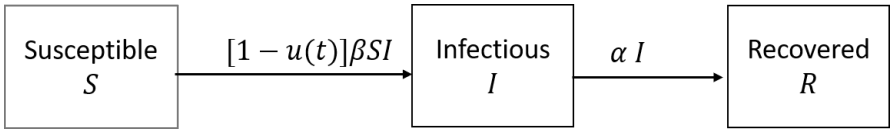

Figure 4.1: **Scheme of Susceptible-Infectious-Recovered (SIR) Model of ITHIR-strategy of NPIs.** Boxes represent compartments and arcs represent flux between compartments.

4.2 Cost functions

The total cost (TC) of an outbreak will be assessed by considering two components as follows. Overview of cost functions we use:

$$TC(k, u_*; \alpha, \beta, S_0) := \text{Disease Burden Cost} + \text{ NPIs Cost},$$

where $k \in (0, 1)$ is the threshold level of starting the intervention and $u_* \in [0, 1]$ is the control intensity of NPIs. One particular type of cost functions is the quadratic total cost (TC_{qq}) of an outbreak, which is quadratic in the disease burden and quadratic in the control intensity. The disease burden cost of this type of cost functions is calculated as a quadratic integral of the density of infected individuals during the course of an outbreak (denoted by $\tilde{I}_q$) multiplied by the cost factor C_1 and the NPIs cost is calculated as the duration of intervention in months (denoted by $\tilde{T}$) multiplied by the cost C_2 of a single month and the quadratic of the control intensity u_*. Hence the quadratic total cost is the following:

$$TC_{qq} \;\; := \;\; C_1\tilde{I}_q + C_2\tilde{T}u_*^2, \tag{4.2}$$

where

$$\tilde{I}_q := \int_0^\infty I^2(t)dt. \tag{4.3}$$

We also define several structures for the total cost function (as in [26] for example) such as the linear cost function, which is linear in disease burden and in intensity of control, and exponential cost function, which is discounted in time in disease burden (meaning that immediate of the disease are considered higher than future costs), and we use a mixture of them. In these cost functions (see Table 4.1) we use the following notations:

$$\tilde{I}_l := \int_0^\infty [1-u(t)]\beta S(t)I(t)dt = \alpha\int_0^\infty I(t)dt, \tag{4.4}$$

and

$$\tilde{I}_e \;\; := \;\; \int_0^\infty I(t)e^{-\phi t}dt, \qquad \phi > 0. \tag{4.5}$$

Table 4.1: ***An overview of cost functions we use:***

The cost function type	**The cost function**
Linear in disease burden and linear in control intensity	$TC_{ll} \coloneqq C_1\tilde{I}_l + C_2\tilde{T}u_*.$
Discounting in disease burden while growing in duration of intervention exponentially	$TC_{ee} \coloneqq C_1\tilde{I}_e + C_2u_*e^{\tilde{T}}$
Linear in disease burden and quadratic in control intensity	$TC_{lq} \coloneqq C_1\tilde{I}_l + C_2\tilde{T}u_*^2.$
Linear in disease burden and growing in duration exponentially	$TC_{le} \coloneqq C_1\tilde{I}_l + C_2u_*e^{\tilde{T}}.$
Quadratic in disease burden and growing in duration exponentially	$TC_{qe} \coloneqq C_1\tilde{I}_q + C_2u_*e^{\tilde{T}}.$
Linear in disease burden, quadratic in control intensity, and growing in duration exponentially	$TC_{lqe} \coloneqq C_1\tilde{I}_l + C_2u_*^2e^{\tilde{T}}$
Quadratic in disease burden, quadratic in control intensity, and growing in duration exponentially	$TC_{qqe} \coloneqq C_1\tilde{I}_q + C_2u_*^2e^{\tilde{T}}$

There has been a number of studies using SIR model with optimal control theory to find the control function $u(t)$ that minimizes some (typically linear, quadratic, exponential) cost function (see [20, 26, 39, 51] for examples). However, a continuously changing $u(t)$, which is the common output from that approach for nonlinear cost functions, is not feasible to be realized as a public health policy. Hence we aim to define a strategy $u(t)$ in a simpler way, and we assume that $u(t)$ is a piecewise constant function, taking values of either 0 (control is off), or some $0 < u_* \leq 1$ (control is on). This means that we propose to apply the NPIs with a given rate on some time interval. We assume that the starting point of intervention is when the density of infecteds reaches a threshold value k as in [33, 49]. Stopping the intervention when the density of infecteds becomes less than the threshold value k is not always appropriate. Moreover, relaxing the NPIs has significant impact on the size of epidemic if we stop interventions before herd immunity is achieved [4]. To avoid next waves of the epidemic we propose to stop the intervention only when herd immunity is reached in the population. We call such an intervention a *ITHIR*-strategy of (k, u_*)-type, referring to *intervene till herd immunity reached* with parameters (k, u_*). In mathematical terms, the *ITHIR*-strategy of (k, u_*)-type is defined as follows. Let

$$u(t) = \begin{cases} 0, & t \notin J, \\ u_*, & t \in J, \end{cases} \tag{4.6}$$

where J is the intervention interval $J = [T_{\text{start}}, T_{\text{end}}]$ with

$$T_{\text{start}} = \min\{t \geq 0 : I(t) \geq k\}$$

and

$$T_{\text{end}} = \min\{t \geq 0 : \beta S(t) - \alpha \leq 0\}.$$

The time T_{start} is well defined as long as $k \in [I_0, I_{\max}]$, where $I_{\max}$ is the peak of the SIR-epidemic in the absence of any intervention, which is given by (2.4).

Let $\tilde{S}(k, u_*) := \lim_{t\to\infty} S(t)$ when (k, u_*) strategy applied, the proportion of the susceptible population in the community who had never been infected during an outbreak and NPIs implementation. Clearly, in the absence of any intervention we have $I'(t_*) = 0$ when $S(t_*) = \alpha/\beta = \mathcal{R}_0^{-1}$, and $I'(t) < 0$ for any $t > t_*$ regardless we apply NPIs or not at some $t > t_*$, that is the herd immunity is reached in the community, and hence T_{end} is well defined if and only if $\tilde{S}(k, u_*) < \mathcal{R}_0^{-1}$. The epidemic in this case eventually dies out, and the duration of the intervention (denoted by $\tilde{T}$) is well defined as follows:

$$\tilde{T} \coloneqq T_{\text{end}} - T_{\text{start}}.$$

However, if $\tilde{S}(k, u_*) \geq \mathcal{R}_0^{-1}$, then we never stop the intervention before the vaccine becomes available. Since the vaccine may take a long time to be produced and ready for use, the length of intervention $\tilde{T}$ and hence the total cost is unbounded.

Figure 4.2 depicts how the epidemic plays out with two different strategies. In one, we start NPIs early with a low rate; in the other we start NPIs later but with a higher rate. As Figure 4.2 shows, it is unclear which of these two strategies is better, hence We will systematically explore this in the coming sections by computer simulations as the simulations simulate seasonal and pandemic influenza, see Table 4.2 for the model parameters.

Table 4.2: ***Model parameters***

Epidemic	$\mathcal{R}_0$	α^{-1}**(month)**	**Reference**
Seasonal Influenza	1.28	0.167	[5]
Pandemic Influenza	2.3	0.167	[5, 22]

Let us emphasize that if $\tilde{S}(k, u_*) \geq \mathcal{R}_0^{-1}$, then the herd immunity will never be reached in the population, in which case the intervention is not feasible as its total cost exceeds any given bound. Therefore, considering the feasible region we have the following results.

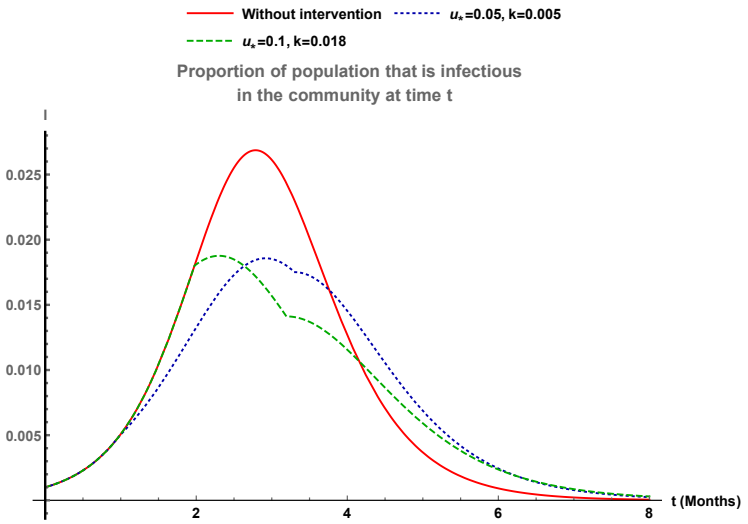

Figure 4.2: The proportion of population that is infectious in the community as a function of time (months) during the epidemic for different strategies. The solid red curve is the epidemic curve in the absence of intervention. Parameters are $\mathcal{R}_0 = 1.28$, $\alpha^{-1} = 1/6$ month, $\beta = 7.68$.

4.3 The relation between the quadratic total cost and the control intensity u_*

To see how the quadratic cost function depends on the control intensity u_*, we shall consider various fixed k-s and vary u_*. The change in the total cost then depends on

$$\frac{d}{du_*}TC_{qq}(k, u_*) = C_1\frac{d\tilde{I}_q}{du_*} + C_2(\frac{d\tilde{T}}{du_*}u_*^2 + 2\tilde{T}u_*). \tag{4.7}$$

From Figure 4.3 we can see that $\tilde{I}_q$ decreasing while $\tilde{T}$ increasing in u_*, thus the sign of the rate of change of the quadratic total cost function is determined by the ratio of C_1 and C_2 relative to the rate of change in $\tilde{I}_q$ and $-(\frac{d\tilde{T}}{du_*}u_*^2 + 2\tilde{T}u_*)$. In the sequel we always normalize the cost of disease burden $C_1 = 100$, and we will vary C_2 to compare different scenarios. Considering the feasible region of limited costs, what we can see in Figure 4.4 is that for a given threshold level k, when $C_2 >> C_1$, the quadratic total cost is increasing in u_*, and hence the minimal cost is obtained when $u(t) = 0$, meaning that when NPIs cost is very expensive compared with the disease burden cost, the minimal cost is attained by not controlling at all. This result is what one would expect, however there is a curious situation when C_1 and C_2 are of similar magnitudes: there is a possibility that the total cost is non-monotone in u_*. This scenario is represented by the dashed red curve in Figure 4.4 (left), in this case we can determine which strategy gives the minimal

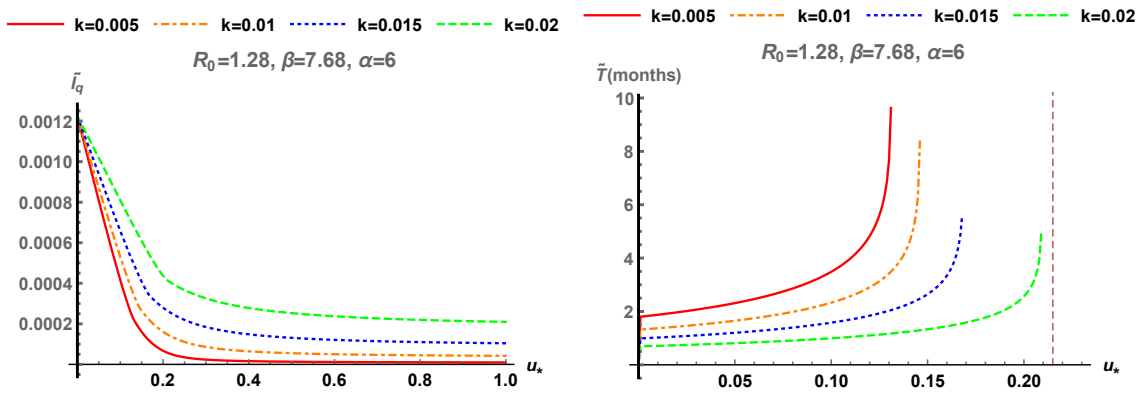

Figure 4.3: $\tilde{I}_q(k, u_*)$ (left) and the length of intervention ($\tilde{T}(k, u_*)$) (right) as a function of the control intensity u_* for four different threshold levels. Parameters are $\mathcal{R}_0 = 1.28$, $\alpha^{-1} = 1/6$ month, $\beta = 7.68$.

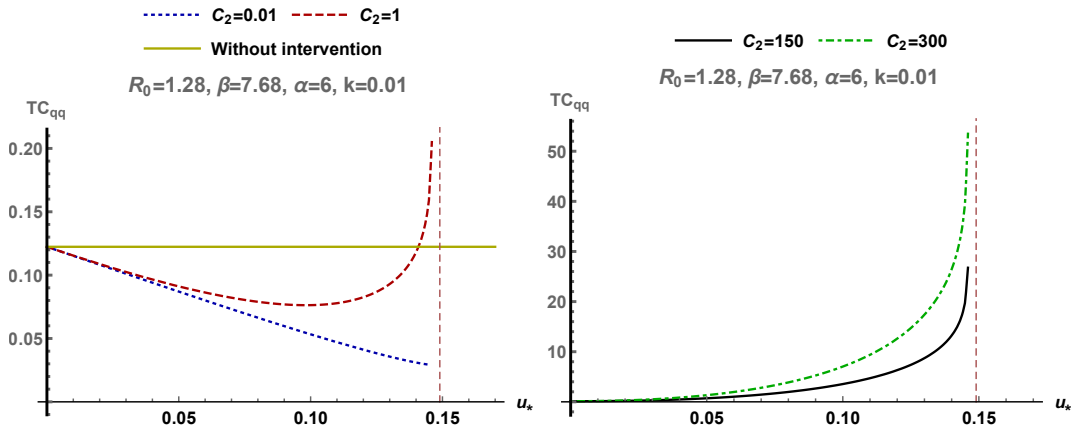

Figure 4.4: The quadratic total cost as a function of u_* for four different NPIs costs. The total cost is unbounded to the right of the dashed vertical pink line. The dark yellow horizontal line is the total cost in the absence of any intervention. Parameters are $k = 0.01$; $\beta = 7.68$; $\alpha^{-1} = 1/6$ month; $\mathcal{R}_0 = 1.28$.

total cost. Also another counter intuitive situation when $C_2 << C_1$, the quadratic total cost is decreasing in u_*, meaning that when the cost of NPIs is very small compared to the cost of disease burden, the optimal strategy lies on the boundary between the two regions, which is again not feasible. In this case we impose a restriction: we maximized the possible length of intervention, and we could find the optimal strategy with such restriction.

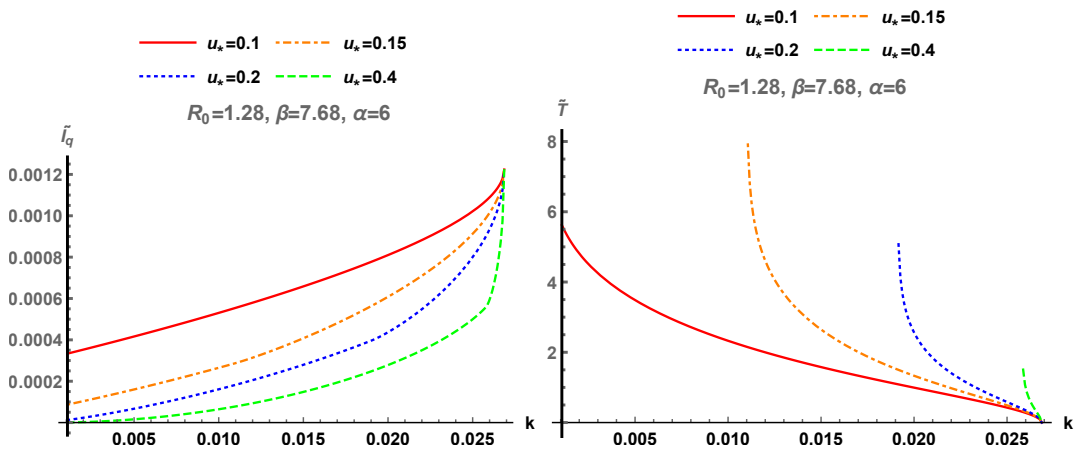

Figure 4.5: $\tilde{I}_q(k, u_*)$ (left) and the length of intervention ($\tilde{T}(k, u_*)$) (right) as a function of the threshold level k for four different control intensities. Parameters are $\mathcal{R}_0 = 1.28$, $\alpha^{-1} = 1/6$ month, $\beta = 7.68$.

4.4 The relation between the quadratic total cost and the threshold level k

Next we consider how the quadratic total cost changes when we vary k for fixed values of u_*. The change in the total cost then depends on

$$\frac{d}{dk} TC_{qq}(k, u_*) = C_1 \frac{d\tilde{I}_q}{dk} + C_2 \frac{d\tilde{T}}{dk} u_*^2. \tag{4.8}$$

Figure 4.5 shows that by increasing k, that is we start intervention later, $\tilde{I}_q$ increasing while the duration of intervention decreasing. Again, the change in total depends on how $C_1 : C_2$ relates to $-\frac{d\tilde{T}}{dk} u_*^2 : \frac{d\tilde{I}_q}{dk}$. This is depicted in Figure 4.6 for various values of C_2. Similarly as before, considering the feasible region of limited costs, when the NPI is very expensive, the minimal cost is achieved by non-intervention ($k \geq I_{\max}$). On the other hand, when the cost of NPIs is very small compared to the cost of disease burden, the optimal strategy lies on the boundary between the two regions, which is again not feasible. In this case we maximized the possible length of intervention, and we could find the optimal strategy with such restriction. When these costs are of similar magnitudes, the total cost can be a non-monotone function in the threshold level k, and in this case we can determine which strategy gives the minimal total cost.

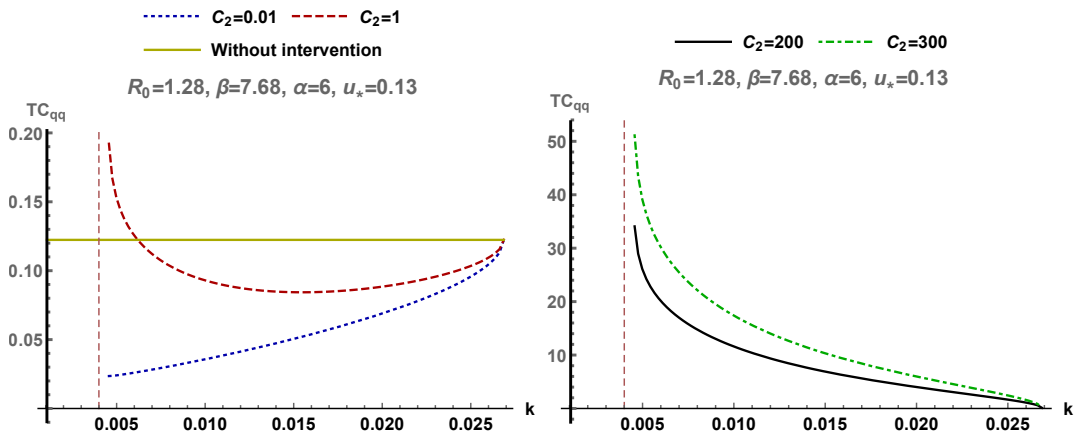

Figure 4.6: Quadratic total cost as a function of threshold level k for four different NPIs costs. The total cost is unbounded to the left dashed vertical pink line. Parameters are $\beta = 7.68$; $\alpha = 6$; $\mathcal{R}_0 = 1.28$; $u_* = 0.13$.

4.5 Discussion and the global optimum

We have proposed a family of temporary NPI strategies in the framework of the SIR model. These strategies are characterized by parameters (k, u_*), where NPIs start when the number of infected hosts reaches the threshold value k, and with rate u_* we continue the intervention till herd immunity is reached (ITHIR). The advantages of ITHIR-strategy are the following: First, it has a clear and meaningful definition: We start NPIs with a control intensity u_* when a threshold k is reached in the level of infection, then the density of susceptibles drops below $\mathcal{R}_0^{-1}$, that is the herd immunity is reached in the population, the density of infected will decrease anyway. Second, it is determined only by the parameters (k, u_*), hence all strategies from this family can be explored in a two dimensional parameter space. We have assigned a different total cost to each strategy composed of cost of disease burden and cost of NPIs, and systematically investigated the dependence of the total cost on the parameters for seasonal and pandemic influenza. As we see in the plots of Figure 4.7, the whole parameter domain is divided into two regions where the total cost is unbounded in the white region and bounded in the colored region. Essentially, considering the feasible region of limited costs, we have found three types of behaviours (hereandafter the next A,B,C denote the first, second, third behaviours with its optimal strategy res.) :

(A) *NPIs cost is very low compared to the cost associated with the disease burden*: in this case the optimal strategy lies on the boundary between the two regions, which is not feasible. Hence we maximized the possible length of intervention, and we could find the optimal strategy with such restriction;

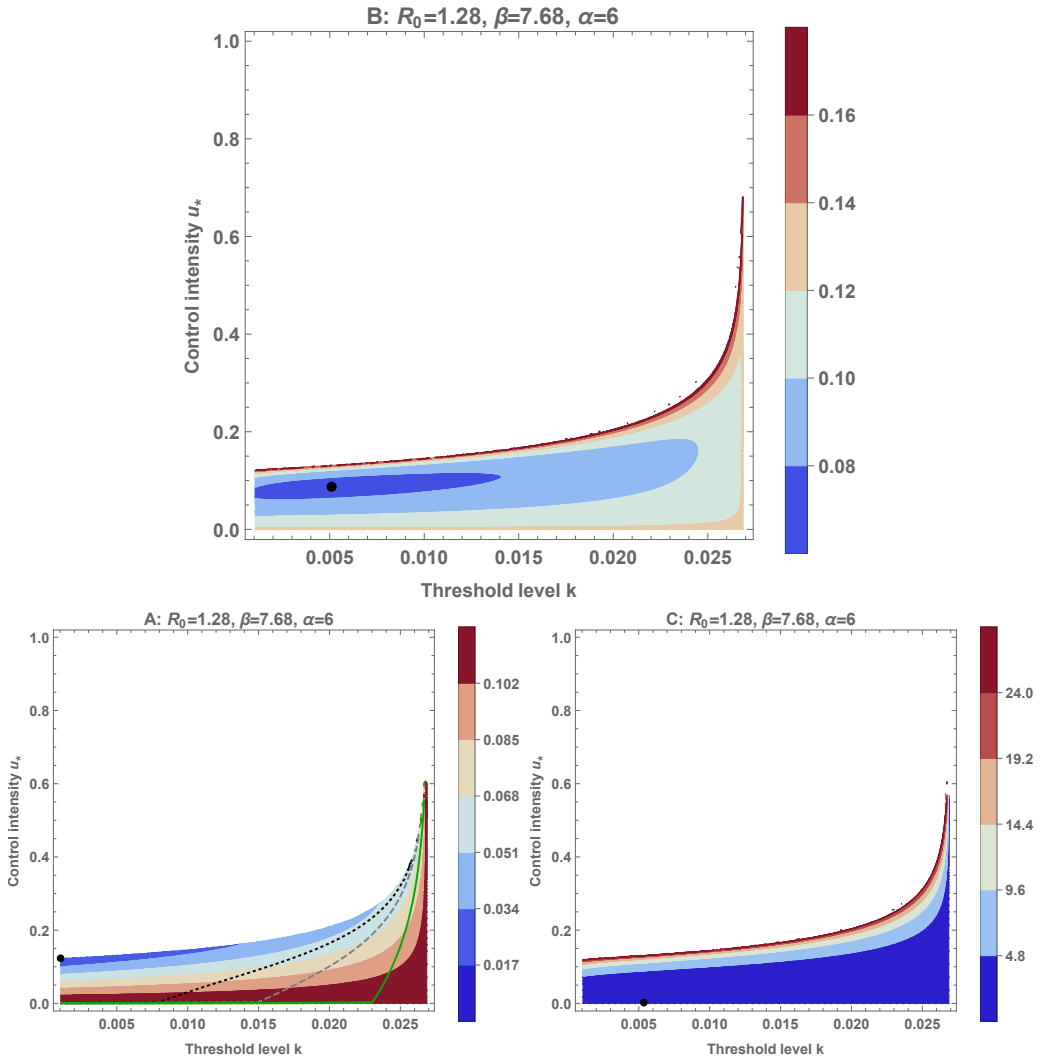

Figure 4.7: Dependence of the quadratic total cost on (k, u_*) in three typical situations: (A) $C_2 = 0.01 \ll C_1$, (C) $C_2 = 200 \gg C_1$, and (B) C_2 and C_1 are of similar magnitude. The white regions represent the unbounded total cost. The plots A and C show the monotone cases, while the plot B where $C_2 = 1$ we can find non-monotonicity in both k and u_*. In plot A the dotted black, dashed gray, and solid green curves represent the duration of NPIs for $1.5, 1, 0.5$ months respectively. The black point represents the infimum of the total cost in plot A, and it represents the minimum of the total cost in plot B and C.

(B) *intervention cost and disease burden cost are of similar magnitudes*: there may be non-monotone relationships between the control intensity, the starting threshold and the total cost, and in this case we can determine which strategy gives the minimal total cost;

(C) *intervention cost is very high compared to the cost associated to disease burden*: in this case the minimal cost is attained by not controlling at all.

These three typical behaviors are plotted into a heatmap in Figure 4.7. In case (A) (see Figure 4.7 bottom left), if we consider the maximized possible length of the intervention that represented by black dotted curve, which equals two months in this example, then the boundary between the two bounded and unbounded cost regions lies out the restriction domain, meaning that the optimal strategy lies in the feasible region where we could find it. If we maximized the possible control intensity in the feasible region, say that $0 < u_* \leq u_{\max}$ then the optimal strategy is to start the NPIs as early as possible with control intensity $u_* = u_{\max}$. Furthermore, if we maximized both of the possible length of intervention and the possible control intensity, then their intersected point is the optimal strategy. In case (B), the black point in the Figure 4.7 (top) represents the global minimum of the quadratic total cost of seasonal flu when $C_2 = 1$, meaning that the optimal strategy is to start NPIs when $k = 0.005$ with control intensity $u_* = 0.088$.

Depending on the available resources and public health capacities, there may be constraints on the parameters, such as $k_{\min} \leq k \leq I_{\max}$ and $0 \leq u_* \leq u_{\max}$ in the feasible region. Finding the optimal strategy with such constraints can be found even in these cases from the graphs in Figures 4.4, 4.6, 4.7. It is very easy when the total cost depends monotonically on the parameters, for example with $0 \leq u_* \leq u_{\max}$ and in the situation of $C_2 = 0.01$ in Figure 4.4, the optimal strategy is always $u_* = u_{\max}$. In contrast, for $C_2 = 200$ (see Figure 4.4 right), $u_* = 0$ is the strategy that gives the minimal cost, but in the situation of $C_2 = 1$ the optimal strategy exists at the minimum.

Another interesting phenomenon is depicted in Figure 4.8, showing that for a fixed u_*, the non-monotonicity of the total cost in k for seasonal influenza can be monotone increasing for pandemic influenza. In that particular situation of Figure 4.8, for seasonal influenza, to minimize the cost we apply the strategy at the minimum while for pandemic influenza the lowest cost comes from start NPIs as early as possible. This important insight shows that pandemic influenza should be treated differently than seasonal by public health authorities.

Also another interesting phenomenon is depicted in Figure 4.9, showing that for a fixed k, the monotonicity of the total cost in u_* can reverse varying the cost function type. We can see the monotone increasing in u_* for $TC_{ee}, TC_{le}, TC_{qe}, TC_{qqe}$ while monotone decreasing for TC_{lq}, and non-monotone for $TC_{ll}, TC_{qq}, TC_{lqe}$. Thus, the type of cost function plays an interesting vital role in determining the optimal temporary intervention strategy in the case of seasonal and pandemic influenza as shown in the tables 4.3 and 4.4.

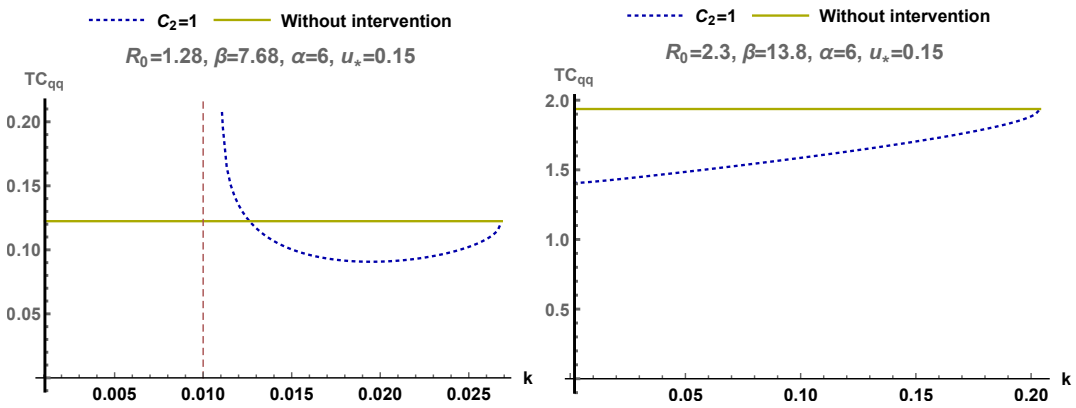

Figure 4.8: Effect of $\mathcal{R}_0$ on the monotonicity of the quadratic cost curve. Parameters are $u_* = 0.15$, $C_2 = 1$, $\alpha^{-1} = 1/6$ month and $\beta = 7.68$, resp. $\beta = 13.8$. For seasonal influenza, ($\mathcal{R}_0 = 1.28$), the optimal strategy is achieved by starting NPIs at the minimum while for pandemic influenza, ($\mathcal{R}_0 = 2.3$), it is better to start NPIs early.

Table 4.3: **The effect of the total cost function type in the case of seasonal influenza on the optimal strategy**. A,B, and C refer to the behaviour of the cost function and the corresponding optimal strategy (see the discussion section). Parameters are $\mathcal{R}_0 = 1.28$; $\alpha^{-1} = 1/6$ month; $\beta = 7.68$; $C_1 = 100$; $k = 0.01$.

The cost function	$C_2 = 1$	$C_2 = 25$	$C_2 = 70$
CT_{ll}	A	B	C
CT_{qq}	B	B	C
CT_{ee}	B	C	C
CT_{lq}	A	A	B
CT_{le}	B	C	C
CT_{qe}	C	C	C
CT_{lqe}	C	B	C
CT_{qqe}	B	C	C

Table 4.4: **The effect of the total cost function type in the case of the pandemic on the monotonicity**. A,B, and C refer to the behaviour of the cost function and the corresponding optimal strategy (see the discussion section). Parameters are $\mathcal{R}_0 = 2.3$; $\alpha^{-1} = 1/6$ month; $\beta = 13.8$; $C_1 = 100$,and $k = 0.01$.

The cost function	$C_2 = 1$	$C_2 = 25$	$C_2 = 70$
CT_{ll}	A	B	C
CT_{qq}	B	B	B
CT_{ee}	B	C	C
CT_{lq}	A	A	B
CT_{le}	B	C	C
CT_{qe}	B	C	C
CT_{lqe}	A	B	B
CT_{qqe}	B	B	B

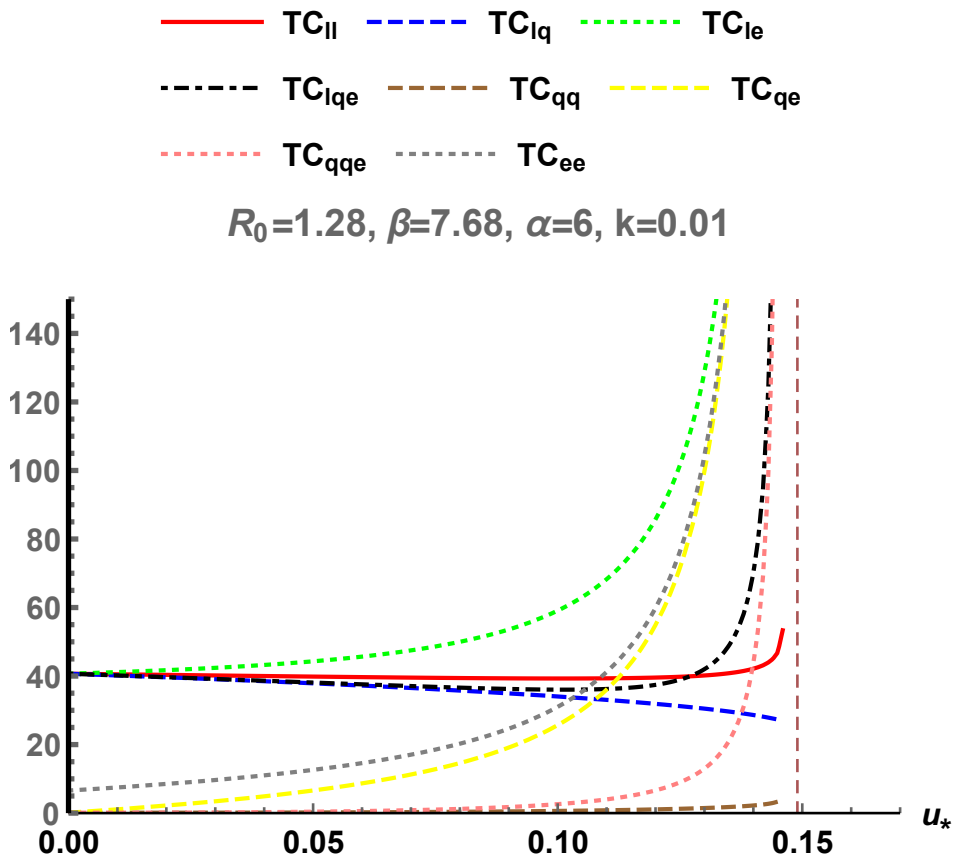

Figure 4.9: The effect of type of cost function on the monotonicity of the cost curve for eight cost functions. Parameters are $k = 0.01$; $\mathcal{R}_0 = 1.28$; $\alpha = 6$; $\beta = 7.68$; $C_2 = 25$.

5

Final epidemic size with temporary intervention strategies during infectious disease outbreaks

Reducing the final epidemic size of any infectious disease is a major goal for national and international public health organizations. Besides vaccination interventions, the most cost-effective preventive measures against many infectious diseases, integrating also non-pharmaceutical interventions and treatment and isolation interventions into control programs is one of the key actions to control epidemics.

In this chapter, we introduce temporary intervention strategies to control infectious disease outbreaks. The analysis of these strategies is based on the SIR framework. We apply a given control when the number of infected reaches a prescribed threshold level, and continue with the same intensity until the number of susceptible individuals drops below a critical level such that herd immunity is reached without further intervention.

We construct the final size system for the aforementioned methods of intervention, investigate how the final epidemic size depends on the parameters of the temporary intervention strategies, and show that the minimal final epidemic size is attained by starting intervention as early as possible and as high rate as possible.

5.1 The final susceptible population size system for the VUHIA-strategy

To understand the following discussion in this section, the reader is referred to Section 3.1 where the specification of the *VUHIA*-strategy including the model description can be found. We only consider the following first two equations of (3.1) with (3.5) as they

are independent of the third one of (3.1):

$$\begin{aligned} S'(t) &= -\beta S(t)I(t) - v(t)S(t), \\ I'(t) &= \beta S(t)I(t) - \alpha I(t), \end{aligned} \tag{5.1}$$

where

$$v(t) = \begin{cases} 0, & t \notin J, \\ p, & t \in J, \end{cases}$$

J is the intervention interval $J = [T_{\text{start}}, T_{\text{end}}]$ with

$$T_{\text{start}} = \min\{t \geq 0 : I(t) \geq k\} \quad \text{and} \quad T_{\text{end}} = \min\{t \geq 0 : \beta S(t) - \alpha \leq 0\},$$

and k is the threshold of infection density when the vaccination is triggered.

Let (Sys_V) denote System (5.1). Note that (Sys_V) consists of the following two systems: First, the free system (denoted by Sys_{free}) is

$$\begin{aligned} S'(t) &= -\beta S(t)I(t), \\ I'(t) &= \beta S(t)I(t) - \alpha I(t). \end{aligned} \tag{5.2}$$

Second, the control system of *VUHIA*-strategy (denoted by Sys_{Vc}) is

$$\begin{aligned} S'(t) &= -\beta S(t)I(t) - pS(t), \\ I'(t) &= \beta S(t)I(t) - \alpha I(t). \end{aligned} \tag{5.3}$$

It is well known (see Chapter 2.1) that

$$\Phi_1(t) \coloneqq I(t) + S(t) - \mathcal{R}_0^{-1} \log S(t) \tag{5.4}$$

is an invariant of (Sys_{free}), and hnce there is a unique solution curve connecting each equilibrium point in the interval $\alpha/\beta < S < 1$ to one in the interval $0 < S < \alpha/\beta$.

For the (Sys_{Vc}), it is not difficult to see that $(0, 0)$ is the only equilibrium point for (Sys_{Vc}) and it attracts the set $\{(S, I) \in [0, 1]^2 : S + I \leq 1\}$. Next, one can use a similar technique to the way of constructing $\Phi_1(t)$ in Chapter 2.1 to obtain $\Phi_2(t)$ that given in the next Proposition.

Proposition 5.1.1.

$$\Phi_2(t) = I(t) + S(t) - \frac{\alpha}{\beta} \log S(t) + \frac{p}{\beta} \log I(t) \tag{5.5}$$

is an invariant of System 5.3.

Proof. If $\Phi_2'(t) = 0$ for all t, then the proof is complete. The derivative of the function $\Phi_2(t)$, given in (5.5), with respect to t is

$$\Phi_2'(t) = S'(t) + I'(t) - \frac{\alpha}{\beta}\frac{S'(t)}{S(t)} + \frac{p}{\beta}\frac{I'(t)}{I(t)}. \tag{5.6}$$

Then one can substitute the $S'(t)$ and $I'(t)$ equations of Sys_{Vc} into (5.6) to obtain

$$\Phi_2'(t) = -\beta S(t)I(t) - pS(t) + \beta S(t)I(t) - \alpha I(t) \\ - \frac{\alpha}{\beta}\frac{-\beta S(t)I(t) - pS(t))}{S(t)} + \frac{p}{\beta}\frac{\beta S(t)I(t) - \alpha I(t)}{I(t)},$$

which can be simplified to

$$\Phi_2'(t) = -pS(t) - \alpha I(t) - \frac{\alpha}{\beta}(-\beta I(t) - p) + \frac{p}{\beta}(\beta S(t) - \alpha).$$

That is $\Phi_2'(t) = 0$. □

Note that the solution of (Sys_V) only coincides with the solution of (Sys_{Vc}) in the interval $S(T_{start}) \leq S \leq \alpha/\beta$. Now we are able to analyze the vector field of (Sys_V) and rely on $\Phi_1(t)$ and $\Phi_2(t)$ to construct the final size system for the *VUHIA*-strategy of (k, p)-type.

The final susceptible population size $\tilde{S}(k, p) := \lim_{t\to\infty} S(t)$ when (k, p) of *VUHIA*-strategy applied is the proportion of the susceptible population in the community who had never been infected during an outbreak and *VUHIA*-strategy implementation.

Theorem 5.1.1. *The final susceptible population size system for the VUHIA-strategy of (k, p)-type is*

$$\begin{aligned} k + S(T_{\text{start}}) - \mathcal{R}_0^{-1}\log S(T_{\text{start}}) &= 1 - \mathcal{R}_0^{-1}\log S_0, \\ k + S(T_{\text{start}}) - \mathcal{R}_0^{-1}\log S(T_{\text{start}}) + \frac{p}{\beta}\log k &= I(T_{\text{end}}) + \mathcal{R}_0^{-1} - \mathcal{R}_0^{-1}\log\mathcal{R}_0^{-1} + \frac{p}{\beta}\log I(T_{\text{end}}), \\ I(T_{\text{end}}) + \mathcal{R}_0^{-1} - \mathcal{R}_0^{-1}\log\mathcal{R}_0^{-1} &= \tilde{S}(k, p) - \mathcal{R}_0^{-1}\log\tilde{S}(k, p). \end{aligned} \tag{5.7}$$

Proof. From the first equation of (Sys_V), one can observe that S is decreasing for all $t \geq 0$. From the second equation, we can see that I-nullclines are $I = 0$ and the vertical line $S = \alpha/\beta = \mathcal{R}_0^{-1}$. $I' > 0$ if $S > \mathcal{R}_0^{-1}$ and $I' < 0$ if $S < \mathcal{R}_0^{-1}$. Hence for the initial data (S_0, I_0), $S_0 \approx 1$ and $I_0 << 1$ and $I(T_{start}) = k$, during the time interval $[0, T_{start}]$, S decreases monotonically while I rises, coinciding with the solution of (Sys_{free}) (see Figure 5.1), and hence one can use the invariant function $\Phi_1(t)$ of (Sys_{free}), given in (5.4), to find $S(T_{start})$ as in the first equation of the final susceptible population size system (5.7).

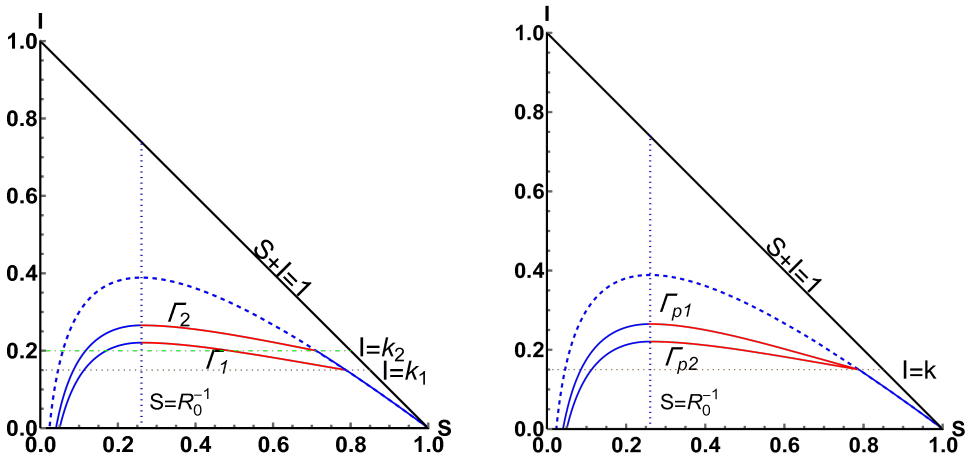

Figure 5.1: The solution $(S, I) = (S(.; S_0, I_0), I(.; S_0, I_0))$ of (Sys_V) for $(k_1, 10)$-strategy and $(k_2, 10)$-strategy (left) and $(0.15, p_1)$-strategy and $(0.15, p_2)$-strategy (right), where $k_1 = 0.15$, $k_2 = 0.2$, $p_1 = 5$, $p_2 = 10$, $I_0 << 1$ and $S_0 \approx 1$. The solution of (Sys_{free}) is represented by the dashed curve. The vertical dotted line is $S = \alpha/\beta = \mathcal{R}_0^{-1}$. Parameters are $\mathcal{R}_0 = 3.83$, $\alpha = 6$, $\beta = 23$.

.

Then, during the interval $[T_{start}, T_{end}]$, $S(t)$ and $I(t)$ are coinciding with a solution of (Sys_{Vc}), and hence one can use the invariant function $\Phi_2(t)$, given in the Proposition 5.1.1 to find $I(T_{end})$ as in the second equation of the final susceptible population size system. Finally, for all $t \in [T_{end}, \infty)$, $S(t)$ and $I(t)$ are coinciding with a solution of (Sys_{Vf}), and hence using the invariant function $\Phi_1(t)$ to find $\tilde{S}(k, p)$ as in the third equation of the final susceptible population size system. By this way the three equations of the final susceptible population size system (5.7) have constructed. □

5.2 Dependence of the final susceptible population on (k, p)

Lemma 5.2.1. *Let $p > 0$ be a fixed vaccination rate. The final susceptible population size for VUHIA-strategy of (k, p)-type is decreasing in the threshold level k.*

Proof. Let $I(T_{start_1}) = k_1$ and $I(T_{start_2}) = k_2$ be arbitrary threshold levels of starting vaccination such that $k_1 < k_2$ and $k_1, k_2 \in [I_0, I_{\max}]$. We consider the $I - S$ plane and denote the solutions of (Sys_V) for (k_1, p)-strategy and (k_2, p)-strategy by (S_{k_1}, I_{k_1}), (S_{k_2}, I_{k_2}) respectively (see Figure 5.1). We consider phase curves $I(S)$ and claim that $I_{k_2}(S) > I_{k_1}(S)$ for each S in the interval $\tilde{S}(k_1, p) \leq S < S(T_{start_1})$. Indeed, we note that

$I_{k_2}(S(T_{start_1})) = I_{k_1}(S(T_{start_1})) = k_1$

$$\frac{dI_{k_2}}{dS_{k_2}} = \frac{\beta S_{k_2} k_1 - \alpha k_1}{-\beta S_{k_2} k_1} < \frac{\beta S_{k_1} k_1 - \alpha k_1}{-\beta S_{k1} k_1 - p S_{k_1}} = \frac{dI_{k_1}}{dS_{k_1}}, \quad \text{at } S_{k_1} = S_{k_2} = S(T_{start_1}).$$

Now suppose for contradiction that the solutions (S_{k_1}, I_{k_1}) and (S_{k_2}, I_{k_2}) are intersected at (S_*, I_*), where $S(T_{start_2}) \leq S_* < S(T_{start_1})$. Then it is necessary that $dI_{k_1}/dS_{k_1} \leq dI_{k_2}/dS_{k_2}$, at $S_{k_1} = S_{k_2} = S_*$. That is

$$\frac{\beta S_* I_* - \alpha I_*}{-\beta S_* I_* - p S_*} \leq \frac{\beta S_* I_* - \alpha I_*}{-\beta S_* I_*},$$

and hence $pS_* \leq 0$, which is not true. This implies that $I_{k_2}(S) > I_{k_1}(S)$ for each S in the interval $S(T_{start_2}) \leq S < S(T_{start_1})$. Since both solutions (S_{k_1}, I_{k_1}) and (S_{k_2}, I_{k_2}) coincide with the same system for each $\tilde{S}(k_1, p) \leq S \leq S(T_{start_2})$, they will not intersect each other and $I_{k_2}(S) > I_{k_1}(S)$ for each S in this interval. Hence $\tilde{S}(k_1, p) > \tilde{S}(k_2, p)$. That is the final susceptible population size is decreasing in k.

□

In the next Lemma, we uncover a counter-intuitive phenomenon about the relationship between the final susceptible population size and the vaccination rate. Indeed, the final size of the susceptible population after achieving herd immunity by applying the *VUHIA*-strategy of (k, p)-type and eliminating the epidemic increases in the vaccination rate p, for a fixed threshold level k.

Lemma 5.2.2. *Let $k \in [I_0, I_{\max}]$ be a fixed threshold level of starting vaccination. The final susceptible population size for VUHIA-strategy of (k, p)-type is increasing in the vaccination rate p.*

Proof. Let p_1 and p_2 be arbitrary vaccination rates such that $p_2 > p_1 > 0$. Similar to the proof of Lemma 5.2.1, we consider the $I - S$ plane and denote the solutions of (Sys_V) for (k, p_1)-strategy and (k, p_2)-strategy by (S_{p_1}, I_{p_1}), (S_{p_2}, I_{p_2}) respectively (see Figure 5.1). We consider phase curves $I(S)$ and claim that $I_{p_1}(S) > I_{p_2}(S)$ for each S in the interval $\alpha/\beta \leq S < S(T_{start})$. Indeed, we note that $I_{p_1}(S(T_{start})) = I_{p_2}(S(T_{start})) = k$ and

$$\frac{dI_{p_1}}{dS_{p_1}} = \frac{\beta S_{p_1} k - \alpha k}{-\beta S_{p_1} k - p_1 S_{p_1}} < \frac{\beta S_{p_2} k - \alpha k}{-\beta S_{p_2} k - p_2 S_{p_2}} = \frac{dI_{p_2}}{dS_{p_2}}, \quad \text{at } S_{p_1} = S_{p_2} = S(T_{start}).$$

Now suppose for contradiction that (S_{p_1}, I_{p_1}) and (S_{p_2}, I_{p_2}) are intersected at (S_*, I_*), where $\alpha/\beta \leq S_* < S(T_{start})$. Then it is necessary that $dI_{p_1}/dS_{p_1} \geq dI_{p_2}/dS_{p_2}$, at $S_{p_1} = S_{p_2} = S_*$. That is

$$\frac{\beta S_* I_* - \alpha I_*}{-\beta S_* I_* - p_1 S_*} \geq \frac{\beta S_* I_* - \alpha I_*}{-\beta S_* I_* - p_2 S_*},$$

which contradicts $p_2 > p_1$. This means that each solution of (S_{p_1}, I_{p_1}) and (S_{p_2}, I_{p_2}) coincides with the solution of (Sys_{Vc}) in the interval $\alpha/\beta \leq S \leq S(T_{start})$ and $I_{p_1}(S) > I_{p_2}(S)$ for each S in the interval $\alpha/\beta \leq S < S(T_{start})$. Since both solutions (S_{p_1}, I_{p_1}) and (S_{p_2}, I_{p_2}) coincide with the solution of (Sys_{Vf}) in the interval $\tilde{S}(k, p_2) \leq S < \alpha/\beta$, they will not intersect each other and $I_{p_1}(S) > I_{p_2}(S)$ for each S in this interval because $I_{p_1}(\alpha/\beta) > I_{p_2}(\alpha/\beta)$. Hence $\tilde{S}(k, p_2) > \tilde{S}(k, p_1)$. That is the final susceptible population size is increasing in p. □

Next, we prove the previous two Lemmas by another way depending on the final susceptible population size system given in Theorem 5.1.1.

Alternative proof of Lemma 5.2.1. If $I_0 \leq k \leq I_{\max}$ and $I(T_{\text{start}}) = k$, then any changing in k leads to changing in T_{start}. Since the right side of the first equation of (5.7) is a constant, the derivative of the left-hand side of this equation with respect to k is zero. That is

$$\frac{d(k + S(T_{\text{start}}) - \mathcal{R}_0^{-1} \log S(T_{\text{start}}))}{dk} = \frac{d(1 - \mathcal{R}_0^{-1} \log S_0)}{dk} = 0.$$

Now, we consider the second equation of (5.7) and differentiate both sides w.r.t k, and then do some algebraic manipulation to get the following:

$$\frac{d(k + S(T_{\text{start}}) - \mathcal{R}_0^{-1} \log S(T_{\text{start}}))}{dk} + \frac{p}{\beta k} = \frac{dI(T_{\text{end}})}{dT_{\text{end}}} \frac{dT_{\text{end}}}{dk} + \frac{p}{\beta} \frac{dI(T_{\text{end}})}{dT_{\text{end}}} \frac{dT_{\text{end}}}{dk} \frac{1}{I(T_{\text{end}})},$$

Which is equivalent to

$$\frac{p}{\beta k} = \frac{dI(T_{\text{end}})}{dT_{\text{end}}} \frac{dT_{\text{end}}}{dk} (1 + \frac{p}{\beta} \frac{1}{I(T_{\text{end}})}).$$

Simple algebraic manipulation leads to

$$\frac{dI(T_{\text{end}})}{dT_{\text{end}}} \frac{dT_{\text{end}}}{dk} = \frac{p}{k} \frac{I(T_{\text{end}})}{\beta I(T_{\text{end}}) + p}.$$

Differentiation both sides of the third equation of (5.7) w.r.t. k gives

$$\frac{dI(T_{\text{end}})}{dT_{\text{end}}} \frac{dT_{\text{end}}}{dk} = \frac{d\tilde{S}(k, p)}{dk} (1 - \mathcal{R}_0^{-1} \frac{1}{\tilde{S}(k, p)}),$$

and hence

$$\frac{d\tilde{S}(k, p)}{dk} = \left(\frac{p}{k} \frac{I(T_{\text{end}})}{\beta I(T_{\text{end}}) + p} \right) \left(\frac{\tilde{S}(k, p)}{\tilde{S}(k, p) - \mathcal{R}_0^{-1}} \right) < 0$$

because $\tilde{S}(k, p) < \mathcal{R}_0^{-1}$ for all $p > 0$. □

Alternative proof of Lemma 5.2.2. Similar to the previous alternative proof of Lemma 5.2.1, differentiation the second equation of System (5.7) w.r.t. p and algebraic manipulation give

$$\frac{dI(T_{\text{end}})}{dT_{\text{end}}}\frac{dT_{\text{end}}}{dp} = \frac{I(t_2)}{\beta I(T_2)+p}[\log k - \log I(T_{\text{end}})]. \tag{5.8}$$

Do similar steps to the third equation of (5.7) and use (5.8) to get

$$\frac{d\tilde{S}(k,p)}{dp} = \frac{I(t_2)}{\beta I(T_2)+p}\left[\log k - \log I(T_{\text{end}})\right]\frac{\tilde{S}(k,p)}{\tilde{S}(k,p)-\mathcal{R}_0^{-1}} > 0. \tag{5.9}$$

□

5.3 Numerical simulation for FES of the VUHIA-strategy

Remember that $\tilde{V}(k,p)$ is the proportion of the population that get vaccinated during the course of the epidemic and *VUHIA*-strategy of (k,p)-type implementation, it is given by (3.8). The final epidemic size (FES) of *VUHIA*-strategy of (k,p)-type (with $N=1$) is

$$\tilde{I}(k,p) := 1-\tilde{S}(k,p)-\tilde{V}(k,p) = \int_0^\infty \beta S(t)I(t)dt = \alpha\int_0^\infty I(t)dt, \tag{5.10}$$

the total number of infected people during the course of the epidemic and *VUHIA*-strategy of (k,p)-type.

Next, we systematically investigate the dependence of the final epidemic size $\tilde{I}(k,p)$ of the *VUHIA*-strategy on the parameters (k,p).

To see how the final epidemic size $\tilde{I}(k,p)$ depends on the vaccination rate p, we shall consider various fixed k-s and vary p. The change in the $\tilde{I}(k,p)$ then depends on

$$\frac{d}{dp}\tilde{I}(k,p) = -\frac{d}{dp}\tilde{S}(k,p) - \frac{d}{dp}\tilde{V}(k,p).$$

From Figure 5.2, we can see that the final susceptible population size $\tilde{S}(k,p)$ and the total vaccinated people $\tilde{V}(k,p)$ increasing in p, thus the sign of the rate of change of the final epidemic size is positive for all $p>0$. Hence, the final epidemic size $\tilde{I}(k,p)$ is decreasing in p, which we can see in the top plot of Figure 5.2, meaning that the optimal strategy to reduce the final epidemic size is to vaccinate as high rate as possible. In addition, we can also observe that (with $N=1$) $\tilde{I}(k,p)\to 1-S_\infty$ as $p\to 0$.

Next, we consider how the final epidemic size changes when we vary k for fixed values of p. Figure 5.3 shows that by increasing k, that is we start vaccinating later, both the final susceptible population $\tilde{S}(k,p)$ and total vaccinated people $\tilde{V}(k,p)$ are decreasing.

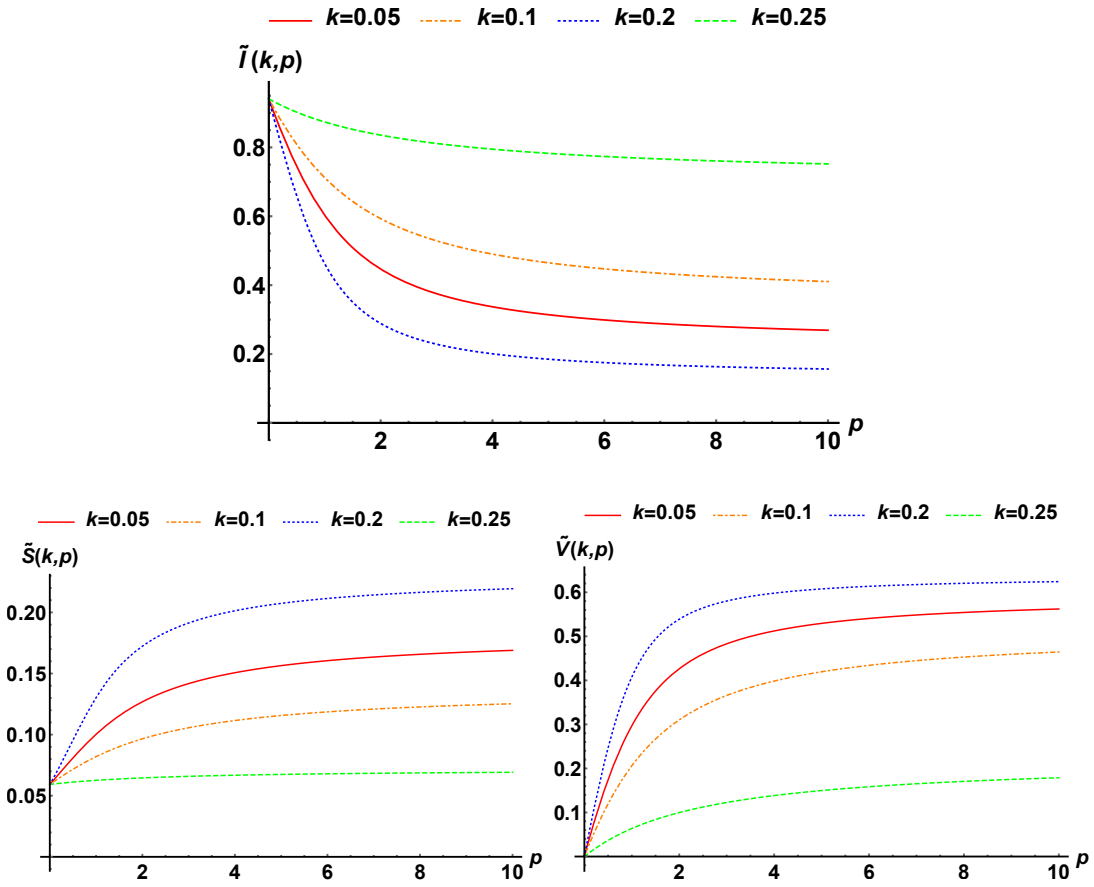

Figure 5.2: The final susceptible population size (bottom left), the total vaccinated people (bottom right), and the final epidemic size (top) as functions of the vaccination rate p. Parameters are $\mathcal{R}_0 = 3$, $\alpha^{-1} = (1/3)$ month, $\beta = 9$.

Hence, $d\tilde{I}(k,p)/dk < 0$ for all $k \in [I_0, I_{\max}]$ and the final epidemic size is increasing in k for all $k \in [I_0, I_{\max}]$, see the top plot in Figure 5.3. Thus the optimal strategy to minimize the final epidemic size is to start vaccination as early as possible. In addition, one can note that the graphs of all four curves meet at the right when $k \to I_{\max}$. That is, (with $N = 1$) the FES of *VUHIA*-strategy of (k,p)-type $[1 - \tilde{S}(k,p) - \tilde{V}(k,p)] \to 1 - S_\infty$ as $k \to I_{\max}$, the final epidemic size without vaccination.

Figure 5.4 represents the dependence of the final size of the susceptible population after achieving herd immunity by applying the *VUHIA*-strategy and eliminating the epidemic (bottom left), the total vaccinated people (bottom right), and the final epidemic size (top) on (k,p). The plots are heatmaps. From the top plot of this figure, we can see that the minimal final epidemic size is attained when $(k,p) \to (I_0, p_{max})$, where p_{max} is the maximal possible vaccination rate. Hence, the optimal strategy to reduce the final

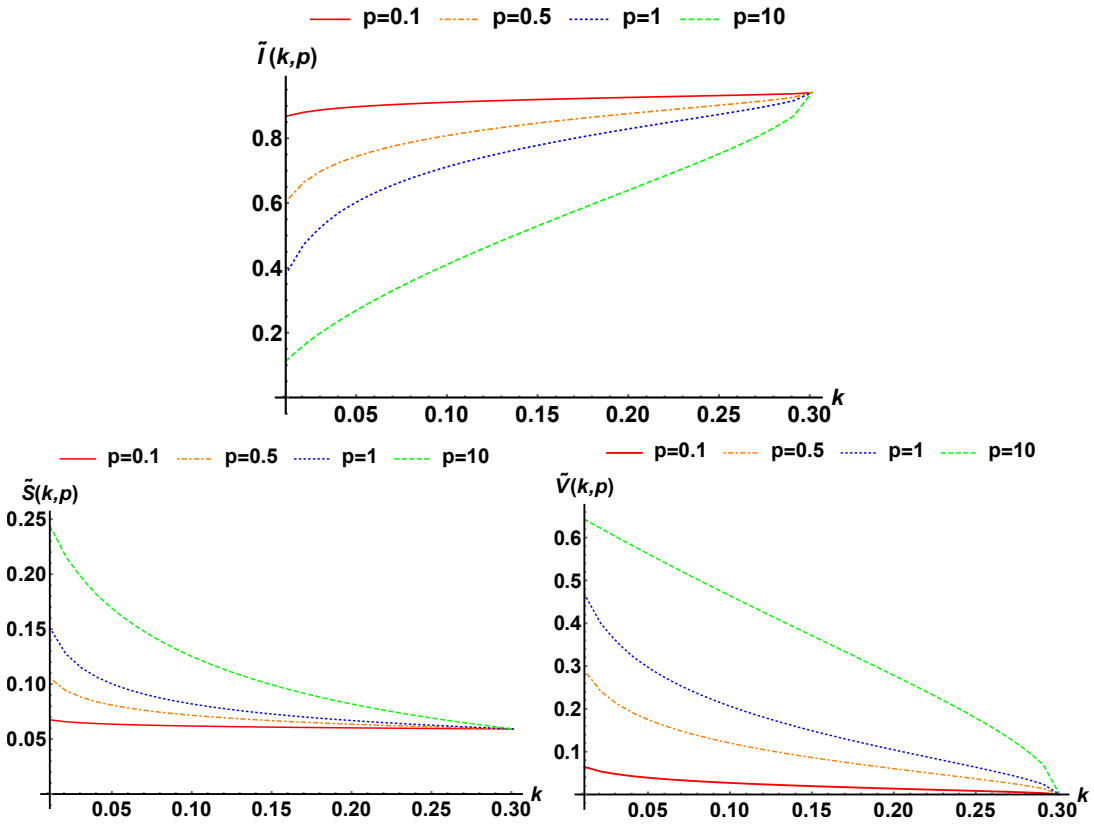

Figure 5.3: The final susceptible population size, the total vaccinated people, and the final epidemic size as functions of the threshold level k. Parameters are $\mathcal{R}_0 = 3$, $\alpha^{-1} = (1/3)$ month, $\beta = 9$.

epidemic size is to start vaccination as early as possible as high rate as possible.

5.4 The final size system for the *ITHIR*-strategy of NPIs

To understand the following discussion in this section, the reader is referred to Section 4.1 where the specification of the *ITHIR*-strategy including the model description of non-pharmaceutical interventions (NPIs) is given. We only consider the following first two equations of (4.1) with (4.6) as they are independent of the third one of (4.1):

$$\begin{aligned} S'(t) =& -[1-u(t)]\beta S(t)I(t), \\ I'(t) =& [1-u(t)]\beta S(t)I(t) - \alpha I(t), \end{aligned} \tag{5.11}$$

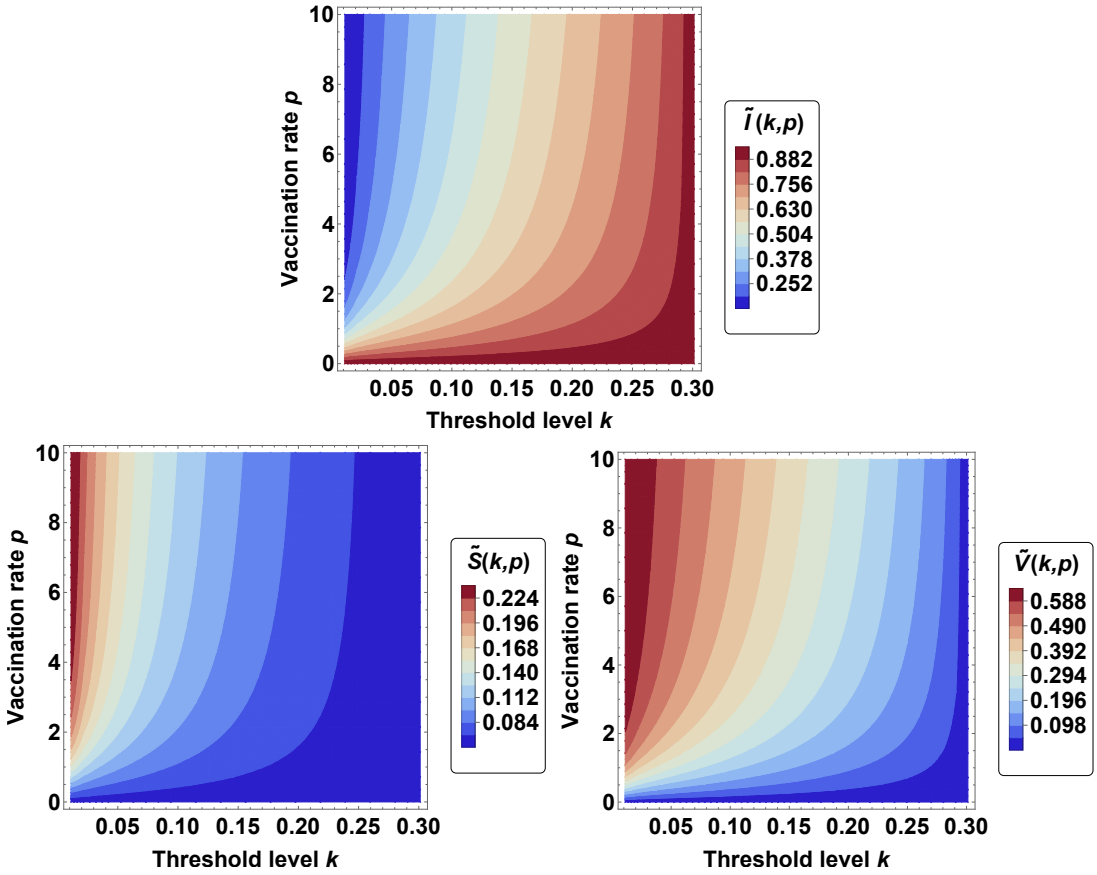

Figure 5.4: Dependence of the final susceptible population size (bottom left), the total vaccinated people (bottom right), and the final epidemic size on (k, p) (top). Parameters are $\mathcal{R}_0 = 3$, $\alpha^{-1} = (1/3)$ month, $\beta = 9$.

where

$$u(t) = \begin{cases} 0, & t \notin J, \\ u_*, & t \in J, \end{cases}$$

and J is the intervention interval $J = [T_{\text{start}}, T_{\text{end}}]$ with

$$T_{\text{start}} = \min\{t \geq 0 : I(t) \geq k\} \quad \text{and} \quad T_{\text{end}} = \min\{t \geq 0 : \beta S(t) - \alpha \leq 0\},$$

and k is the threshold level where we start NPIs.

Let (Sys_{NPI}) denote System (5.11). Note that (Sys_{NPI}) consists of the following two systems: First, the free system (Sys_{free}) from any interventions, which is given in (5.2). Second, the control system of *ITHIR*-strategy of NPIs (denoted by Sys_{NPIc}) is

$$\begin{aligned} S'(t) =& -[1 - u_*]\beta S(t)I(t), \\ I'(t) =& [1 - u_*]\beta S(t)I(t) - \alpha I(t). \end{aligned} \tag{5.12}$$

Let us emphasize that these are 2-dimensional systems consisting of the S- and I-equations of a basic SIR model. The transmission rate is β for (Sys_{free}), and it is $(1-u_*)\beta$ for (Sys_{NPIc}). Hence we take the following observation without proof:

Proposition 5.4.1.

$$\Phi_3(t) = I(t) + S(t) - \frac{\alpha}{[1-u_*]\beta}\log S(t) \tag{5.13}$$

is an invariant of System 5.12.

Remember that $\tilde{S}(k,u_*) = \lim_{t\to\infty} S(t)$ when (k,u_*) of *ITHIR*-strategy applied, the proportion of the susceptible population in the community who had never been infected during an outbreak and *ITHIR*-strategy implementation.

Now we are able to construct the final size system for the *ITHIR*-strategy of (k,u_*)-type in a similar manner to the final size system (5.7).

Theorem 5.4.1. *If $k \in [I_0, I_{\max}]$, then we distinguish two cases:*
Case 1: If $\tilde{S}(k,u_*) \geq \mathcal{R}_0^{-1}$, then the final size system for ITHIR-strategy of NPIs is

$$\begin{aligned} k + S(T_{\text{start}}) - \mathcal{R}_0^{-1}\log S(T_{\text{start}}) &= 1 - \mathcal{R}_0^{-1}\log S_0, \\ k + S(T_{\text{start}}) - \frac{\mathcal{R}_0^{-1}}{(1-u_*)}\log S(T_{\text{start}}) &= \tilde{S}(k,u_*) - \frac{\mathcal{R}_0^{-1}}{(1-u_*)}\log \tilde{S}(k,u_*). \end{aligned} \tag{5.14}$$

Case 2: If $\tilde{S}(k,u_*) < \mathcal{R}_0^{-1}$, then the final size system for ITHIR-strategy of NPIs is

$$\begin{aligned} k + S(T_{\text{start}}) - \mathcal{R}_0^{-1}\log S(T_{\text{start}}) &= 1 - \mathcal{R}_0^{-1}\log S_0, \\ k + S(T_{\text{start}}) - \frac{\mathcal{R}_0^{-1}}{(1-u_*)}\log S(T_{\text{start}}) &= I(T_{\text{end}}) + \mathcal{R}_0^{-1} - \frac{\mathcal{R}_0^{-1}}{(1-u_*)}\log \mathcal{R}_0^{-1}, \\ I(T_{\text{end}}) + \mathcal{R}_0^{-1} - \mathcal{R}_0^{-1}\log \mathcal{R}_0^{-1} &= \tilde{S}(k,u_*) - \mathcal{R}_0^{-1}\log \tilde{S}(k,u_*). \end{aligned} \tag{5.15}$$

Proof. From the first equation of (Sys_{NPI}), we see that S is decreasing for all $t \geq 0$, and from the second equation we can note that I-nullclines are $I = 0$ and the vertical line $S = \alpha/[1-u(t)]\beta = \mathcal{R}_0^{-1}/[1-u(t)]$. $I' > 0$ if $S > \mathcal{R}_0^{-1}/[1-u(t)]$ and $I' < 0$ if $S < \mathcal{R}_0^{-1}/[1-u(t)]$. Hence for the initial data (S_0, I_0) and $I(T_{start}) = k$, if $t \in [0, \mathrm{T}_{\text{start}})$, then $u(t) = 0$ and the solution of (Sys_{NPI}) coincide with the solution of (Sys_{free}), and hence one can use the invariant function $\Phi_1(t)$ of the (Sys_{free}), given in (5.4), to find $S(T_{start})$ as in the first equation of the final size system (5.14) and (5.15). Next we distinguish two cases depending on the $\tilde{S}(k,u_*)$, see Figure 5.5:
Case 1: If $\tilde{S}(k,u_*) \geq \mathcal{R}_0^{-1}$, then $u(t) = u_*$ for all $t \geq \mathrm{T}_{\text{start}}$ and the solution of (Sys_{NPI}) coincides with the solution of (Sys_{NPIc}) for all $t \geq \mathrm{T}_{\text{start}}$ as we never stop the intervention

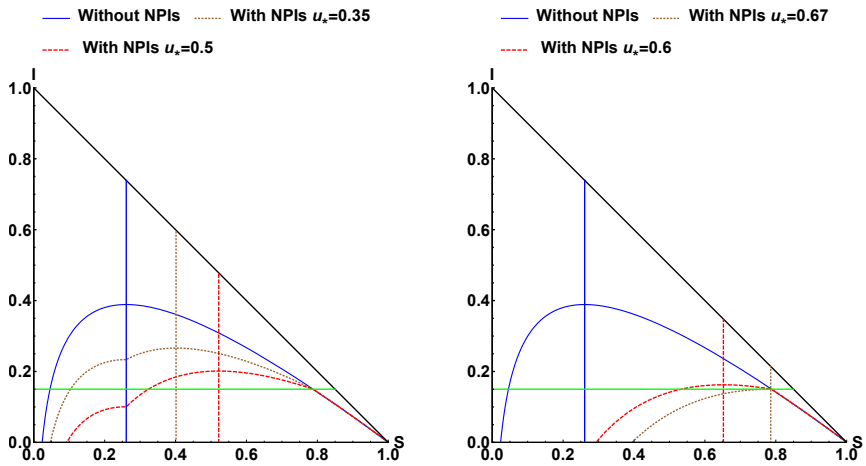

Figure 5.5: The solution $(S, I) = (S(.; S_0, I_0), I(.; S_0, I_0))$ of (Sys_{NPI}), where $I_0 << 1$ and $S_0 \approx 1$, is represented by the dashed and dotted curves for different *ITHIR*-strategy of NPIs . $\tilde{S}(k, u_*) < \mathcal{R}_0^{-1}$ (left) while $\tilde{S}(k, u_*) > \mathcal{R}_0^{-1}$ (right). The solid blue curve is the solution of (Sys_{free}). The solid vertical blue line is $S = \mathcal{R}_0^{-1}$. The other vertical lines are $S = \mathcal{R}_0^{-1}/(1 - u_*)$. The horizontal solid line is the threshold level k. Parameters are $\mathcal{R}_0 = 3.83$, $\alpha = 6$, $\beta = 23$.

in this case. Hence one can use the invariant function $\Phi_3(t)$, given in the Proposition 5.4.1 to find $\tilde{S}(k, u_*)$ as in the second equation of the final size system (5.14).
Case 2: If $\tilde{S}(k, u_*) < \mathcal{R}_0^{-1}$, then the solution of (Sys_{NPI}) coincides with the solution of (Sys_{NPIc}) for all $t \in [\mathrm{T_{start}}, \mathrm{T_{end}}]$, and hence one can use the invariant function $\Phi_3(t)$, given in the Proposition 5.4.1 to find $I(T_{end})$ as in the second equation of the final size system (5.15). Finally, for all $t \in [T_{end}, \infty)$, $S(t)$ and $I(t)$ are coinciding with the solution of (Sys_{free}), and hence using the invariant function $\Phi_1(t)$ to find $\tilde{S}(k, u_*)$ as in the third equation of the final size system(5.15). By this way, the final size system for *ITHIR*-strategy of NPIs is constructed for both cases. □

Next we give a condition that determines whether we are in Case 1) or case 2) of the previous theorem. Set

$$\eta(k) := 1 - \mathcal{R}_0^{-1} \frac{\log \frac{\mathcal{R}_0^{-1}}{S(T_{\mathrm{start}})}}{\mathcal{R}_0^{-1} - k - S(T_{\mathrm{start}})}. \tag{5.16}$$

Proposition 5.4.2. *Let $k \in [I_0, I_{\max}]$ be a given threshold level. If $\mathcal{R}_0^{-1} \leq \tilde{S}(k, u_*) < S(T_{\mathrm{start}})$, then $\eta(k) \leq u_* \leq 1$.*

Proof. From the second equation of (5.14), algebraic manipulation gives

$$1 - u_* = \frac{\alpha}{\beta} \frac{\log \frac{\tilde{S}(k,u_*)}{S(T_{\mathrm{start}})}}{\tilde{S}(k, u_*) - k - S(T_{\mathrm{start}})}. \tag{5.17}$$

For simplicity, we set the right-hand side of (5.17) as follows:

$$g(x) = \rho\frac{\log x - \log s_1}{x - k - s_1}, \quad \rho = \frac{\alpha}{\beta}, \quad s_1 = S(T_{\text{start}}), \quad x = \tilde{S}(k, u_*).$$

In the next step, we show that g is decreasing on $[\rho, s_1]$. Therefore,

$$g'(x) = \rho\frac{x - k - s_1 - x\log x + x\log s_1}{x(x - k - s_1)^2},$$

and $g'(x) < 0$ if

$$x + x\log s_1 - k - s_1 - x\log x < 0.$$

In addition, we set

$$f(x) = x + x\log s_1 - k - s_1 - x\log x,$$

and prove that the absolute maximum value of f is negative. Indeed, $f'(x) = \log s_1 - \log x$, $f'(x) > 0$ for every $\rho < x < s_1$, and has an absolute maximum value at $x = s_1$, which is $f(s_1) = -k < 0$. Thus $g(x)$ is a decreasing on $[\rho, s_1]$. Hence, $g(x)$ has an absolute maximum at $x = \rho$ and has an absolute minimum at $x = s_1$, which implies that $g(s_1) \leq g(x) \leq g(\rho)$, and hence $0 \leq 1 - u_* \leq 1 - \eta(k)$. Thus $\eta(k) \leq u_* \leq 1$. □

As a consequence of Proposition 5.4.2, $0 \leq u_* < \eta(k)$ if $\tilde{S}(k, u_*) < \mathcal{R}_0^{-1}$. . The final epidemic size of *ITHIR*-strategy of (k, u_*)-type (with $N = 1$) is

$$\tilde{I}(k, u_*) := 1 - \tilde{S}(k, u_*) = \int_0^\infty (1 - u_*)\beta S(t)I(t)dt = \alpha\int_0^\infty I(t)dt. \tag{5.18}$$

5.5 Dependence of the FES of the ITHIR-strategy on (k, u_*)

Lemma 5.5.1. *Let $0 < u_* \leq 1$ be a fixed control intensity. Then the final epidemic size $(1 - \tilde{S}(k, u_*))$ of ITHIR-strategy of (k, u_*)-type of NPIs (with $N = 1$) is increasing in the threshold value k.*

Proof. The proof is divided into two parts related to the two cases in Theorem 5.4.1. In the first part we assume that $\tilde{S}(k, u_*) \geq \mathcal{R}_0^{-1}$. Differentiation the first equation of System 5.14 w.r.t k gives

$$\frac{d(k + S(T_{\text{start}}) - \mathcal{R}_0^{-1}\log S(T_{\text{start}}))}{dk} = \frac{d(1 - \mathcal{R}_0^{-1}\log S_0)}{dk} = 0,$$

that is

$$1 + \frac{dS(T_{\text{start}})}{dT_{\text{start}}}\frac{dT_{\text{start}}}{dk} - \mathcal{R}_0^{-1}\frac{dS(T_{\text{start}})}{dT_{\text{start}}}\frac{dT_{\text{start}}}{dk}\frac{1}{S(T_{\text{start}})} = 0,$$

and hence

$$\frac{dS(T_{\text{start}})}{dT_{\text{start}}}\frac{dT_{\text{start}}}{dk}\frac{1}{S(T_{\text{start}})} = \frac{-1}{S(T_{\text{start}}) - \mathcal{R}_0^{-1}}. \tag{5.19}$$

Similarly, differentiate the second equation of System (5.14) w.r.t. k to get

$$1 + \frac{dS(T_{\text{start}})}{dT_{\text{start}}}\frac{dT_{\text{start}}}{dk} - \frac{\mathcal{R}_0^{-1}}{1-u_*}\frac{dS(T_{\text{start}})}{dT_{\text{start}}}\frac{dT_{\text{start}}}{dk}\frac{1}{S(T_{\text{start}})} = \frac{d\tilde{S}(k,u_*)}{dk} - \frac{\mathcal{R}_0^{-1}}{1-u_*}\frac{d\tilde{S}(k,u_*)}{dk}\frac{1}{\tilde{S}(k,u_*)}.$$

which is equivalent to

$$1 + \frac{dS(T_{\text{start}})}{dT_{\text{start}}}\frac{dT_{\text{start}}}{dk}\frac{1}{S(T_{\text{start}})}[S(T_{\text{start}}) - \frac{\mathcal{R}_0^{-1}}{1-u_*}] = \frac{d\tilde{S}(k,u_*)}{dk}\frac{1}{\tilde{S}(k,u_*)}[\tilde{S}(k,u_*) - \frac{\mathcal{R}_0^{-1}}{1-u_*}].$$

Using (5.19) and then algebraic manipulation give the following:

$$1 + \frac{-1}{S(T_{\text{start}}) - \mathcal{R}_0^{-1}}[S(T_{\text{start}}) - \frac{\mathcal{R}_0^{-1}}{1-u_*}] = \frac{d\tilde{S}(k,u_*)}{dk}\frac{1}{\tilde{S}(k,u_*)}[\tilde{S}(k,u_*) - \frac{\mathcal{R}_0^{-1}}{1-u_*}],$$

$$\frac{1}{S(T_{\text{start}}) - \mathcal{R}_0^{-1}}[S(T_{\text{start}}) - \mathcal{R}_0^{-1} - S(T_{\text{start}}) + \frac{\mathcal{R}_0^{-1}}{1-u_*}] = \frac{d\tilde{S}(k,u_*)}{dk}\frac{1}{\tilde{S}(k,u_*)}[\tilde{S}(k,u_*) - \frac{\mathcal{R}_0^{-1}}{1-u_*}],$$

$$\frac{1}{S(T_{\text{start}}) - \mathcal{R}_0^{-1}}[\frac{\mathcal{R}_0^{-1}}{1-u_*} - \mathcal{R}_0^{-1}] = \frac{d\tilde{S}(k,u_*)}{dk}\frac{1}{\tilde{S}(k,u_*)}[\tilde{S}(k,u_*) - \frac{\mathcal{R}_0^{-1}}{1-u_*}],$$

$$\frac{d\tilde{S}(k,u_*)}{dk} = \frac{[\frac{\mathcal{R}_0^{-1}}{1-u_*} - \mathcal{R}_0^{-1}]\tilde{S}(k,u_*)}{[S(T_{\text{start}}) - \mathcal{R}_0^{-1}][\tilde{S}(k,u_*) - \frac{\mathcal{R}_0^{-1}}{1-u_*}]} < 0 \tag{5.20}$$

by using the fact that $\tilde{S}(k,u_*) < \frac{\mathcal{R}_0^{-1}}{1-u_*}$ (see the proof of Theorem 5.4.1). And this completes the proof of the Case 1.

Next we consider Case 2 of Theorem 5.4.1 and assume that $\tilde{S}(k,u_*) < \mathcal{R}_0^{-1}$. Similarly as in the first part, Differentiation the first equation of (5.15) w.r.t k and simple algebraic manipulation give

$$\frac{dS(T_{\text{start}})}{dT_{\text{start}}}\frac{dT_{\text{start}}}{dk} = \frac{-S(T_{\text{start}})}{S(T_{\text{start}}) - \mathcal{R}_0^{-1}}. \tag{5.21}$$

From the second equation of (5.15) and using (5.21) we get

$$\frac{\frac{\mathcal{R}_0^{-1}}{1-u_*} - \mathcal{R}_0^{-1}}{S(T_{\text{start}}) - \mathcal{R}_0^{-1}} = \frac{dI(T_{\text{end}})}{dT_{\text{end}}}\frac{dT_{\text{end}}}{dk}. \tag{5.22}$$

From the third equation of (5.15) and using (5.22) we obtain

$$\frac{d\tilde{S}(k,u_*)}{dk} = \frac{\tilde{S}(k,u_*)[\frac{\mathcal{R}_0^{-1}}{1-u_*} - \mathcal{R}_0^{-1}]}{[S(T_{\text{start}}) - \mathcal{R}_0^{-1}][\tilde{S}(k,u_*) - \mathcal{R}_0^{-1}]} < 0. \tag{5.23}$$

From (5.23) and (5.20), in both cases $d(1-\tilde{S}(k,u_*))/dk > 0$. □

Lemma 5.5.2. *Let $k \in [I_0, I_{\max}]$ be a fixed threshold level. Then the final epidemic size $(1 - \tilde{S}(k, u_*))$ of ITHIR-strategy of NPIs is decreasing in control intensity u_*.*

Proof. First, we assume that $\tilde{S}(k, u_*) \geq \mathcal{R}_0^{-1}$, and hence we use System (5.14) and differentiate the second equation of it w.r.t. u_*, we obtain

$$\frac{-\mathcal{R}_0^{-1}}{(1-u_*)^2} \log S(T_{\text{start}}) = \frac{d\tilde{S}(k, u_*)}{du_*} - \frac{\mathcal{R}_0^{-1}}{(1-u_*)} \frac{\frac{d\tilde{S}(k,u_*)}{du_*}}{\tilde{S}(k, u_*)} - \frac{\mathcal{R}_0^{-1}}{(1-u_*)^2} \log \tilde{S}(k, u_*),$$

that is

$$\frac{d\tilde{S}(k, u_*)}{du_*} = \frac{-\mathcal{R}_0^{-1}[\log S(T_{\text{start}}) - \log \tilde{S}(k, u_*)]}{(1-u_*)^2} \frac{\tilde{S}(k, u_*)}{\tilde{S}(k, u_*) - \frac{\mathcal{R}_0^{-1}}{(1-u_*)}} > 0.$$

Similarly, let $\tilde{S}(k, u_*) < \mathcal{R}_0^{-1}$. By differentiation the second and the third equations of system (5.15) w.r.t. u_* and using algebraic manipulation one can show that

$$\frac{d\tilde{S}(k, u_*)}{du_*} = \frac{-\mathcal{R}_0^{-1}[\log S(T_{\text{start}}) - \log \mathcal{R}_0^{-1}]}{(1-u_*)^2} \frac{\tilde{S}(k, u_*)}{\tilde{S}(k, u_*) - \mathcal{R}_0^{-1}} > 0.$$

Thus, in both cases $d(1 - \tilde{S}(k, u_*))/du_* < 0$. □

5.6 Numerical simulation for the ITHIR-strategy of NPIs

Figure 5.6 shows that by increasing k, that is we start NPIs later, the FES increasing, and hence the minimal FES is attained when $k \to I_0$, meaning that for a fixed u_* the optimal strategy to minimize the FES is to start NPIs as early as possible.

Moreover, herd immunity against seasonal influenza will be reached if this proportion $1 - \mathcal{R}_0^{-1} = 0.219531 = HIT$ (herd immunity threshold) of the population are recovered from the disease (see the turning points of the curves in Figure 5.6). We can see that in the case of the solid red curve ($u_* = 0.1$) herd immunity is reached for any k because $1 - \tilde{S}(k, 0.1) > HIT$). However, the other curves show that in lower levels of k (to the left of the turning points) herd immunity will never be reached. The strategies at the turns give the minimal FES such that the herd immunity is reached. We will discuss later if there is a risk if the strategy is accidentally changed to be in the case of herd immunity will never be reached.

Furthermore, we can see that the delay in initiating the intervention strategy implies to a larger control intensity is needed to get a similar magnitude of the FES (see how the turns shift to the right), that is, if we start intervention later, then a larger u_* is

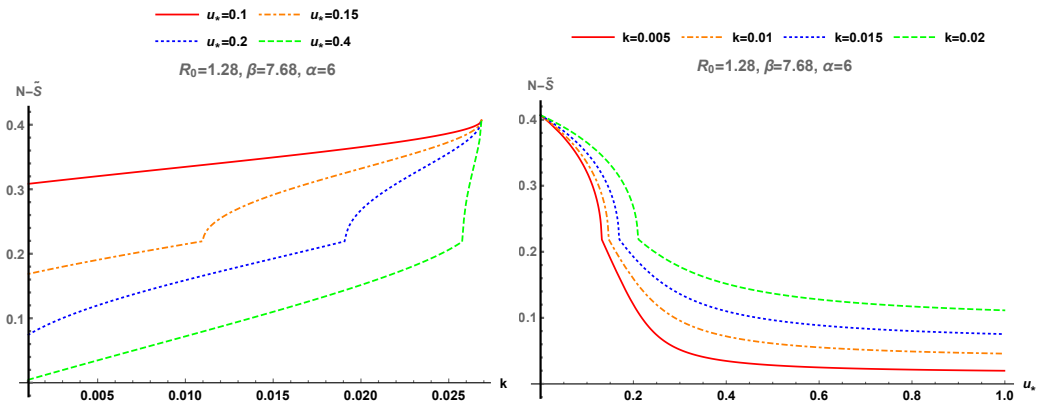

Figure 5.6: Final epidemic size of *ITHIR*-strategy of NPIs as a function of threshold level k (left) for four different values of control intensity u_* and as a function of control intensity u_* (right) for four different threshold levels. The final epidemic size without any intervention (with $N = 1$) is $1 - S_\infty = 0.406805$. Parameters are $\mathcal{R}_0 = 1.28$, $1/\alpha = 1/6$ month, $\beta = 8.4$, $I_{\max} = 0.0268647$, $1 - \mathcal{R}_0^{-1} = 0.219531$.

required to get the same FES (0.219531) of the population. In addition, we can observe that $\tilde{I}(k, u_*) \to 1 - S_\infty = 0.406805$ as $k \to I_{\max} = 0.0268647$.

Next we will see how the final epidemic size of *ITHIR*-strategy depends on the control intensity u_*. Figure 5.6 shows that the FES of NPIs is decreasing in u_* and the minimal FES of NPIs is attained when $u_* \to 1$, meaning that the optimal strategy to minimize the FES is to impose NPIs as strict as possible. The FES equals the herd immunity threshold at the turns. We may ask here whether there is a risk if our plan was to apply a strategy at one of the turns but accidentally u_* has turned out to be stronger, leading to a situation where herd immunity will never be reached? In fact, the risk could be here from an economic point of view if we continue by the same control intensity. However, carefully relaxing the measures to come back to the prescribed strategy may offer a solution to this situation. We also observe that for various k-s the FES curves do not intersect each other and they are placed in order, meaning that to minimize FES we start NPIs as early as possible besides as high rate as possible.

Figure 5.7 depicts the dependence of the final epidemic size on the threshold level k and the control intensity u_* together, where the plot is a heatmap. From this figure, we can see that the FES is increasing in k while decreasing in u_*, and the global minimum of the FES is attained by applying $(k, u_*) \to (I_0, 1)$-strategy. The green solid curve represents $(k, \eta(k))$-strategies, the boundary between Case (1) and Case (2) of Theorem 5.4.1. The herd immunity will never be reached in the population if the applied (k, u_*)-strategies are in the region above the green curve, on contrast, in the other region below the green curve. Handel found that the best control strategy is the strategy that achieves

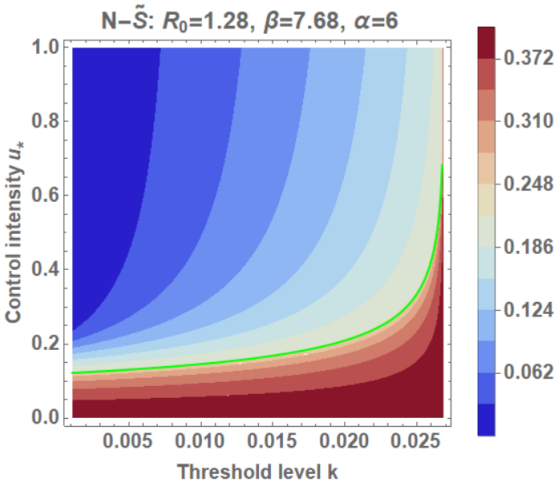

Figure 5.7: **Dependence of the final epidemic size on (k, u_*)-strategies**. The final epidemic size on the green curve (with $N = 1$) is $1-\tilde{S}(k, \eta(k)) = 1-\mathcal{R}_0^{-1} = 0.219531$. Herd immunity will never be reached in the region above the green curve. The final epidemic size without any interventions (with $N = 1$) is $1 - S_\infty = 0.406805$. Parameters are $\mathcal{R}_0 = 1.28$, $1/\alpha = 1/6$ month, $\beta = 8.4$, which are the parameters of seasonal influenza.

this condition $(\tilde{S}(k, u_*), I_\infty) \to (\mathcal{R}_0^{-1}, 0)$ (see [17]). According to our finding this occurs at the combination of (k, u_*) represented by the green solid curve and determined by the formula (5.16).

Depending on the available resources and public health capacities, there may be constraints on the parameters, such as $k_{\min} \leq k \leq I_{\max}$ and also $0 < u_* \leq u_{\max}$ in the region where the herd immunity can be reached. Then the optimal strategy that minimizes FES of NPIs in this restricted domain is $(k_{\min}, u_{\max})$.

Let us emphasize that the same magnitude of the final epidemic size exists along the curves, which are level sets the final epidemic size and are represented by the values on the scale beside the plot (see Figure 5.7). These curves indicate that any delay in starting the NPIs leads to more control intensity is needed to get the same magnitude of the final epidemic size.

5.7 Treatment and isolation strategies (TISs) for epidemic outbreak

Antiviral drugs of seasonal influenza may be a treatment option. In addition, antiviral drugs can lessen symptoms and shorten the duration of the infection by 1 or 2 days [8]. Besides, isolating infected individuals is another option to reduce the period of infection.

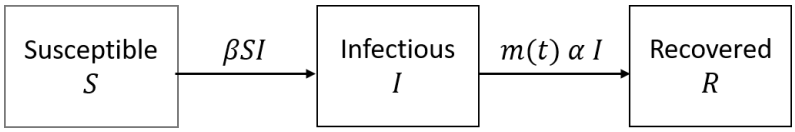

Figure 5.8: **Scheme of Susceptible-Infectious-Recovered (SIR) Model of treatment and isolation strategies.** Boxes represent compartments and arcs represent flux between compartments.

In this section, we investigate the effectiveness of treating and isolating the infected in preventing or containing the epidemic in terms of the final size of the epidemic. Our goal is to construct the final size system for the treatment and isolation strategies (TISs) and then find the optimal strategy that minimizes the final epidemic size of this type of intervention.

Modelling framework

To understand the following discussion, the reader is referred to Figure 5.8. We consider a constant population divided into susceptible ($S(t)$), infected ($I(t)$), and removed ($R(t)$) compartments. New infections occur with transmission coefficient β. Although in the classical SIR model, infected individuals recover with rate α, here we assume that the recovery rate depends on the number of infected individuals and the number of susceptible individuals: If the number of infecteds reaches a threshold level k, then in this section we assume that the authorities adopt a therapeutic protocol to treat the infecteds, and impose isolation on the infected individuals to shorten the infectious period, and thereby α^{-1} is reduced to $(m_*\alpha)^{-1}$, where $m_* > 1$. If the number of susceptibles drops below a critical level such that the herd immunity is reached in the community, then the interventions are relaxed and the recovery rate is α. Hence we consider the following system of differential equations:

$$\begin{aligned} S'(t) &= -\beta S(t)I(t), \\ I'(t) &= \beta S(t)I(t) - m(t)\alpha I(t), \\ R'(t) &= m(t)\alpha I(t), \end{aligned} \tag{5.24}$$

where

$$m(t) = \begin{cases} 1, & t \notin J, \\ m_*, & t \in J, \end{cases}$$

$m_* > 1$, and and J is the intervention interval $J = [T_{\text{start}}, T_{\text{end}}]$ with

$$T_{\text{start}} = \min\{t \geq 0 : I(t) \geq k\} \quad \text{and} \quad T_{\text{end}} = \min\{t \geq 0 : \beta S(t) - \alpha \leq 0\}.$$

5.8 The final size system for the ITHIR-strategy of TISs

We only consider the following first two equations of (5.24) as they are independent of the third one of (5.24):

$$\begin{aligned} S'(t) = & -\beta S(t)I(t), \\ I'(t) = & \beta S(t)I(t) - m(t)\alpha I(t). \end{aligned} \tag{5.25}$$

Let (Sys_{TI}) denote (5.25). Note that (Sys_{TI}) consists of the following two systems: First, the free system (Sys_{free}) from any interventions, which is given in (5.2). Second, the control system of *ITHIR*-strategy of treatment and isolation interventions (denoted by Sys_{TI})

$$\begin{aligned} S'(t) = & -\beta S(t)I(t), \\ I'(t) = & \beta S(t)I(t) - m_*\alpha I(t). \end{aligned} \tag{5.26}$$

Let us emphasize that these are 2-dimensional systems consisting of the S- and I-equations of a basic SIR model. The recovery rate is α for (Sys_{free}), and it is $m_*\alpha$ for (Sys_{TIc}). Hence we take the following observation without proof:

Proposition 5.8.1.

$$\Phi_4(t) = I(t) + S(t) - \frac{m_*\alpha}{\beta}\log S(t) = 1 - \frac{m_*\alpha}{\beta}\log S_0. \tag{5.27}$$

is an invariant of System 5.26.

Let $\tilde{S}(k, m_*) \coloneqq \lim_{t\to\infty} S(t)$ when (k, m_*) of *ITHIR*-strategy applied, the proportion of the susceptible population in the community who had never been infected during an outbreak and *ITHIR*-strategy implementation of (k, m_*)-type. The final epidemic size of *ITHIR*-strategy of (k, m_*)-type (with $N = 1$) is

$$\tilde{I}(k, m_*) := 1 - \tilde{S}(k, m_*) = \int_0^\infty \beta S(t)I(t)dt = m_*\alpha \int_0^\infty I(t)dt. \tag{5.28}$$

Now we are ready to construct the final size system for *ITHIR*-strategy of (k, m_*)-type in a similar way to the final size system 5.4.1.

Theorem 5.8.1. *If $k \in [I_0, I_{\max}]$, then we distinguish two cases: Case 1: If $\tilde{S}(k, m_*) \geq \mathcal{R}_0^{-1}$, then the final size system for ITHIR-strategy of treatment and isolation interventions is*

$$\begin{aligned} k + S(T_{\text{start}}) - \mathcal{R}_0^{-1}\log S(T_{\text{start}}) &= 1 - \mathcal{R}_0^{-1}\log S_0, \\ k + S(T_{\text{start}}) - m_*\mathcal{R}_0^{-1}\log S(T_{\text{start}}) &= \tilde{S}(k, m_*) - m_*\mathcal{R}_0^{-1}\log \tilde{S}(k, m_*). \end{aligned} \tag{5.29}$$

Case 2: If $\tilde{S}(k, m_*) < \mathcal{R}_0^{-1}$, then the final size system for ITHIR-strategy of treatment and isolation strategies is

$$\begin{aligned} k + S(T_{\text{start}}) - \mathcal{R}_0^{-1} \log S(T_{\text{start}}) &= 1 - \mathcal{R}_0^{-1} \log S_0, \\ k + S(T_{\text{start}}) - m_* \mathcal{R}_0^{-1} \log S(T_{\text{start}}) &= I(T_{\text{end}}) + \mathcal{R}_0^{-1} - m_* \mathcal{R}_0^{-1} \log \mathcal{R}_0^{-1}, \\ I(T_{\text{end}}) + \mathcal{R}_0^{-1} - \mathcal{R}_0^{-1} \log \mathcal{R}_0^{-1} &= \tilde{S}(k, m_*) - \mathcal{R}_0^{-1} \log \tilde{S}(k, m_*). \end{aligned} \tag{5.30}$$

One can proof this theorem in a similar way to Theorem 5.4.1. So, the proof is left to the reader.

Next we give a condition that determines whether we are in Case 1) or case 2) of the previous theorem.

Proposition 5.8.2. *Let $k \in [I_0, I_{\max}]$ be a given threshold level. If $\mathcal{R}_0^{-1} \leq \tilde{S}(k, m_*) < S(T_{\text{start}})$ then $m_* \geq \nu(k)$ where*

$$\nu(k) := \frac{\mathcal{R}_0^{-1} - k - S(T_{\text{start}})}{\mathcal{R}_0^{-1} \log(\frac{\mathcal{R}_0^{-1}}{S(T_{\text{start}})})}.$$

It is not difficult to prove Proposition 5.8.2 by the similar way of proving Proposition 5.4.2.

Clearly, as consequence of Proposition 5.8.2 the values of the treatment and isolation rate m_* where we can stop *ITHIR*-strategy of (k, m_*)-type is

$$1 < m_* < \frac{\mathcal{R}_0^{-1} - k - S(T_{\text{start}})}{\mathcal{R}_0^{-1} \log(\frac{\mathcal{R}_0^{-1}}{S(T_{\text{start}})})}. \tag{5.31}$$

5.9 Dependence of FES of *ITHIR*-strategy on (k, m_*)

Lemma 5.9.1. *Let $m_* > 1$ be a fixed treatment and isolation rate. Then the final epidemic size $\tilde{I}(k, m_*)$ is increasing in the threshold value k.*

The proof of this lemma is similar to that of Lemma 5.5.1.

Lemma 5.9.2. *Let $k \in [I_0, I_{\max}]$ be a fixed threshold level. Then the final epidemic size $\tilde{I}(k, m_*)$ is decreasing in the treatment rate m_*.*

The proof is similar to that of Lemma 5.5.2

5.10 Numerical simulation for *ITHIR*-strategy of TIIs and conclusions

We systemically investigate the dependence of the final epidemic size on the threshold level k and the treatment and isolation rate m_*. We found the same observations of

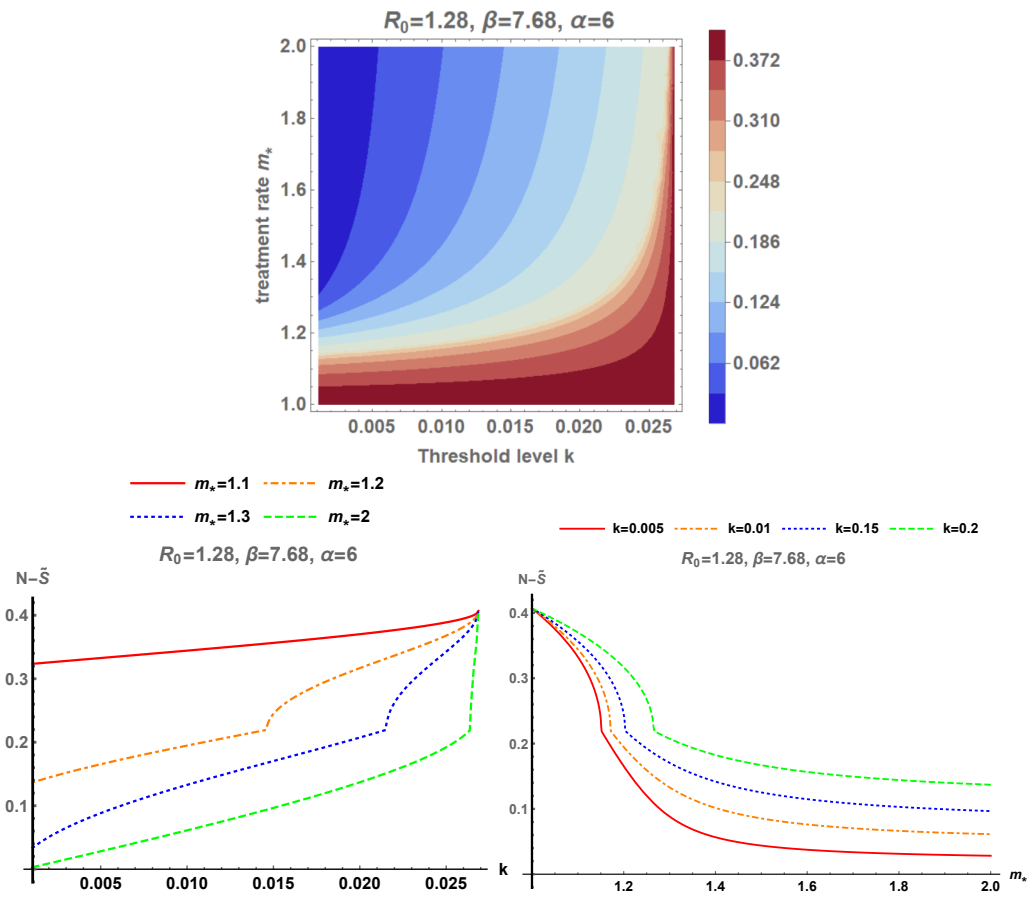

Figure 5.9: Dependence of the final epidemic size on (k, m_*) (top). The FES of *ITHIR*-strategy of (k, m_*)-type as a function of k (left bottom) and as a function of m_* (right bottom). The final epidemic size without any intervention (with $N = 1$) is $1 - S_\infty = 0.406805$. Parameters are $\mathcal{R}_0 = 1.28$, $1/\alpha = 1/6$ month, $\beta = 8.4$.

ITHIR-strategy of (k, u_*)-type. Briefly, from Figure 5.9 the FES of *ITHIR*-strategy on (k, m_*) is increasing in k while is decreasing in m_*, meaning that the global minimum of the FES is attained when we start treatment and isolation as early as possible as high rate as possible.

We have proposed and analyzed a family of temporary intervention strategies in terms of final epidemic size and its dependence on the intervention parameters. For simplicity, our analysis depends on the SIR framework. We have constructed the final size system for *VUHIA*-strategy of (k, p)-type, *ITHIR*-strategy of (k, u_*)-type, and *ITHIR*-strategy of (k, m_*)-type, where k is the threshold level, p is the vaccination rate, u_* is the control intensity in the reduction of transmission, and m_* is the treatment and isolation rate. We have showed that the final epidemic size is increasing in k while decreasing in p,u_*, and m_*. We also systematically investigated the dependence of the final epidemic size on

the parameters of seasonal influenza. We found that the optimal strategy to minimize the final epidemic size is to start the intervention as early as possible as high rate as possible.

It is well known that vaccination is the most cost-effective preventive measure against many infectious disease. In fact, we here also emphasize that our results demonstrate that *VUHIA*-strategy of (k, p)-type is the most successful from minimizing the finial epidemic size point of view in addition to cost-effectiveness, where herd immunity can be achieved for all (k, p)-strategies on the contrary to a big part of (k, u_*) and (k, m_*) strategies.

6

Periodic orbits and global stability for a discontinuous SIR model with delayed control

We propose and analyse a mathematical model for infectious disease dynamics with a discontinuous control function, where the control is activated with some time lag after the density of the infected population reaches a threshold. The model is mathematically formulated as a delayed relay system, and the dynamics is determined by the switching between two vector fields (the so-called free and control systems) with a time delay with respect to a switching manifold. First we establish the usual threshold dynamics: when the basic reproduction number $\mathcal{R}_0 \leq 1$, then the disease is eradicated, while for $\mathcal{R}_0 > 1$ the disease persists in the population. Then, for $\mathcal{R}_0 > 1$, we divide the parameter domain into three regions, and prove results about the global dynamics of the switching system for each case: we find conditions for the global convergence to the endemic equilibrium of the free system, for the global convergence to the endemic equilibrium of the control system, and for the existence of periodic solutions that oscillate between the two sides of the switching manifold. The proof of the latter result is based on the construction of a suitable return map on a subset of the infinite dimensional phase space. Our results provide insight into disease management, by exploring the effect of the interplay of the control efficacy, the triggering threshold and the delay in implementation.

6.1 Model description

The population N is divided into three compartments: susceptible (S), infected (I) and recovered (R). All individuals are born susceptible, and the birth rate is $\mu > 0$ for each compartment. The death rate is also μ for each class, and hence the total population

$N = S + I + R$ is constant, which we normalize to unity, $N = 1$. Although in classical SIR models with mass action incidence, the new infections occur with some constant transmission coefficient $\beta > 0$, here we assume that the transmission coefficient depends on the number of infected individuals: If the density of infected individuals reaches a threshold level $k \in (0, 1)$, then the society implements certain control measures, and thereby the transmission rate is reduced from β to $(1 - u_*)\beta$ with $u_* \in (0, 1)$. The constant u_* represents the efforts and the efficacy of the control measures. It is reasonable to assume that this reduction takes place with a time delay $\tau > 0$. If the density of the infected individuals becomes less than k, then the control measures are stopped, again with delay $\tau > 0$. Infected individuals recover with rate $\gamma > 0$, and full lifelong immunity is assumed upon recovery. With these assumptions above, we obtain the following SIR model with delay:

$$\begin{aligned} \frac{dS(t)}{dt} &= \mu - \mu S(t) - [1 - u(I(t-\tau))]\beta S(t)I(t), \\ \frac{dI(t)}{dt} &= [1 - u(I(t-\tau))]\beta S(t)I(t) - \gamma I(t) - \mu I(t), \\ \frac{dR(t)}{dt} &= \gamma I(t) - \mu R(t), \end{aligned} \tag{6.1}$$

where

$$u(I) = \begin{cases} 0 & \text{if } I < k, \\ u_* & \text{if } I \geq k, \end{cases} \tag{6.2}$$

$k \in (0, 1)$ and $u_* \in (0, 1)$.

In the special case $\tau = 0$ we obtain a model studied in [49].

A dynamical system is called a delayed relay system [40], if it is governed by a differential equation of the form

$$\frac{dx(t)}{dt} = \begin{cases} f^1(x(t)) & \text{if } g(x(t-\tau)) < 0, \\ f^2(x(t)) & \text{if } g(x(t-\tau)) \geq 0, \end{cases}$$

where $\tau > 0$, and f^1, f^2 are Lipschitz continuous. The switching function g is typically a piecewise smooth Lipschitz continuous function. The set $\{x : g(x) = 0\}$ is called the switching manifold.

Let (Sys_d) denote the system consisting of the first two equations of (6.1). We consider only these two equations as they are independent of the third one in (6.1). Note that (Sys_d) is a delayed relay system with $x = (S, I)$,

$$\begin{aligned} f^1(S, I) &= \begin{pmatrix} f_1^1(S, I) \\ f_2^1(S, I) \end{pmatrix}^T = \begin{pmatrix} \mu - \mu S - \beta SI \\ \beta SI - \gamma I - \mu I \end{pmatrix}^T, \\ f^2(S, I) &= \begin{pmatrix} f_1^2(S, I) \\ f_2^2(S, I) \end{pmatrix}^T = \begin{pmatrix} \mu - \mu S - (1 - u_*)\beta SI \\ (1 - u_*)\beta SI - \gamma I - \mu I \end{pmatrix}^T \end{aligned} \tag{6.3}$$

and $g(S,I) = I - k$. Now the switching manifold is the set $\{(S,I) : I = k\}$.

Hereinafter (Sys_f) denotes the free system

$$(S'(t), I'(t)) = f^1(S(t), I(t)),$$

and (Sys_c) is for the control system

$$(S'(t), I'(t)) = f^2(S(t), I(t)).$$

Let us emphasize that these are 2-dimensional systems consisting of the S- and I-equations of a classical ordinary SIR model. The transmission rate is β for (Sys_f), and it is $(1-u_*)\beta$ for (Sys_c).

As it is well-known, the set

$$\Delta = \{(S,I) \in [0,1]^2 : \quad S + I \leq 1\} \tag{6.4}$$

is positively invariant for both (Sys_f) and (Sys_c). For all $(S_0, I_0) \in \Delta$ and for both $* \in \{f, c\}$, let

$$(S_*, I_*) = (S_*(\cdot; S_0, I_0), I_*(\cdot; S_0, I_0))$$

denote the solution of (Sys_*) with

$$S_*(0) = S_*(0; S_0, I_0) = S_0 \qquad \text{and} \qquad I_*(0) = I_*(0; S_0, I_0) = I_0.$$

Solution (S_*, I_*) exists on the positive real line. It is also important that if $I_0 = 0$, then $I_*(t) = 0$ for all $t \geq 0$. Condition $I_0 > 0$ guarantees that I_* remains positive on the positive real line. In other words,

$$\Delta_1 = \{(S,I) \in \Delta : I > 0\} \tag{6.5}$$

is positively invariant w.r.t. both (Sys_f) and (Sys_c).

Because of the delay τ, the phase space for (Sys_d) has to be chosen as

$$X = \{(S_0, \varphi) \in [0,1] \times C([-\tau, 0], [0,1]) : S_0 + \varphi(0) \leq 1\}.$$

Given any $(S_0, \varphi) \in X$, the solution $(S,I) = (S(\cdot; S_0, \varphi), I(\cdot; S_0, \varphi))$ of (Sys_d) is a pair of real functions with the following properties: S is defined and continuous on $[0, \infty)$ with $S(0) = S_0$, I is defined and continuous on $[-\tau, \infty)$ with $I|_{[-\tau,0]} = \varphi$, furthermore, (S,I) satisfies the integral equation system

$$\begin{aligned} S(t) =& S_0 + \int_0^t \{\mu - \mu S(\xi) - [1 - u(I(\xi - \tau))]\beta S(\xi) I(\xi)\} \, \mathrm{d}\xi, \\ I(t) =& \varphi(0) + \int_0^t \{[1 - u(I(\xi - \tau))]\beta S(\xi) I(\xi) - \gamma I(\xi) - \mu I(\xi)\} \, \mathrm{d}\xi \end{aligned}$$

for all $t > 0$.

It is obvious that the solutions of (Sys_d) are absolutely continuous, and the first two equations in (6.1) are satisfied almost everywhere. Throughout this chapter $S'(t)$ and $I'(t)$ will mean the right-hand derivative when $I(t-\tau) = k$; this will not cause any confusion.

For all $t \geq 0$, let I_t denote the element of $C([-\tau, 0], [0, 1])$ defined by $I_t(\xi) = I(t+\xi)$, $\xi \in [-\tau, 0]$.

Consider the following subset of X:

$$X_0 = \{(S_0, \varphi) \in X : [-\tau, 0] \ni t \mapsto \varphi(t) - k \in \mathbb{R} \text{ has a finite number of sign changes}\}.$$

In this chapter we only study solutions with initial data in X_0. A further subset of X is

$$X_1 = \{(S_0, \varphi) \in X_0 : \varphi(0) > 0\},$$

the collection of endemic states, when the disease is present in the population. We will show in Section 6.3 that both X_0 and X_1 are positively invariant for (Sys_d).

6.2 Equilibria

In case of the free system (Sys_f), the basic reproduction number is

$$\mathcal{R}_0 = \frac{\beta}{\gamma + \mu}.$$

The reproduction number of the control system (Sys_c), what we call control reproduction number, is given by

$$\mathcal{R}_{u_*} = \frac{(1-u_*)\beta}{\gamma + \mu} = (1-u_*)\mathcal{R}_0.$$

Next we recall the equilibria and their stability properties for the ordinary systems (Sys_f) and (Sys_c).

The disease-free equilibrium for both (Sys_f) and (Sys_c) is

$$E_0^* = (S_0^*, I_0^*) \in \Delta, \qquad \text{where} \quad S_0^* = 1 \text{ and } I_0^* = 0.$$

The endemic equilibrium for (Sys_f) is

$$E_1^* = (S_1^*, I_1^*) \in \Delta, \qquad \text{where} \quad S_1^* = \frac{1}{\mathcal{R}_0} \text{ and } I_1^* = \frac{\mu}{\beta}(\mathcal{R}_0 - 1).$$

It exists only if $\mathcal{R}_0 > 1$.

It is known (see [23]) that E_0^* is globally asymptotically stable w.r.t the free system (Sys_f) if $\mathcal{R}_0 \leq 1$, and it is unstable if $\mathcal{R}_0 > 1$. The endemic state E_1^* is asymptotically stable w.r.t (Sys_f) if $\mathcal{R}_0 > 1$, and its region of attraction is Δ_1.

The endemic equilibrium for (Sys_c) is

$$E_2^* = (S_2^*, I_2^*) \in \Delta, \quad \text{where} \quad S_2^* = \frac{1}{\mathcal{R}_{u_*}} \text{ and } I_2^* = \frac{\mu}{(1-u_*)\beta}(\mathcal{R}_{u_*} - 1).$$

It exists for $\mathcal{R}_{u_*} > 1$.

E_2^* is asymptotically stable w.r.t (Sys_c) and attracts Δ_1 if $\mathcal{R}_{u_*} > 1$. The disease free equilibrium E_0^* is globally asymptotically stable w.r.t (Sys_c) if $\mathcal{R}_{u_*} \leq 1$, and it is unstable if $\mathcal{R}_{u_*} > 1$.

Next we examine what are the equilibria for (Sys_d).

For all $I^* \in [0,1]$, let I^* also denote the constant function in $C([-\tau, 0], [0,1])$ with value I^*. This will not cause any confusion but ease the notation. If we write $(S^*, I^*) \in \Delta$, then I^* is considered to be a real number in $[0,1]$. Notation $(S^*, I^*) \in X_0$ means that I^* is an element of $C([-\tau, 0], [0,1])$. In accordance, we may consider E_0^*, E_1^* and E_2^* as elements of X_0.

$(S^*, I^*) \in X_0$ is an equilibrium for (Sys_d) if and only if $(S^*, I^*) \in \Delta$ satisfies the algebraic equation system

$$\begin{aligned} 0 &= \mu - \mu S^* - [1 - u(I^*)]\beta S^* I^*, \\ 0 &= [1 - u(I^*)]\beta S^* I^* - \gamma I^* - \mu I^*. \end{aligned} \tag{6.6}$$

As above, we call an equilibrium (S^*, I^*) disease-free if $I^* = 0$, and endemic if $I^* > 0$.

By calculating the solutions of (6.6), we obtain the following result.

Proposition 6.2.1.
The unique disease-free equilibrium for the delayed relay system (Sys_d) is $E_0^* \in X_0$, and it exists for all choices of parameters.
If $\mathcal{R}_0 \leq 1$, then there is no endemic equilibrium for (Sys_d). If $\mathcal{R}_0 > 1$, then we distinguish three cases.
(a) If

$$\mathcal{R}_0 > 1 \quad \textit{and} \quad \mathcal{R}_0[\mu - (\mu + \gamma)k] < \mu, \tag{C.1}$$

then $E_1^* \in X_0$ is the unique endemic equilibrium for (Sys_d).
(b) If

$$\mu \leq \mathcal{R}_0[\mu - (\mu + \gamma)k] < \mu/(1 - u_*), \tag{C.2}$$

then there is no endemic equilibrium for (Sys_d).
(c) If

$$\mathcal{R}_0[\mu - (\mu+\gamma)k] \geq \mu/(1-u_*), \tag{C.3}$$

then $E_2^* \in X_0$ *is the unique endemic equilibrium.*

Note that if either (C.2) or (C.3) holds, then necessarily $\mathcal{R}_0 > 1$. In addition, conditions (C.1), (C.2) and (C.3) together cover the case $\mathcal{R}_0 > 1$.

Proof. It is easy to see that $(S^*, 0)$ satisfies (6.6) if and only if $S^* = S_0^* = 1$. Moreover, $(S_0^*, I_0^*) = (1, 0)$ is a solution of (6.6) without any restrictions on the parameters. So the first statement of the proposition is true.

We may now assume that $I_* > 0$ and thus $S^* < 1$. Let us divide (6.6) by $(\mu+\gamma)$ and examine the equivalent form

$$\begin{aligned} 0 &= \frac{\mu}{\gamma+\mu}(1-S^*) - [1-u(I^*)]\mathcal{R}_0 S^* I^*, \\ 0 &= [[1-u(I^*)]\mathcal{R}_0 S^* - 1]I^*. \end{aligned}$$

As $I^* \neq 0$, the second equation gives that

$$\mathcal{R}_0[1-u(I^*)]S^* = 1. \tag{6.7}$$

It comes from $S^* < 1$ and the definition of u that (6.7) cannot be satisfied if $\mathcal{R}_0 \leq 1$, so in that case there is no endemic equilibrium.

If $\mathcal{R}_0 > 1$, then we need to distinguish two cases. If $0 < I^* < k$ and hence $u(I_*) = 0$, then one can easily see that $(S^*, I^*) = (S_1^*, I_1^*)$. If $I^* \geq k$ and $u(I_*) = u_*$, then $(S^*, I^*) = (S_2^*, I_2^*)$.

To complete the proof, we need to guarantee that $0 < I_1^* < k$ and $I_2^* \geq k$. Using $\beta = \mathcal{R}_0(\mu+\gamma)$, one can show that inequality

$$0 < I_1^* = \frac{\mu}{\beta}(\mathcal{R}_0 - 1) < k$$

is satisfied if and only if

$$1 < \mathcal{R}_0 \quad \text{and} \quad \mathcal{R}_0[\mu - (\mu+\gamma)k] < \mu.$$

Similarly, $I_2^* \geq k$ is equivalent to

$$\mathcal{R}_0[\mu - (\mu+\gamma)k] \geq \mu/(1-u_*).$$

Statements (a)-(c) of the proposition follow from the calculations above. □

In Fig. 6.1 we divide the (k, u_*) plane into three regions according to Cases (a)-(c) of Proposition 6.2.1 in order to show the interplay between threshold level k and control intensity u_*.

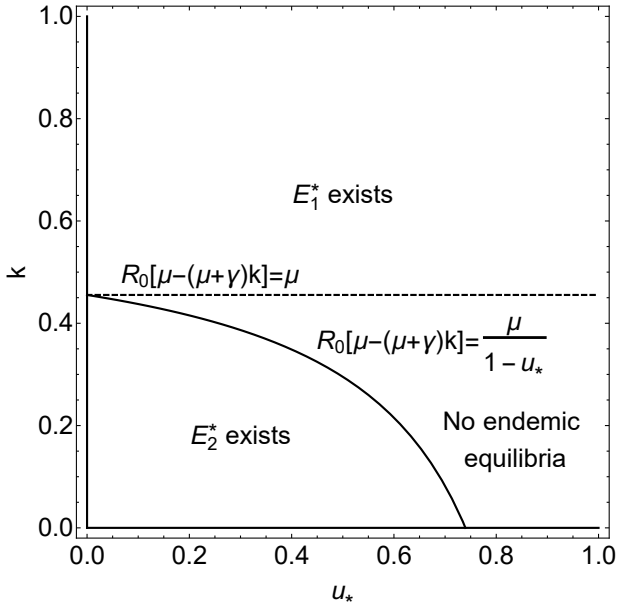

Figure 6.1: A 2-parameter bifurcation diagram giving the endemic equilibria in the (k, u_*) plane for $\mathcal{R}_0 > 1$. The parameters are $\gamma = 0.25$, $\beta = 2.5$ and $\mu = 0.4$.

6.3 Construction of solutions

In this section we show that if $(S_0, \varphi) \in X_0$ ($(S_0, \varphi) \in X_1$), then the solution (S, I) exists, and $(S(t), I_t) \in X_0$ ($(S(t), I_t) \in X_1$) for each $t \geq 0$.

First we need the following result for the ordinary systems (Sys_f) and (Sys_c).

Proposition 6.3.1. *Let $* \in \{f, c\}$. For any $k \in (0, 1)$ and any non-constant solution (S_*, I_*) of (Sys_*), the function*

$$[0, \infty) \ni t \mapsto I_*(t) - k \in \mathbb{R}$$

has a finite number of zeros on each interval of finite length.

Proof. We give a proof for the free system (Sys_f). The proof for (Sys_c) is analogous.

Consider the second equation of (Sys_f):

$$I_f'(t) = \beta S_f(t) I_f(t) - (\gamma + \mu) I_f(t) = (\gamma + \mu)\left(\mathcal{R}_0 S_f(t) - 1\right) I_f(t). \tag{6.8}$$

If $R_0 \leq 1$ and $I_f(t) = k \in (0, 1)$ for some $t \geq 0$, then $S_f(t) \leq 1 - I_f(t) < 1$ and $I_f'(t) < 0$. The statement is clearly true in this case.

Now assume that $R_0 > 1$. Recall from [23] that

$$V(S, I) = S_1^* \left(\frac{S}{S_1^*} - \log \frac{S}{S_1^*} \right) + I_1^* \left(\frac{I}{I_1^*} - \log \frac{I}{I_1^*} \right)$$

is a Lyapunov function for (Sys_f), and $\dot{V}(S,I) < 0$ for all $(S,I) \in \Delta_1 \setminus \{E_1^*\}$. For any $k \in (0,1) \setminus \{I_1^*\}$, consider the nontrivial level set

$$H_k = \left\{ (S,I) \in \Delta_1 : \quad V(S,I) = S_1^* + k - I_1^* \log \frac{k}{I_1^*} \right\},$$

which is a simple closed curve. The property $\dot{V}(S,I) < 0$ guarantees that $int(H_k)$ is positively invariant for (Sys_f), where $int(H_k)$ denotes the interior of H_k.

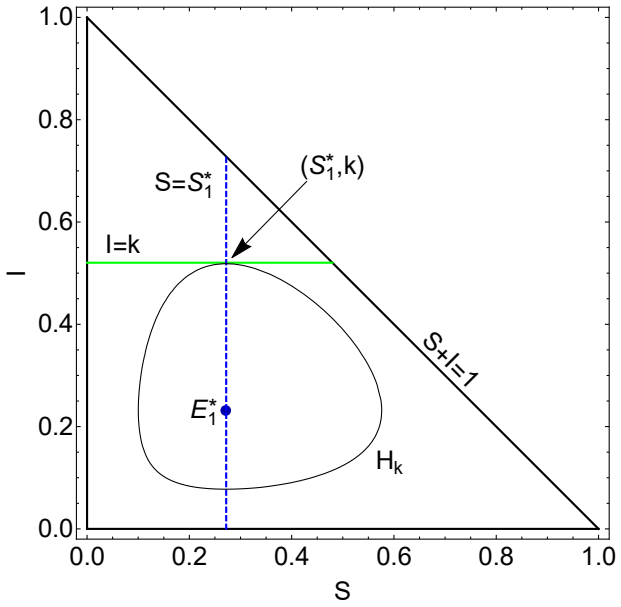

Figure 6.2: The segment $I = k$ and the level set H_k of the Lyapunov function V.

Observe that $(S_1^*, k) \in H_k$. One can easily check that $[0,1] \ni S \mapsto V(S,k) \in \mathbb{R}$ has a strict minimum at $S = S_1^*$, which implies that the segment $I = k$ and H_k have no common point besides (S_1^*, k). The segment $I = k$ is tangential to H_k at (S_1^*, k), see Fig. 6.2.

We also see from (6.8) that if $I_f(t) > 0$ for some $t \in \mathbb{R}$, then

$$I_f'(t) = 0 \quad \text{if and only if} \quad S_f(t) = 1/R_0 = S_1^*, \tag{6.9}$$

and

$$I_f'(t) > 0 \ (I_f'(t) < 0) \quad \text{if and only if} \quad S_f(t) > S_1^* \ (S_f(t) < S_1^*). \tag{6.10}$$

A direct consequence of (6.9) is the following observation for a non-constant solution (S_f, I_f). If there exists $\tilde{t} \geq 0$ such that $I_f\left(\tilde{t}\right) = k$ and $I_f'\left(\tilde{t}\right) = 0$, then $S_f\left(\tilde{t}\right) = S_1^*$ by (6.9). Due to the Lyapunov function, there are no periodic solutions, hence there is no

$t \neq \tilde{t}$ such that $(S_f(t), I_f(t)) = (S_1^*, k)$. This yields, again by (6.9), that if $I_f(t) = k$ for some $t \in [0, \infty) \setminus \{\tilde{t}\}$, then $I_f'(t) \neq 0$.

Now suppose for contradiction that for some $k \in (0, 1)$ and non-constant solution (S_f, I_f), the function $[0, \infty) \ni s \mapsto I_f(s) - k \in \mathbb{R}$ has an infinite number of zeros in a finite closed interval $J \subset [0, \infty)$. Let $B = \{t \in J \colon I_f(t) = k\}$. The compactness of J ensures that B has an accumulation point t_a in J. Necessarily $I_f(t_a) = k$.

Let $\varepsilon > 0$ be arbitrary. Next we show that B has elements $t_1 < t_2 < t_3$ in $(t_a - \varepsilon, t_a + \varepsilon)$ such that

$$I_f'(t_1) < 0, \quad I_f'(t_2) > 0, \quad I_f'(t_3) < 0,$$

$$I_f(t) < k \text{ for } t \in (t_1, t_2) \quad \text{and} \quad I_f(t) > k \text{ for } t \in (t_2, t_3).$$

One can prove this claim as follows. Either $(t_a - \varepsilon, t_a)$ or $(t_a, t_a + \varepsilon)$ contains elements of B arbitrary close to t_a. Suppose $(t_a - \varepsilon, t_a)$ is such an interval. By decreasing ε, we may assume that the point $\tilde{t}$ (if exists) is not in $(t_a - \varepsilon, t_a)$, and hence

$$I_f'(t) \neq 0 \text{ for all } t \in B \cap (t_a - \varepsilon, t_a). \tag{6.11}$$

Choose any $t_1 \in B \cap (t_a - \varepsilon, t_a)$ with $I_f'(t_1) < 0$. It is easy to see that such t_1 exists, otherwise we cannot have several zeros in $(t_a - \varepsilon, t_a)$. Then one can give $\delta_1 > 0$ with $t_1 + \delta_1 < t_a$ such that $I_f(t) < k$ for $t \in (t_1, t_1 + \delta_1)$. As $B \cap (t_1 + \delta_1, t_a)$ is bounded and nonempty (actually it has an infinite number of elements), the infimum $t_2 = \inf\{B \cap (t_1 + \delta_1, t_a)\}$ exists. It is clear that $t_1 < t_2 < t_a$, and $I_f(t_2) = k$ by the continuity of I_f. Observation (6.11) guarantees that $I_f'(t_2) \neq 0$. It comes from the definition of t_2 that $I_f(t) < k$ for $t \in (t_1, t_2)$ and $I_f'(t_2) > 0$. As next step, one can give $\delta_2 > 0$ such that $t_2 + \delta < t_a$ and $I_f(t) > k$ for $t \in (t_2, t_2 + \delta_2)$. Set $t_3 = \inf\{B \cap (t_2 + \delta_2, t_a)\}$. Then t_3 satisfies the properties given in the claim. In the second case, when B has infinite elements in $(t_a, t_a + \varepsilon)$, we can find t_3 first, then t_2 and t_1 in an analogous way.

We claim that $I_f'(t_a) = 0$, and therefore $S_f(t_a) = S_1^*$ (that is, $t_a = \tilde{t}$). Indeed, if $I_f'(t_a)$ is positive (negative), then $I_f'(t)$ is positive (negative) for all $t \in B$ in a small neighbourhood of t_a by the continuous differentiability of I_f. This contradicts our previous claim. So $S_f(t_a) = S_1^*$.

As the solution is non-constant, $(S_f(t_a), I_f(t_a)) = (S_1^*, k) \neq (S_1^*, I_1^*)$, and we conclude that $k \neq I_1^*$. We consider the case $k > I_1^*$. (The case $k < I_1^*$ can be handled in similarly.)

Recall that $(S_f(t_a), I_f(t_a)) = (S_1^*, k)$ is the intersection point of the segment $I = k$ and H_k. We have seen that there exist t_1 and t_2 arbitrary close to t_a such that $I_f(t_1) = I_f(t_2) = k$, $I_f'(t_1) < 0 < I_f'(t_2)$ and $I_f(t) < k$ for $t \in (t_1, t_2)$. Remark (6.10) implies that $S_f(t_1) < S_1^* < S_f(t_2)$. We may also achieve (using the boundedness of S_f' and I_f') that $(S_f(t), I_f(t))$ is arbitrary close to (S_1^*, k) on (t_1, t_2). This gives the existence of

$t_* \in (t_1, t_2)$ with $(S_f(t_*), I_f(t_*)) \in int(H_k)$. The positive invariance of $int(H_k)$ then gives $(S_f(t), I_f(t)) \in int(H_k)$ for all $t \geq t_*$ contradicting $I_f(t_2) = k$.

This means that our initial assumption was wrong, and the proposition is true also in the $R_0 > 1$ case. □

Now we ready to prove the positive invariance of X_0.

Proposition 6.3.2. *If $(S_0, \varphi) \in X_0$, then a unique solution (S, I) exists, and $(S(t), I_t) \in X_0$ for each $t \geq 0$.*

Proof. Set

$$0 = t_0 < t_1 < ... < t_{N-1} < t_N = \tau$$

such that $\varphi(\xi) < k$ on intervals of the form $(-\tau + t_{2n}, -\tau + t_{2n+1})$ and $\varphi(\xi) > k$ on intervals of the form $(-\tau + t_{2n-1}, -\tau + t_{2n})$, where $n \in [0, N/2]$ is an integer. (We omit the case when $\varphi(\xi) > k$ on $(-\tau + t_{2n}, -\tau + t_{2n+1})$ and $\varphi(\xi) < k$ on $(-\tau + t_{2n-1}, -\tau + t_{2n})$ because that can be handled analogously.)

Under the assumptions above, $I(t - \tau) < k$ and $u(I(t - \tau)) = 0$ for $t \in (0, t_1)$. Hence the solution (S, I) of (Sys_d) coincides with a solution of (Sys_f) on $[0, t_1]$:

$$S(t; S_0, \varphi) = S_f(t; S_0, \varphi(0)), \quad I(t; S_0, \varphi) = I_f(t; S_0, \varphi(0))$$

for $t \in [0, t_1]$. Since $I(t - \tau) > k$ and thus $u(I(t - \tau)) = u_*$ for $t \in (t_1, t_2)$, we see that

$$S(t; S_0, \varphi) = S_c(t - t_1; S(t_1), I(t_1)), \quad I(t; S_0, \varphi) = I_c(t - t_1; S(t_1), I(t_1))$$

for $t \in [t_1, t_2]$. Similarly, (S, I) is given by a specific solution of (Sys_f) or (Sys_c) on all intervals of the form $[t_{m-1}, t_m]$, where $m \in \{1, ..., N\}$. Hence the solution exists on $[0, \tau]$.

As the functions $t \mapsto I_f(t) - k$ and $t \mapsto I_c(t) - k$ have finite number of sign changes on intervals of finite length by Proposition 6.3.1, we deduce that $t \mapsto I(t) - k$ also admits a finite number of sign changes on $[0, \tau]$.

Iterating this argument first for $[\tau, 2\tau]$, then for all intervals of the form $[j\tau, (j + 1)\tau]$, $j \geq 2$, we see that the solution exists on the positive real line. The uniqueness of (S, I) comes at once from the uniqueness of solutions for (Sys_f) and (Sys_c). In addition, it is clear that $t \mapsto I(t) - k$ has a finite number of sign changes on intervals of finite length. The way we obtain the solutions of (Sys_d) and the positive invariance of Δ for (Sys_f) and (Sys_c) also imply that $S(t) \in [0, 1]$, $I(t) \in [0, 1]$ and $S(t) + I(t) \leq 1$ for all $t \geq 0$. Summing up, $(S(t), I_t) \in X_0$ for all $t \geq 0$. □

Since the solutions of (Sys_d) with initial data in X_0 are determined by the solutions of (Sys_f) and (Sys_c) as in the previous proof, and as the set $\Delta_1 = \{(S, I) \in \Delta : I > 0\}$ is positively invariant for both (Sys_f) and (Sys_c), we see that X_1 is positively invariant for (Sys_d) too.

6.4 Threshold dynamics: disease extinction and persistence

Theorem 6.4.1. *If $\mathcal{R}_0 \leq 1$, then E_0^* is globally asymptotically stable for the delayed relay system (Sys_d) (that is, E_0^* is asymptotically stable and attracts X_0). If $\mathcal{R}_0 > 1$, then E_0^* is unstable w.r.t. (Sys_d), and the disease uniformly persists in the population.*

Proof. First note that the solutions of (Sys_d) coincide with the solutions of the free system (Sys_f) in a small neighbourhood of E_0^*. Therefore E_0^* is a stable equilibrium for (Sys_d) if and only if it is stable for (Sys_f).

Let $\mathcal{R}_0 \leq 1$. We only need to prove the global attractivity of E_0^* on X_0. Suppose for contradiction that $I(t)$ does not converge to 0 as $t \to \infty$ for some solution (S, I). By the second equation of (Sys_d),

$$\frac{dI(t)}{dt} = (\mu + \gamma) \left\{ [1 - u(I(t - \tau))] \mathcal{R}_0 S(t) - 1 \right\} I(t) \leq 0,$$

that is, I is nonincreasing. As I is nonnegative and does not converge to 0, necessarily there exists a constant $c > 0$ such that $I(t) \geq c$ for all $t \geq 0$ and $I(t) \to c$ as $t \to \infty$. Then $S(t) \leq 1 - c$ and

$$\left\{ [1 - u(I(t - \tau))] \mathcal{R}_0 S(t) - 1 \right\} I(t) \leq -c^2$$

for all $t \geq 0$. It follows that

$$I(T) = I(0) + (\mu + \gamma) \int_0^T \left\{ [1 - u(I(\xi - \tau))] \mathcal{R}_0 S(\xi) - 1 \right\} I(\xi) \mathrm{d}\xi \leq I(0) - (\mu + \gamma) c^2 T,$$

which implies $I(T) < 0$ for all sufficiently large T, a contradiction. So $I(t) \to 0$ as $t \to \infty$.

Next we prove that if $\mathcal{R}_0 \leq 1$, then $S(t) \to 1$ as $t \to \infty$ for all solutions (S, I). It is clear from the previous paragraph that there exists $T(\varepsilon)$ for each $\varepsilon > 0$ such that $I(t) < \varepsilon$ for all $t \geq T(\varepsilon)$. Then for $t \geq T(\varepsilon)$,

$$\frac{dS(t)}{dt} = \mu - \mu S(t) - [1 - u(I(t - \tau))] \beta S(t) I(t) \geq \mu - \mu S(t) - \varepsilon \beta S(t),$$

which implies

$$\liminf_{t \to \infty} S(t) \geq \frac{\mu}{\mu + \varepsilon \beta}.$$

Note that $\varepsilon > 0$ can be arbitrary small. Thereby

$$\liminf_{t \to \infty} S(t) \geq \frac{\mu}{\mu} = 1.$$

We know on the other hand that $S(t) \leq 1$ for all $t \geq 0$. Summing up, $\lim_{t\to\infty} S(t)$ exists and equals one.

We have verified that $S(t) \to 1$ and $I(t) \to 0$ as $t \to \infty$ for every solution (S, I) if $\mathcal{R}_0 \leq 1$.

To show the persistence, let $\mathcal{R}_0 > 1$, and consider a solution with $I(0) > 0$. If there exists arbitrarily large t with $I(t) \geq k$, then $\limsup_{t\to\infty} I(t) \geq k$. Otherwise, there is a t_* such that $I(t) < k$ for all $t > t_*$. In this case, the solution follows (Sys_f) for $t \geq t_* + \tau$:

$$\begin{aligned} S(t) =& S_f(t - t_* - \tau; S(t_* + \tau), I(t_* + \tau)), \\ I(t) =& I_f(t - t_* - \tau; S(t_* + \tau), I(t_* + \tau)), \end{aligned} \qquad t \in [t_* + \tau, \infty).$$

Then $\lim_{t\to\infty} I(t) = I_1^*$. In any case, we can conclude that $\limsup_{t\to\infty} I(t) \geq \min\{k, I_1^*\}$, which means uniform weak persistence. Since the solutions of (Sys_f) and (Sys_c) both have uniformly bounded derivatives on Δ, by the Arzelà-Ascoli theorem our solution operators $\Phi(t) : X_0 \ni (S_0, \varphi) \mapsto (S_t, I_t) \in X_0$ are compact for $t > \tau$, hence the semiflow Φ has a compact attractor in X_0. We can apply Corollary 4.8 from [41] to conclude (strongly) uniform persistence: there exists a $\delta > 0$ such that for all solutions with $I(0) > 0$, $\liminf_{t\to\infty} I(t) \geq \delta$. □

6.5 Case (a): E_1^* is GAS for large k

In this section let $\mathcal{R}_0 > 1$ and $k > k_0$, where $k_0 = 1 - 1/\mathcal{R}_0$. It is easy to see that these conditions imply (C.1). Hence Proposition 6.2.1 gives that E_1^* is the unique endemic equilibrium for (Sys_d) and $I_1^* < k$.

Fig. 6.3 shows the segment $I = k_0$ in Δ.

The main result of this section is the following global stability theorem.

Theorem 6.5.1. *If $\mathcal{R}_0 > 1$ and $k > k_0$, then E_1^* is asymptotically stable with respect to (Sys_d), and it attracts the set X_1.*

The proof is based on the next simple observation.

Proposition 6.5.1. *Assume that $\mathcal{R}_0 > 1$ and $k > k_0$. If $I(t_0) < k$ for some $t_0 \geq 0$, then $I(t) < k$ for all $t \in [t_0, \infty)$.*

Proof. Suppose for contradiction that there exists $t_* > t_0$ such that $I(t) < k$ for $t \in [t_0, t_*)$ and $I(t_*) = k$. Then necessarily $I'(t_*) \geq 0$. On the other hand,

$$S(t_*) \leq 1 - I(t_*) = 1 - k < 1 - k_0 = 1/\mathcal{R}_0,$$

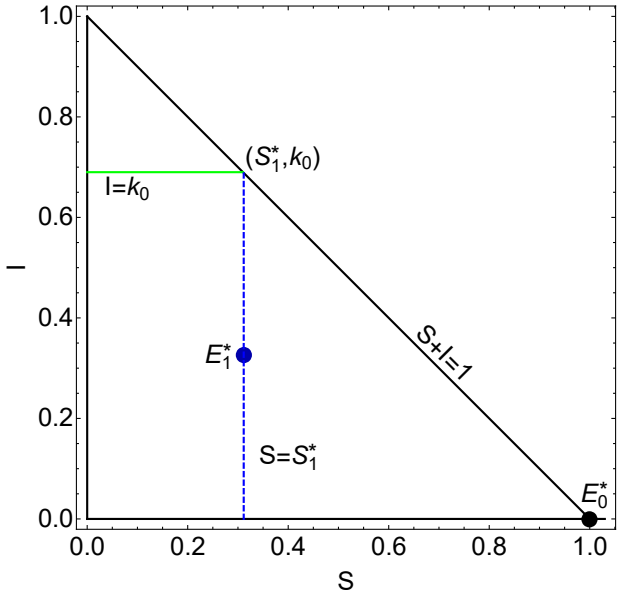

Figure 6.3: The segment $I = k_0$.

and thus

$$\frac{dI(t_*)}{dt} = (\gamma+\mu)[[1-u(I(t_*-\tau))]\mathcal{R}_0 S(t_*) - 1]I(t_*) < 0,$$

independently of the value of $I(t_* - \tau)$. This is a contradiction, so the proposition is true. □

Proof of Theorem 6.5.1. As $I_1^* < k$, the solutions of (Sys_d) coincide with solutions of the free system (Sys_f) in a small neighborhood of E_1^*. Since E_1^* is stable for (Sys_f), this fact implies that E_1^* is a stable equilibrium also for (Sys_d). We only need to prove that the region of attraction is X_1.

Consider an arbitrary solution (S, I) of (Sys_d) with initial data in X_1.

We claim there exists $t_0 \geq 0$ such that $I(t_0) < k$. Indeed, suppose for contradiction that $I(t) \geq k$ for all $t \in [0, \infty)$. Then we have

$$I(t) = I_c(t-\tau; S(\tau), I(\tau)) \quad \text{for } t \in [\tau, \infty).$$

If $\mathcal{R}_{u_*} > 1$, then E_2^* attracts the set $\Delta_1 = \{(S, I) \in \Delta : I > 0\}$ w.r.t. (Sys_c), and hence $I(t) \to I_2^* < k$ as $t \to \infty$. If $\mathcal{R}_{u_*} \leq 1$, then $I(t) \to 0 < k$ as $t \to \infty$ by the global attractivity of E_0^* for (Sys_c). In both cases we obtained a contradiction.

One can now use Proposition 6.5.1 with this t_0 to obtain that $I(t) < k$ for $t \in [t_0, \infty)$. Then (S, I) coincides with the subsequent solution of (Sys_f) on $[t_0 + \tau, \infty)$:

$$\begin{aligned} S(t) &= S_f(t - t_0 - \tau; S(t_0+\tau), I(t_0+\tau)), \\ I(t) &= I_f(t - t_0 - \tau; S(t_0+\tau), I(t_0+\tau)), \end{aligned} \qquad t \in [t_0+\tau, \infty).$$

Recall that E_1^* attracts Δ_1 w.r.t. (Sys_f). Also note that $I(t) > 0$ for all $t \geq 0$ by the positive invariance of X_1. We conclude that $(S(t), I(t)) \to E_1^*$ as $t \to \infty$.

Summing up, E_1^* is asymptotically stable and attracts X_1 w.r.t. (Sys_d). □

6.6 Case (b): Periodic orbits in the absence of endemic equilibria

Recall from Proposition 6.2.1 that (Sys_d) has no endemic equilibria if

$$\mu < \mathcal{R}_0[\mu - (\mu + \gamma)k] < \mu/(1 - u_*). \tag{6.12}$$

In more detail, condition (6.12) implies that the second coordinate I_1^* of E_1^* is greater than k (see the proof of Proposition 6.2.1), and hence E_1^* is not an equilibrium for (Sys_d). If $\mathcal{R}_{u_*} > 1$, then E_2^* exists for (Sys_c), but $I_2^* < k$, and thus E_2^* is not an equilibrium for (Sys_d) either. If $\mathcal{R}_{u_*} \leq 1$, then E_0^* is the unique equilibrium for both (Sys_c) and (Sys_d).

The aim of this section is to show that the absence of endemic equilibria implies the existence of periodic orbits in the $\mathcal{R}_0 > 1$ case – at least for small τ.

Theorem 6.6.1. *If* (6.12) *holds and τ is small enough, then the delayed relay system (Sys_d) has a periodic solution.*

In order to prove this theorem, first we need to recall how the solutions of (Sys_f) and (Sys_c) behave in Δ_1.

If $\mathcal{R}_0 > 1$, i.e., $E_1^* = (S_1^*, I_1^*)$ is an endemic equilibrium for (Sys_f), then the curves $S = S_1^*$ and $(\mu + \beta I)S = \mu$ are the null-isoclines for (Sys_f), see Figure 6.4.(a). Analyzing the vector field, one sees that

$$\begin{aligned}
&S_f'(t) \leq 0 \text{ and } I_f'(t) > 0 \text{ if} \\
&\qquad (S_f(t), I_f(t)) \in A_1 = \{(S, I) \in \Delta_1 : \quad S > S_1^*, (\mu + \beta I)S \geq \mu\}, \\
&S_f'(t) < 0 \text{ and } I_f'(t) \leq 0 \text{ if} \\
&\qquad (S_f(t), I_f(t)) \in A_2 = \{(S, I) \in \Delta_1 : \quad S \leq S_1^*, (\mu + \beta I)S > \mu\}, \\
&S_f'(t) \geq 0 \text{ and } I_f'(t) < 0 \text{ if} \\
&\qquad (S_f(t), I_f(t)) \in A_3 = \{(S, I) \in \Delta_1 : \quad S < S_1^*, (\mu + \beta I)S \leq \mu\}, \\
&S_f'(t) > 0 \text{ and } I_f'(t) \geq 0 \text{ if} \\
&\qquad (S_f(t), I_f(t)) \in A_4 = \{(S, I) \in \Delta_1 : \quad S \geq S_1^*, (\mu + \beta I)S < \mu\}.
\end{aligned}$$

Moreover, the above inequalities are strict in the interior of A_i, $i \in \{1, 2, 3, 4\}$.

It is clear from these observations and the positive invariance of Δ_1 that the solutions of (Sys_f) behave as follows.

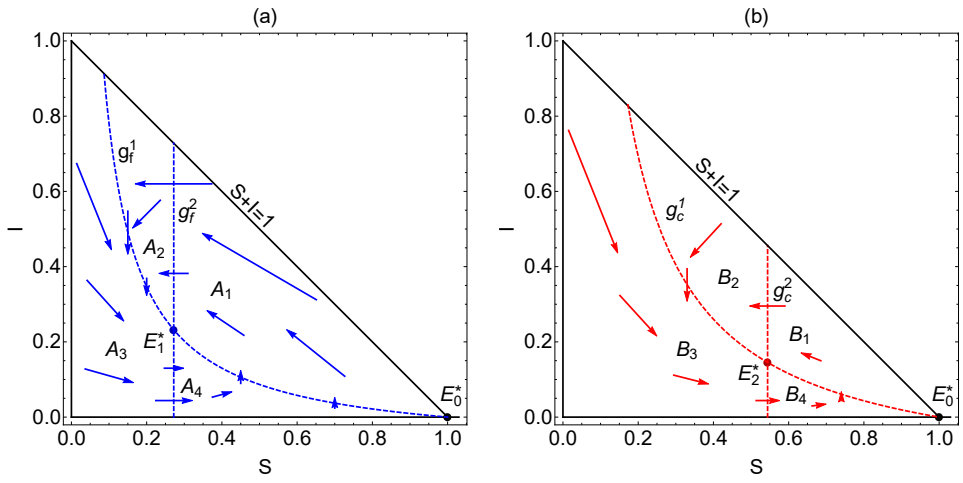

Figure 6.4: The null-isoclines and the vector field for (a): the free system (Sys_f) in case $\mathcal{R}_0 > 1$, (b): the control system (Sys_c) in case $\mathcal{R}_{u_*} > 1$. The isoclinic curves for the free system (Sys_f) are $g_f^1 = \{(S,I) \in \Delta_1 : \mu - \mu S - \beta SI = 0\}$ and $g_f^2 = \{(S,I) \in \Delta_1 : S = S_1^*\}$. The isoclinic curves for the control system (Sys_c) are $g_c^1 = \{(S,I) \in \Delta_1 : \mu - \mu S - (1-u_*)\beta SI = 0\}$ and $g_c^2 = \{(S,I) \in \Delta_1 : S = S_2^*\}$.

Remark 6.6.2. *Let $\mathcal{R}_0 > 1$.*
(i) Assume that $(S_0, I_0) \in A_i$, where $i \in \{1,3\}$. Then either

$$(S_f(t), I_f(t)) = (S_f(t; S_0, I_0), I_f(t; S_0, I_0)) \in A_i \quad \text{for all } t \geq 0$$

(in this case the solution converges to E_1^* in A_i), or there exist $0 < T_1 < T_2$ such that

$$(S_f(t), I_f(t)) \in A_i \quad \text{for } t \in [0, T_1) \tag{6.13}$$

and

$$(S_f(t), I_f(t)) \in A_{i+1} \quad \text{for } t \in [T_1, T_2) \tag{6.14}$$

(that is, the solution leaves A_i through the boundary of A_{i+1}).
(ii) Each solution leaves A_i, $i \in \{2,4\}$, through the boundary of A_{i+1}: If $(S_0, I_0) \in A_i$, where $i \in \{2,4\}$, then there exist $0 < T_1 < T_2$ such that (6.13) and (6.14) hold. Here the index is considered modulo 4, so A_5 stands for A_1.
(iii) Assume that $k < I_1^*$. If $0 < I_f(t_*) < k$ for some t_*, then there exists $t_{**} > t_*$ such that

$$S_f(t_{**}) \in [S_1^*, 1-k] \quad \text{and} \quad I_f(t_{**}) = k.$$

Let us now consider (Sys_c). If $\mathcal{R}_{u_*} > 1$, i.e., if E_2^* is an endemic equilibrium for (Sys_c), then $\Delta_1 \setminus \{E_2^*\}$ can be divided up into four subsets B_1, B_2, B_3, B_4 in an analogous way using the null-isoclines $S = S_2^*$ and $(\mu + (1-u_*)\beta I)S = \mu$, see Fig. 6.4.(b). By analyzing the vector field, we get the subsequent information on the behavior of solutions.

Remark 6.6.3. *If $\mathcal{R}_{u_*} > 1$, then the analogues of Remark 6.6.2.(i) and (ii) hold for the solutions of (Sys_c) with B_i standing instead of A_i, $i \in \{1,2,3,4\}$. In addition, if $k > I_2^*$ and $I_c(t_*) > k$ for some t_*, then there exist $t_{**} > t_*$ such that $S_c(t_{**}) \in [0, S_2^*]$ and $I_c(t_{**}) = k$.*

Theorem 6.6.1 is the consequence of the subsequent two propositions.

Proposition 6.6.1. *Assume* (6.12).

(i) Consider a solution (S_f, I_f) of (Sys_f) with $S_f(0) = S_0 \in [S_1^*, 1-k]$ and $I_f(0) = k$. There exists a time $T_f > 0$ (independent of S_0) such that $I_f(t) > k$ for $t \in (0, T_f]$.

(ii) Assume in addition that $\mathcal{R}_{u_*} > 1$. Consider a solution (S_c, I_c) of (Sys_c) with $S_c(0) = S_0 \in [0, S_2^*]$ and $I_c(0) = k$. There exists a time $T_c > 0$ (independent of S_0) such that $I_c(t) < k$ for $t \in (0, T_c]$.

Proof. (i) Condition (6.12) implies that $I_1^* > k$. Therefore $(S_f(0), I_f(0)) = (S_0, k) \in A_4 \cup A_1$, see Fig. 6.4.(a). It follows from Remark 6.6.2.(i) and (ii) that either $I_f(t) > k$ for all $t > 0$ (the proof is complete in this case with any $T_f > 0$), or there exists $T > 0$ such that $I_f(t) > k$ for all $t \in (0, T)$ and $I_f(T) = k$. In the latter case the total change of I_f on the interval $[0, T]$ is greater than $2(I_1^* - k)$. On the other hand, it comes from the I_f-equation that $|I_f'(t)| \leq \beta + \gamma + \mu$ for all $t \geq 0$. Therefore

$$T > \frac{2(I_1^* - k)}{\beta + \gamma + \mu}.$$

So set $T_f = 2(I_1^* - k)/(\beta + \gamma + \mu)$.

(ii) Under the assumptions of the proposition, E_2^* is an endemic equilibrium for (Sys_c) with $I_2^* < k$, and $(S_0, k) \in B_2 \cup B_3$, see Fig. 6.4.(b). One may apply a reasoning analogous to the proof of statement (i) to show that statement (ii) is true with

$$T_c = \frac{2(k - I_2^*)}{(1-u_*)\beta + \gamma + \mu}.$$

□

Now consider the subset

$$\mathcal{A} = \{(S_0, \varphi) \in X_1 : S_0 \in [S_1^*, 1-k], \varphi(\theta) < k \text{ for } \theta \in [-\tau, 0) \text{ and } \varphi(0) = k\}.$$

Proposition 6.6.2. *If $(S_0, \varphi) \in \mathcal{A}$, then the solution $(S, I) = (S(.; S_0, \varphi), I(.; S_0, \varphi))$ of (Sys_d) is independent of φ. If* (6.12) *holds and τ is small enough, then there exists a smallest $t_1 = t_1(S_0) > 0$ such that $(S(t_1), I_{t_1}) \in \mathcal{A}$. Moreover, $S(t_1)$ depends continuously on S_0.*

Proof. For any $(S_0, \varphi) \in \mathcal{A}$, the solution $(S, I) = \Big(S(.; S_0, \varphi), I(.; S_0, \varphi)\Big)$ coincides with the subsequent solution of (Sys_f) on $[0, \tau]$:

$$\begin{aligned} S(t) &= S_f(t; S_0, k), \qquad t \in [0, \tau], \\ I(t) &= I_f(t; S_0, k), \qquad t \in [0, \tau], \end{aligned} \tag{6.15}$$

see curve Γ_1 on Fig. 6.5.

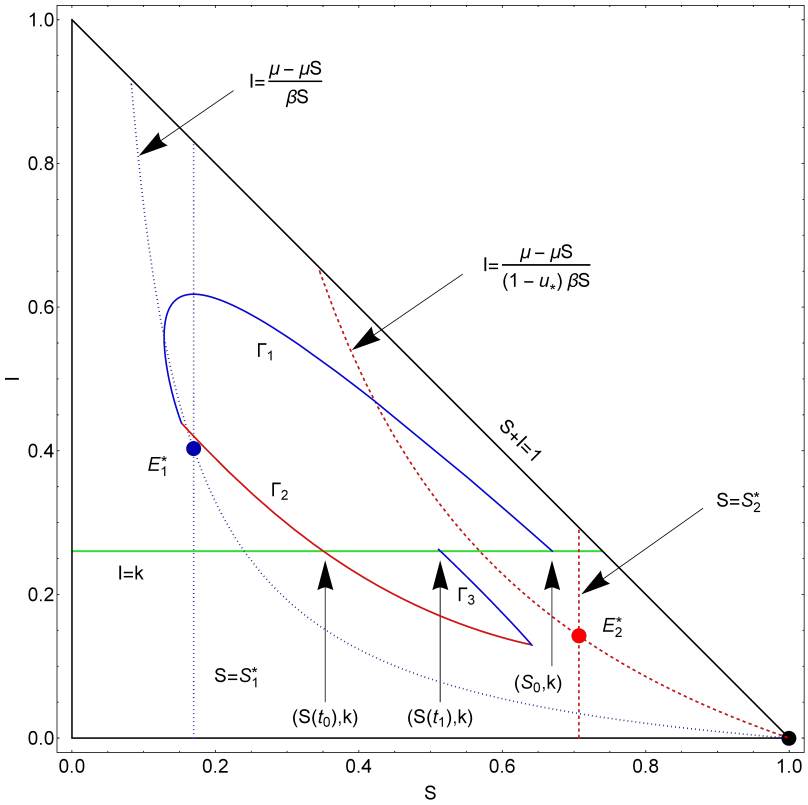

Figure 6.5: The solution $(S, I) = (S(.; S_0, \varphi), I(.; S_0, \varphi))$ of (Sys_d) for $(S_0, \varphi) \in \mathcal{A}$ under conditions (6.12) and $\mathcal{R}_{u_*} > 1$. The blue solid curves Γ_1 and Γ_3 represent (S, I) when it follows (Sys_f). The solid red curve Γ_2 represents (S, I) when it follows (Sys_c). The null-isoclines of (Sys_f) and (Sys_c) are the dotted blue and dashed red curves, respectively. The parameters are: $k = 0.26$, $\gamma = 1.38$, $\beta = 15.8$, $\mu = 1.3$, $\tau = 1$, $u_* = 0.76$, $S_0 = 0.58$.

It comes from Proposition 6.6.1.(i) that if $\tau \leq T_f$, then $I(t) = I_f(t; S_0, k) > k$ for $t \in (0, \tau]$.

Observe that if $I(t) \geq k$ for $t \in [0, T]$ with any $T > \tau$, then (S, I) coincides with the following solution of (Sys_c) on $[\tau, T + \tau]$:

$$\begin{aligned} S(t) &= S_c(t - \tau; S(\tau), I(\tau)), \qquad t \in [\tau, T + \tau], \\ I(t) &= I_c(t - \tau; S(\tau), I(\tau)), \qquad t \in [\tau, T + \tau], \end{aligned} \tag{6.16}$$

see curve Γ_2 on Fig. 6.5.

Next we show the existence of $t_0 > \tau$ such that $I(t_0) = k$ and $I(t) > k$ for $t \in (0, t_0)$. We need to distinguish two cases.

Case $\mathcal{R}_{u_*} \leq 1$: Suppose for contradiction that $I(t) > k$ for all $t \in (0, \infty)$ and hence $I(t) = I_c(t - \tau; S(\tau), I(\tau))$ for $t \in [\tau, \infty)$. The disease free equilibrium E_0^* is globally asymptotically stable for (Sys_c) if $\mathcal{R}_{u_*} \leq 1$, i.e., $I_c(t) \to 0$ as $t \to \infty$. This is a contradiction.

Case $\mathcal{R}_{u_*} > 1$: The existence of t_0 comes from $I(\tau) > k > I_2^*$, observation (6.16) and Remark 6.6.3. In this case $S(t_0) \in [0, S_2^*]$.

It is clear that for $t \in [t_0, t_0 + \tau]$,

$$\begin{aligned} S(t) &= S_c(t - t_0; S(t_0), k), \\ I(t) &= I_c(t - t_0; S(t_0), k). \end{aligned} \tag{6.17}$$

Next we claim that $I(t) < k$ for $(t_0, t_0 + \tau]$ if τ is small enough. If $\mathcal{R}_{u_*} \leqslant 1$, then it comes from the I_c-equation and $S(t) < 1$ that $I'(t) < 0$ for $t \in [t_0, t_0 + \tau)$. So the claim holds in this case. If $\mathcal{R}_{u_*} > 1$, then we apply Proposition 6.6.1.(ii). It yields that $I(t) = I_c(t - t_0; S(t_0), k) < k$ for $(t_0, t_0 + \tau]$ if $\tau < T_c$.

Our last observation implies that

$$\begin{aligned} S(t) &= S_f(t - t_0 - \tau; S(t_0 + \tau), I(t_0 + \tau)), \\ I(t) &= I_f(t - t_0 - \tau; S(t_0 + \tau), I(t_0 + \tau)) \end{aligned} \tag{6.18}$$

for $t \in [t_0 + \tau, t_0 + 2\tau]$. Moreover, if $I(t) < k$ for $t \in (t_0, t_1)$ with some $t_1 > t_0 + \tau$, then equations (6.18) hold for all $t \in [t_0 + \tau, t_1 + \tau]$. Arguing as before, one can actually verify the existence of $t_1 > t_0 + \tau$ such that $I(t) < k$ for $t \in (t_0, t_1)$, $S(t_1) \in [S_1^*, 1 - k]$ and $I(t_1) = k$. See curve Γ_3 on Fig. 6.5.

As $S(t_1) \in [S_1^*, 1 - k]$, $I_{t_1}(\theta) < k$ for $\theta \in [-\tau, 0)$ and $I_{t_1}(0) = k$, we conclude that $(S(t_1), I_{t_1}) \in \mathcal{A}$.

The statement that (S, I) is independent of φ is clear from the first step of the proof.

The continuous dependence of $S(t_1)$ from S_0 comes from the fact the solutions of (Sys_f) and (Sys_c) depend continuously on initial data. □

Proof of Theorem 6.6.1. Proposition 6.6.2 allows us to define a continuous return map

$$P : [S_1^*, 1 - k] \to [S_1^*, 1 - k], \qquad S_0 \mapsto S(t_1).$$

By the Schauder fixed-point theorem, P admits a fixed point $\hat{S}_0 \in [S_1^*, 1-k]$. In addition, let $\hat{\varphi} = I_{t_1}(., \hat{S}_0, \varphi)$, where $\varphi \in C([-\tau, 0], \mathbb{R})$ is an arbitrary function with $\varphi(0) = k$ and

$\varphi(\theta) < k$ for $\theta \in [-\tau, 0]$. By Proposition 6.6.2, $\hat{\varphi}$ is independent of φ and $(\hat{S}_0, \hat{\varphi}) \in \mathcal{A}$. It is now obvious that solution $(S(., \hat{S}_0, \hat{\varphi}), I(., \hat{S}_0, \hat{\varphi}))$ of (Sys_d) is periodic with minimal period t_1. □

It follows from the proof above that Theorem 6.6.1 holds if

$$\tau \leq \min\{T_f, T_c\} = \min\left\{\frac{2(I_1^* - k)}{\beta + \gamma + \mu}, \frac{2(k - I_2^*)}{(1 - u_*)\beta + \gamma + \mu}\right\}.$$

Numerical investigations suggest that the theorem holds for larger choices of τ as well. This is not surprising as our estimates in Proposition 6.6.1 were not sharp.

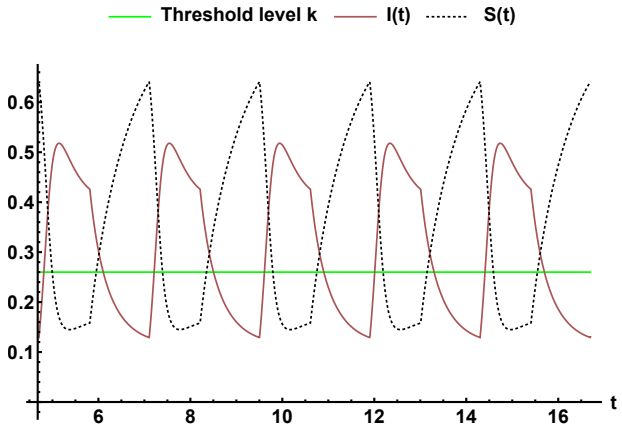

Figure 6.6: The periodic solution for $k = 0.26$, $\gamma = 1.38$, $\beta = 15.8$, $\mu = 1.3$, $\mathcal{R}_0 = 5.9$, $\tau = 1$, $u_* = 0.76$.

6.7 Case (c): E_2^* is GAS for sufficiently small k

The purpose of this section is to show that E_2^* attracts X_1 under certain conditions.

Theorem 6.7.1. *Assume that*

$$\frac{\mu}{\mu + \gamma} + \frac{\mu}{\beta} < 2\sqrt{\frac{\mu}{\beta}} \tag{6.19}$$

and

$$k_1 = \frac{\mu}{\mu + \gamma} - S_2^* = \frac{\mu}{\mu + \gamma} - \frac{\mu + \gamma}{\beta(1 - u_*)} > 0. \tag{6.20}$$

If $k \in (0, k_1)$, then E_2^* is the unique endemic equilibrium for (Sys_d), it is asymptotically stable, and the region of attraction is X_1.

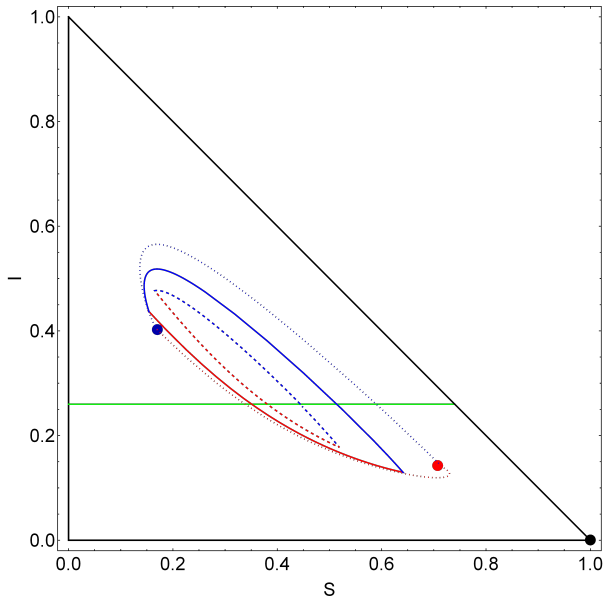

Figure 6.7: The dashed, solid and dotted curves represent the periodic solution for $\tau = 0.4, 1, 4$ respectively. The parameters are $k = 0.26$, $\gamma = 1.38$, $\beta = 15.8$, $\mu = 1.3$, $\mathcal{R}_0 = 5.9$, $u_* = 0.76$.

Note that it is possible to satisfy both inequalities (6.19) and (6.20) at the same time: for example, if $\beta = 15$, $\mu = 0.4$, $\gamma = 1$ and $u_* = 0.5$, then both (6.19) and (6.20) hold.

Also observe that condition $k \in (0, k_1)$ implies (C.3). Therefore Proposition 6.2.1 already guarantees that E_2^* is the unique endemic equilibrium for (Sys_d). For the second coordinate of E_1^*, we have $I_1^* \geq k$.

Fig. 6.8 explains the geometrical position of the segment $I = k_1$.

Set

$$\Delta_2 = \left\{ (S, I) \in \Delta : S + I \geq \frac{\mu}{\mu + \gamma} \right\}.$$

It is straightforward to check that both E_1^* and E_2^* belong to Δ_2.

We need the forthcoming two results before proving Theorem 6.7.1. First we show that all solutions of (Sys_d) leave $\Delta \setminus \Delta_2$ in finite time. Then we verify the positive invariance of Δ_2 independently of the choice of parameters.

Proposition 6.7.1. *Assume (6.19) and suppose that* $(S(0), I(0)) \in \Delta \setminus \Delta_2$ *for a solution* (S, I) *of* (Sys_d). *Then there exists* $t_0 > 0$ *such that* $(S(t_0), I(t_0)) \in \Delta_2$.

Proof. First we claim that if (6.19) holds, then S_f' and S_c' are both positive on the closure

$$\overline{\Delta \setminus \Delta_2} = \left\{ (S, I) \in \Delta : I \leq \frac{\mu}{\mu + \gamma} - S \right\}$$

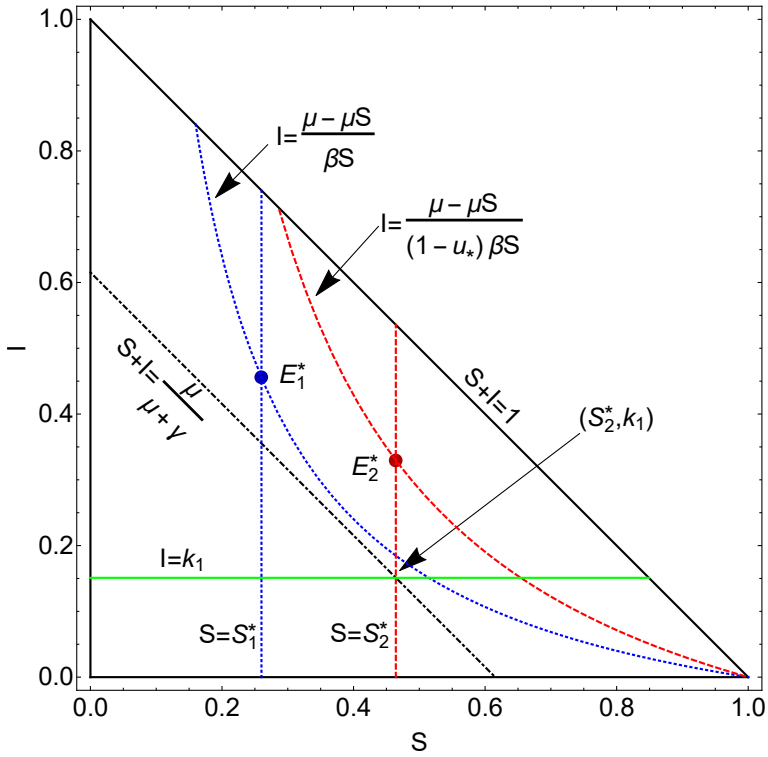

Figure 6.8: The definition of k_1.

of $\Delta \setminus \Delta_2$. Recall from Fig. 6.4 in Section 6.6 that S_f' and S_c' are both positive on the subset

$$\left\{(S,I) \in \Delta : I < \frac{\mu - \mu S}{\beta S}\right\}.$$

Hence it suffices to show that

$$\frac{\mu}{\mu+\gamma} - S < \frac{\mu - \mu S}{\beta S} \quad \text{for } 0 \le S \le \frac{\mu}{\mu+\gamma}.$$

We investigate this inequality in the form

$$\frac{\mu}{\mu+\gamma} + \frac{\mu}{\beta} < S + \frac{\mu}{\beta S} \qquad \text{for all } 0 \le S \le 1. \tag{6.21}$$

The left-hand side is independent of S. Examining the derivative of the right-hand side, it is easy to see that the right-hand side is minimal for $S = \sqrt{\mu/\beta}$, and it takes the value

$$S + \frac{\mu}{\beta S} = 2\sqrt{\frac{\mu}{\beta}} \qquad \text{for } S = \sqrt{\frac{\mu}{\beta}}.$$

We see from assumption (6.19) that inequality (6.21) holds for $S = \sqrt{\mu/\beta}$. Thus it holds for all $S \in [0,1]$. The proof of the claim is complete.

Let M_f and M_c be the minimum of S_f' and S_c' on $\overline{\Delta \setminus \Delta_2}$, respectively. As S_f' and S_c' are both continuous and positive on the compact subset $\overline{\Delta \setminus \Delta_2}$, the constants M_f and M_c are well-defined and positive.

Now suppose that $(S(0), I(0)) \in \Delta \setminus \Delta_2$ for a solution (S, I) of (Sys_d). As long as $(S(t), I(t)) \in \Delta \setminus \Delta_2$, we have $S'(t) \geq \min\{M_f, M_c\} > 0$. The boundedness of $\Delta \setminus \Delta_2$ implies that the solution necessarily leaves $\Delta \setminus \Delta_2$ (through the segment $S + I = \mu/(\mu + \gamma)$). □

Proposition 6.7.2. *If there exists $t_0 \geq 0$ such that $(S(t_0), I(t_0)) \in \Delta_2$, then $(S(t), I(t)) \in \Delta_2$ for all $t \geq t_0$.*

Proof. Consider any solution (S, I) of (Sys_d) with $S(t_0) + I(t_0) \geq \mu/(\mu + \gamma)$. Adding up the equations of (Sys_d), we obtain that

$$\begin{aligned}\frac{d}{dt}(S(t) + I(t)) =& \mu - \mu(S(t) + I(t)) - \gamma I(t) \\ \geq& \mu - (\mu + \gamma)(S(t) + I(t))\end{aligned}$$

for all $t > 0$.

The solution of the ordinary differential equation

$$\frac{du(t)}{dt} = \mu - (\mu + \gamma)u(t), \qquad t \in \mathbb{R},$$

with initial data

$$u(t_0) = S(t_0) + I(t_0) \geq \frac{\mu}{\mu + \gamma}$$

is

$$u(t) = \frac{\mu}{\mu + \gamma} + \left(u(t_0) - \frac{\mu}{\mu + \gamma}\right) e^{(\mu+\gamma)(t_0 - t)}.$$

Then, by the comparison theorem, $S(t) + I(t) \geq u(t) \geq \mu/(\mu + \gamma)$ for all $t \geq t_0$, i.e., $(S(t), I(t)) \in \Delta_2$ for all $t \geq t_0$. □

Now we are ready to prove Theorem 6.7.1.

Proof of Theorem 6.7.1. Assumption $k \in (0, k_1)$ implies that

$$\mathcal{R}_0[\mu - (\mu + \gamma)k] > \mu/(1 - u_*). \tag{6.22}$$

Therefore (C.3) holds, and E_2^* is the unique endemic equilibrium for (Sys_d) by Proposition 6.2.1. Inequality (6.22) is actually equivalent to $I_2^* > k$, see the proof of Proposition 6.2.1. This observation and the fact that E_2^* is stable w.r.t. to (Sys_c) guarantees that it is stable w.r.t. to (Sys_d) too. We only need to show that if (S, I) is an arbitrary solution of (Sys_d) with initial data in X_1, then $(S(t), I(t)) \to E_2^*$ as $t \to \infty$.

It comes from Propositions 6.7.1 and 6.7.2 that there exists $t_0 \geq 0$ such that $(S(t), I(t)) \in \Delta_2$ for all $t \geq t_0$. The rest of the proof comes from two claims.

First we claim that there exists $t_1 \geq t_0$ such that $I(t_1) \geq k$. Indeed, suppose for contradiction that $I(t) < k$ for all $t \in [t_0, \infty)$. Then we have

$$I(t) = I_f(t - t_0 - \tau; S(t_0 + \tau), I(t_0 + \tau)) \quad \text{for } t \in [t_0 + \tau, \infty).$$

As we are in the $\mathcal{R}_0 > 1$ case, E_1^* attracts Δ_1 for (Sys_f). It follows that $I(t) \to I_1^*$ as $t \to \infty$. This is a contradiction since condition (6.22) implies that $I_1^* > k$.

Next we claim that if $I(t_1) \geq k$ for some $t_1 \geq t_0$, then $I(t) \geq k$ for all $t \in [t_1, \infty)$. If this is not true, i.e., $I(t)$ can be smaller than k for some $t > t_1$, then there exists $t_2 > t_1$ such that $I(t_2) = k$ and $I'(t_2) \leq 0$. However, as $(S(t_2), I(t_2)) \in \Delta_2$, we have

$$S(t_2) \geq \frac{\mu}{\mu + \gamma} - I(t_2) = \frac{\mu}{\mu + \gamma} - k > \frac{\mu}{\mu + \gamma} - k_1 = S_2^*.$$

(Fig. 6.8 also shows this property: If $(S(t_2), I(t_2)) \in \Delta_2$ and $I(t_2) = k < k_1$, then necessarily $S(t_2) > S_2^*$.) This means that

$$\begin{aligned} \frac{dI(t_2)}{dt} =& [[1 - u(I(t_2 - \tau))]\beta S(t_2) - (\gamma + \mu)]I(t_2) \\ >& [[1 - u_*]\beta S_2^* - (\gamma + \mu)]k = 0 \end{aligned}$$

independently of the value of $I(t_2 - \tau)$. This contradicts our previous observation that $I'(t_2) \leq 0$. So $I(t) \geq k$ for all $t \in [t_1, \infty)$.

It comes from our last result that solution (S, I) coincides with the subsequent solution of (Sys_c) on $[t_1 + \tau, \infty)$:

$$\begin{aligned} S(t) =& S_c(t - t_1 - \tau; S(t_1 + \tau), I(t_1 + \tau)), \\ I(t) =& I_c(t - t_1 - \tau; S(t_1 + \tau), I(t_1 + \tau)), \end{aligned} \qquad t \in [t_1 + \tau, \infty).$$

As E_2^* attracts Δ_1 w.r.t. (Sys_c), we conclude that $(S(t), I(t)) \to E_2^*$ as $t \to \infty$. The proof is complete. □

6.8 Discussion

We have considered the dynamical consequences of switching to a control system in an SIR epidemic model, when the switch takes place with some delay after the solution crosses a switching manifold (i.e., when the density of infected individuals reaches a threshold level k).

Our results for (6.1)-(6.2) with delay $\tau > 0$ are summarized in Table 6.1. We have found that the behaviour of the system can be significantly different from switching

models without delay. This can be easily seen by comparing Table 6.1 to Table 6.2, which lists the findings of Xiao, Xu, and Tang in [49] for system (6.1)-(6.2) in the case $\tau = 0$.

	Parameters	Results for $\tau > 0$
	$\mathcal{R}_0 \leq 1$	E_0^* is GAS. No endemic equilibria.
(a)	$\mathcal{R}_0 > 1$ and $\mathcal{R}_0[\mu - (\mu+\gamma)k] < \mu$	E_0^* is unstable. E_1^* is the unique endemic equilibrium. E_1^* attracts X_1 for large k.
(b)	$\mu < \mathcal{R}_0[\mu - (\mu+\gamma)k] < \mu/(1-u_*)$	E_0^* is unstable. No endemic equilibria. Periodic solution for small τ.
(c)	$\mathcal{R}_0[\mu - (\mu+\gamma)k] > \mu/(1-u_*)$	E_0^* is unstable. E_2^* is the unique endemic equilibrium. E_2^* attracts X_1 for small k (under certain technical conditions).

Table 6.1: A summary of our results.

	Parameters	Results for $\tau = 0$
(a)	$\mathcal{R}_0 > 1$ and $\mathcal{R}_0[\mu - (\mu+\gamma)k] < \mu$	E_1^* is the unique endemic equilibrium, it attracts Δ_1.
(b)	$\mu < \mathcal{R}_0[\mu - (\mu+\gamma)k] < \mu/(1-u_*)$	A new equilibrium appears on the switching manifold attracting Δ_1.
(c)	$\mathcal{R}_0[\mu - (\mu+\gamma)k] > \mu/(1-u_*)$	E_2^* is the unique endemic equilibrium, it attracts Δ_1.

Table 6.2: The results of Xiao, Xu, and Tang in [49] for $\tau = 0$.

As one can see from Table 6.1, all solutions in Δ_1 converge to an endemic equilibrium if $\tau = 0$ and $R_0 > 1$. However, periodic orbits can exist in the delayed case: we constructed periodic solutions for some range of the parameters and for small positive delay (see Case (b)). These are slowly oscillating between the two sides of the switching manifold (meaning that if $I(t_1) = I(t_2) = k$ for $t_1 < t_2$, then $t_2 - t_1 > \tau$). Numerical observations show that the periodic orbit persists by increasing the delay, and the oscillatory solution tends to approach the two stable equilibria corresponding to the free and the control systems.

On the other hand, our global stability results are delay independent (see Cases (a) and (c)). Based on some numerical simulations, we conjecture that a stable periodic

orbit may coexist with a stable equilibrium for some parameter configurations (when k is slightly smaller than I_2^* or slightly bigger than I_1^*), thus local stability of an endemic equilibrium does not always imply its global stability. We have observed this bistable situation for both small and large values of τ. The investigation of such cases is left for future work.

Fig. 6.9 depicts how the maxima and minima of some solutions (calculated after long time integration) change if parameter k increases. This numerically generated diagram confirms the conjecture that a periodic orbit may coexist with a stable equilibrium for some parameter configurations.

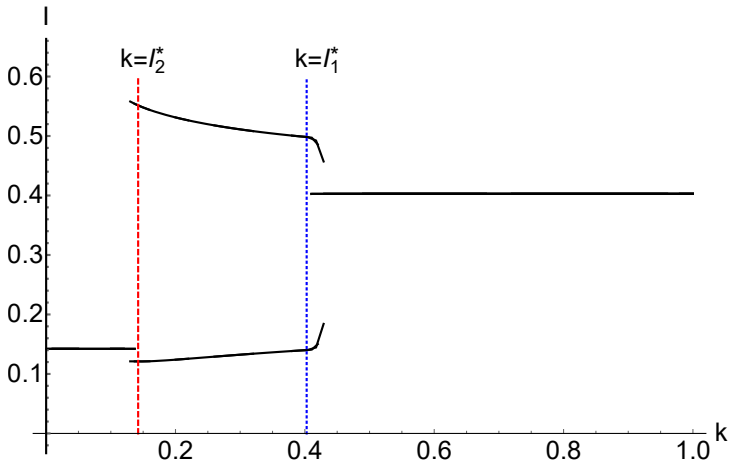

Figure 6.9: Plot of the maxima and minima of the I-terms after long time integration for several initial data. The bifurcation parameter is k. The other parameters are $u_* = 0.76$, $\gamma = 1.38$, $\beta = 15.8$, $\mu = 1.3$ and $\tau = 1$. The solution converges to E_2^* for small k, then to a periodic orbit as k increases, and then to E_1^* for large values of k.

It may seem surprising that we do not necessarily obtain information on the dynamics in the non-delayed case by considering the delayed case with small values of τ. The underlying reason is the following: If $\tau = 0$ in Case (b), then there is a segment within the switching manifold $I = k$ (the so-called sliding domain) along which the vector field corresponding to the free system points up, while the vector field of the control system points down. When a solution reaches the sliding domain, this incompatibility between the free and the control systems can be resolved by a sliding mode control which is forcing the solution to remain on the sliding domain, and the solution may converge to a new equilibrium appearing there. In contrast, the solution curves of the delayed system cross the switching manifold transversally because this system reacts with a positive delay and because both vector fields are transversal to $I = k$ (except at most one point). Therefore in Case (b) with $\tau > 0$ we observe solutions oscillating between the two sides of the

switching manifold but no solutions moving along it.

From our results we can draw some conclusions about the potential intervention strategies. For a large threshold k, the control will eventually be turned off and solutions converge to the endemic equilibrium of the free system, and the control strategy has no effect whatsoever. If $k < I_1^*$, then the control effort u_* also plays a role. If the control effort is weak, then $I_2^* > k$ (see Fig. 6.1) and we can expect the control to be on for large times. Then the control strategy is reducing the infected population. Interestingly, in the presence of time delay, a strong control effort can induce periodic oscillations, and the peak of the periodic solution may be larger than the endemic level what we could achieve by a weaker control. If we do not want to tolerate high peaks in disease prevalence, we may choose a milder control strategy. Alternatively, we may try to reduce the delay as that leads to smaller oscillations, and then the periodic solution can be kept near the threshold k. Our results suggest that it may be worthwhile to continue research to the directions we initiated here, to have a better understanding of the effect of the interplay of control strategies and delays in implementation on the long term transmission dynamics.

7

Summary

The dissertation proposes

(a) a family of temporary vaccination strategies in the framework of the SIR model (see Chapters 3 and 5). These strategies are characterized by parameters (k, p) where vaccination starts when the number of infected hosts reaches a threshold level k, and with rate p we continue vaccination until herd immunity is achieved (VUHIA);

(b) a family of temporary non-pharmaceutical intervention (NPIs) strategies in the framework of the SIR model (see Chapters 4 and 5). These strategies are characterized by parameters (k, u_*) where NPIs start when the number of infected hosts reaches a threshold level k, and with rate u_* we continue intervention till herd immunity is reached (ITHIR);

(c) and analyses of a mathematical model for infectious disease dynamics with a discontinuous control function, where the control is activated with some time lag after the density of the infected population reaches a threshold (see Chapter 6).

The advantages of the *VUHIA*-strategy and *ITHIR*-strategy are the following. First, it has a clear and meaningful definition: we start intervention with rate c ($c = p$ in the case of vaccination interventions and $c = u_*$ in the case of NPIs) when a threshold k is reached in the level of infection, and we continue the intervention then the number of susceptibles drops below $\mathcal{R}_0^{-1}$, that is herd immunity is achieved, and the number of infected will decrease anyway. Second, it is easy to explain to policy makers (in contrast to outputs from optimal control theory). Third, it is determined only by the parameters (k, c), hence all strategies from this family can be explored in a two dimensional parameter space.

In Chapters 3 and 4, we have assigned a total cost for each strategy composed of cost of disease burden and cost of intervention, and systematically investigated the dependence

of the total cost on the parameters. The aim of these two chapters is to find out which strategy gives the minimal cost. Chapter 5 focuses on the final epidemic size of VUHIA and ITHIR strategies. The aim of this chapter is to find out which strategy gives the minimal final epidemic size. Chapter 6 provides insight into disease management, by exploring the effect of the interplay of the control efficacy, the triggering threshold and the delay in implementation.

The dissertation is organized as follows: After the introduction and the mathematical framework, Chapter 3 investigates optimal temporary vaccination strategies for epidemic outbreaks. Specification of the *VUHIA*-strategy and its total cost (model description, the basic reproduction number, the total cost of an outbreak, when to start and when to stop the vaccination) are introduced in Section 3.1. Sections 3.2 and 3.3 illustrate the relation between the total cost, the vaccination rate, and the threshold level. Indeed, the total cost is assessed by considering two components, the disease burden and the cost of vaccination, which are weighted by two factors C_1 and C_2 respectively. We found that the total cost is decreasing in p and k if $C_2 << C_1$ while increasing in p and k if $C_2 >> C_1$. However there is a curious situation when C_1 and C_2 are of similar magnitudes: there is a possibility that the total cost is neither monotone in p nor in k. In section 3.4, we discussed the conclusions. Indeed, we found three types of behaviours:

(i) *vaccination cost is very low compared to the cost associated to disease burden*: in this case increasing the vaccination rate and start vaccination earlier reduce the total cost;

(ii) *vaccination cost is very high compared to the cost associated to disease burden*: In this case the minimal cost is obtained by not vaccinating at all;

(iii) *vaccination cost and disease burden cost are of similar magnitudes*: there may be non-monotone relationships between the vaccination rate, the starting threshold and the total cost. In this case, it may happen that a better strategy is to start earlier but only if we can start sufficiently early, or, it better to increase vaccination rate but only if we can increase it to a sufficiently high level. If we cannot meet those criteria, then the minimal cost is achieved by not vaccinating.

These three typical behaviours are plotted into a heatmap in Figure 3.7. In addition, we found that depending on the available resources and public health capacities, there may be constraints on the parameters, such as $k \geq k_{\min}$ and $p \leq p_{\max}$. The optimal strategy with such constraints can also be found. We demonstrated the effect of $\mathcal{R}_0$ on the monotonicity of the cost curve. Indeed, the monotonicity of the total cost in k can reverse varying the reproduction number.

Chapter 4 proposes and investigates optimal temporary non-pharmaceutical intervention strategies for epidemic outbreaks. We divided this chapter like the previous one. Moreover, we considered different types of cost functions and we identified a parameter region where herd immunity will never be reached, in which case the intervention is not feasible as its cost exceeds any given bound. Considering the feasible region of limited costs, we found the following:

(a) *NPIs cost is very low compared to the cost associated with the disease burden*: in this case the optimal strategy lies on the boundary between the two regions, which is not feasible. In this case we impose a restriction: we maximized the possible length of intervention, and we could find the optimal strategy with such restriction;

(b) *intervention cost and disease burden cost are of similar magnitudes*: there may be non-monotone relationships between the control intensity, the starting threshold and the total cost, and in this case we can determine which strategy gives the minimal total cost;

(c) *intervention cost is very high compared to the cost associated to disease burden*: in this case the minimal cost is attained by not controlling at all.

We also demonstrated that the corresponding optimal strategies can be very different for pandemic and for seasonal influenza. Hence this important insight shows that pandemic influenza should be treated differently than seasonal influenza by public health authorities. We systematically investigated the cost-effectiveness of a newly proposed family of temporary interventions. We uncovered the impact of various cost functions, and provided valuable insights to develop effective control strategies for seasonal and pandemic influenza.

In Chapter 5, Theorem 5.1.1 gives the final susceptible population size system for the *VUHIA*-strategy. Depending on This system we proved that the final susceptible population size is increasing in the vaccination rate p (see see Lemma 5.2.2) while decreasing in the threshold level k (see Lemma 5.2.1). Numerical simulation shows that the final epidemic size of *VUHIA*-strategy of (k, p)-type is decreasing in p while increasing in k, and the optimal strategy to reduce the final epidemic size is to start vaccination as early as possible as strong as possible. Theorems $[(5.4.1), (5.8.1)]$ give the final epidemic size systems for *ITHIR*-strategy of NPIs, and *ITHIR*-strategy of treatment and isolation interventions, where temporary treatment and isolation intervention strategies are investigated in Section 5.7 in terms of the final epidemic size. Dependence of the final epidemic size on (k, u_*)-strategy and (k, m_*)-strategy are investigated, where m_* is the

treatment and isolation rate. Indeed, the final size systems above are used to show that the final epidemic size is increasing in k while decreasing in the intervention rates u_*, and m_*, see Lemmas [(5.5.1), (5.9.1), (5.5.2), (5.9.2)]. We also systematically investigated the dependence of the FES on the parameters, and we found that the optimal strategy to minimize the FES is to start intervention as early as possible as high rate as possible.

In Chapter 6, we considered the dynamical consequences of switching to a control system in an SIR epidemic model, when the switch takes place with some delay after the solution crosses a switching manifold. In Sections 6.1, we mathematically formulated the model as a delayed relay system (denoted by Sys_d), and we determined the dynamics by the switching between two vector fields (the so-called free (Sys_f) and control (Sys_c) systems) with a time delay with respect to a switching manifold. The phase space X for (Sys_d) and subsets X_0 and X_1 of it are chosen, where X_1 is the collection of endemic states, when the disease is present in the population. Section 6.2 recalls the basic and control reproduction numbers, the disease free and endemic equilibria and their stability properties for both (Sys_f) and (Sys_c), and examines what the equilibria for (Sys_d) are. In Section 6.3, we show that if the initial data $(S_0, \varphi) \in X_0$ ($(S_0, \varphi) \in X_1$), then the solution of (Sys_d) exists, and the sets X_0 and X_1 are positively invariant. Section 6.4 establishes the usual threshold dynamics: when the basic reproduction number $\mathcal{R}_0 \leq 1$, then the disease is eradicated, while for $\mathcal{R}_0 > 1$ the disease persists in the population. Then, for $\mathcal{R}_0 > 1$, we divide the parameter domain into three regions, and prove results about the global dynamics of the switching system for each case: we find conditions for the global convergence to the endemic equilibrium of the free system in Section 6.5, for the global convergence to the endemic equilibrium of the control system in Section 6.6, and for the existence of periodic solutions that oscillate between the two sides of the switching manifold in Section 6.7. The proof of the latter result is based on the construction of a suitable return map on a subset of the infinite dimensional phase space. In Section 6.8, first we summarized our results in Table 6.1, and discussed that the behaviour of the system can be significantly different from switching models without delay. This can be easily seen by comparing Table 6.1 to Table 6.2, which lists the findings of Xiao, Xu, and Tang in [49] for system (6.1)-(6.2) in the case $\tau = 0$. Then based on some numerical simulations, we conjectured that a stable periodic orbit may coexist with a stable equilibrium for some parameter configurations, thus local stability of an endemic equilibrium does not always imply its global stability. We have observed this bistable situation for both small and large values of τ. The investigation of such cases is left for future work. Finally, we drew some conclusions about the potential intervention strategies.

This thesis rely on two scientific papers of Attila Dénes, Gabriella Vas, Gergely Röst, and the author of this thesis, see [33] and [34].

Bibliography

[1] Alexander, M. E., Moghadas, S. M., Röst, G., Wu, J., 2008. A delay differential model for pandemic influenza with antiviral treatment. Bulletin of mathematical biology, 70(2), 382-397.

[2] Arino, J. and McCluskey, C.C., 2010. Effect of a sharp change of the incidence function on the dynamics of a simple disease. J. Biol. Dyn., **4**(5), pp.490-505.

[3] Barbarossa, M. V., Dénes, A., Kiss, G., Nakata, Y., Röst, G., Vizi, Z., 2015. Transmission dynamics and final epidemic size of Ebola virus disease outbreaks with varying interventions. PloS one, 10(7).

[4] Barbarossa, M. V., Bogya, N., Dénes, A., Röst, G., Varma, H. V., and Vizi, Z. (2020). Fleeing lockdown and its impact on the size of epidemic outbreaks in the source and target regions-a COVID-19 lesson.

[5] Biggerstaff, Matthew, et al., 2014. "Estimates of the reproduction number for seasonal, pandemic, and zoonotic influenza: a systematic review of the literature." BMC infectious diseases 14.1 : 480.

[6] Bradley, B.T., Bryan, A., 2019. Emerging respiratory infections: The infectious disease pathology of sars, mers, pandemic influenza, and legionella. In: Seminars in Diagnostic Pathology. Elsevier

[7] Brauer, Fred, and Carlos Castillo-Chavez, 2012. "Models for Endemic Diseases." Mathematical Models in Population Biology and Epidemiology. Springer New York, 411-464.

[8] Centers for Disease Control and Prevention, 2011. The CDC guide to strategies to increase physical activity in the community.

[9] M. Drolet, É. Bénard, M. Jit, R. Hutubessy and M. Brisson, 2018. Model Comparisons of the Effectiveness and Cost-effectiveness of Vaccination: A Systematic Review of the Literature. *Value Health* **21**, 1250–1258.

[10] A. Durbin, A. N. Corallo, T. G., Wibisono, D. M. Aleman, B. Schwartz and P. C. Coyte, 2011. A cost effectiveness analysis of the H1N1 vaccine strategy for Ontario, Canada. *J. Infect. Dis. Immun.* **3**(3), 40–49.

[11] Edwards, C., ans Spurgeon, S. K. (1998). Systems and control book series: Vol. 7. Sliding mode control: theory and applications (pp. 15–20). London: Taylor and Francis.

[12] Fan, V.Y., Jamison, D.T., Summers, L.H., 2018. Pandemic risk: how large are the expected losses? Bulletin of the World Health Organization 96(2), 129

[13] Feng, Z., 2007. Final and peak epidemic sizes for SEIR models with quarantine and isolation. Mathematical Biosciences Engineering, 4(4), 675.

[14] Filippov, A. F. (1988). Differential equations with discontinuous righthand sides. Dordrecht: Kluwer Academic.

[15] Fine, P., Eames, K., and Heymann, D. L. (2011). "Herd immunity": a rough guide. Clinical infectious diseases, 52(7), 911-916.

[16] Hale, Jack K.: Ordinary differential equations. Second edition. Robert E. Krieger Publishing Co., Inc., Huntington, N.Y., 1980. xvi+361 pp.

[17] Handel A, Longini IM, Antia R., 2007. What is the best control strategy for multiple infectious disease outbreaks? Proceedings of the Royal Society B: Biological Sciences. 274(1611):833-837. doi:10.1098/rspb.2006.0015.

[18] Hirsch, Morris W., Stephen Smale, and Robert L. Devaney, 2012. Differential equations, dynamical systems, and an introduction to chaos. Academic press.

[19] Iuliano, A.D., Roguski, K.M., Chang, H.H., Muscatello, D.J., Palekar, R., Tempia, S., Cohen, C., Gran, J.M., Schanzer, D., Cowling, B.J., et al., 2018. Estimates of global seasonal influenza-associated respiratory mortality: a modelling study. The Lancet 391(10127), 1285-1300

[20] Kim, B.N., Nah, K., Chu, C., Ryu, S.U., Kang, Y.H., Kim, Y., 2012. Optimal control strategy of plasmodium vivax malaria transmission in korea. Osong public health and research perspectives 3(3), 128,136

[21] Kiss, I. Z., Röst, G., Vizi, Z., 2015 . Generalization of pairwise models to non-Markovian epidemics on networks. Physical review letters, 115(7), 078701.

[22] D. Knipl and G. Röst, 2011. Modelling the strategies for age specific vaccination scheduling during influenza pandemic outbreaks, *Math. Biosci. Eng.* **8**(1), 123–139.

[23] Korobeinikov, A. and Wake, G. C., 2002. Lyapunov functions and global stability for SIR, SIRS, and SIS epidemiological models. Appl. Math. Lett., **15**(8), pp.955–960.

[24] LeBlanc, V.G., 2016. A degenerate Hopf bifurcation in retarded functional differential equations, and applications to endemic bubbles. J. Nonlinear Sci., **26**(1), pp.1-25.

[25] Leekha, Surbhi, et al., 2007. "Duration of influenza A virus shedding in hospitalized patients and implications for infection control." Infection Control. Hospital Epidemiology 28.9 : 1071-1076.

[26] Lin, F., Muthuraman, K., Lawley, M., 2010. An optimal control theory approach to non-pharmaceutical interventions. BMC infectious diseases 10(1), 32

[27] Liu, M., Liz, E. and Röst, G., 2015. Endemic bubbles generated by delayed behavioral response: global stability and bifurcation switches in an SIS model. Siam. J. Appl. Math., **75**(1), pp.75–91.

[28] Liu, M., Röst, G. and Vas, G., 2013. SIS model on homogeneous networks with threshold type delayed contact reduction. Comput Math Appl., **66**(9), pp.1534-1546.

[29] Liu, X. and Stechlinski, P., 2013. Transmission dynamics of a switched multi-city model with transport-related infections. Nonlinear Anal. Real World Appl., **14**(1), pp.264-279.

[30] Liu, X. and Stechlinski, P., 2017. Infectious disease modeling, a hybrid system approach, vol. 19. Springer.

[31] Markel, H., Lipman, H.B., Navarro, J.A., Sloan, A., Michalsen, J.R., Stern, A.M., Cetron, M.S., 2007. Nonpharmaceutical interventions implemented by us cities during the 1918-1919 influenza pandemic. Jama 298(6), 644-654

[32] S. Merler, M. Ajelli, L. Fumanelli, S. Parlamento, A. Pastore y Piontti, N. E. Dean et al., 2016. Containing Ebola at the Source with Ring Vaccination. *PLoS Negl. Trop. Dis.* **10**(11), e0005093.

[33] Muqbel, K., Dénes, A. and Röst, G., 2019. Optimal Temporary Vaccination Strategies for Epidemic Outbreaks. In Trends in Biomathematics: Mathematical Modeling for Health, Harvesting, and Population Dynamics, pp. 299-307. Springer, Cham.

[34] Muqbel, K., Vas, G. Röst, G., 2020. Periodic Orbits and Global Stability for a Discontinuous SIR Model with Delayed Control. *Qual. Theory Dyn. Syst.* **19**, 59 .

[35] Nikbakht, R., Baneshi, M. R., Bahrampour, A., and Hosseinnataj, A. (2019). Comparison of methods to Estimate Basic Reproduction Number (R. Journal of Research in Medical Sciences, 2.

[36] Parija, S. C., 2014. Textbook of Microbiology Immunology-E-book. Elsevier Health Sciences.

[37] Röst, G., Bartha, F. A., Bogya, N., Boldog, P., Dénes, A., Tamás, F., ... and Vizi, Z. (2020). Early phase of the COVID-19 outbreak in Hungary and post-lockdown scenarios. medRxiv.

[38] Röst, G., Vizi, Z., Kiss, I. Z., 2018. Pairwise approximation for SIR-type network epidemics with non-Markovian recovery. Proceedings of the Royal Society A: Mathematical, Physical and Engineering Sciences, 474(2210), 20170695.

[39] Shim, E., 2013. Optimal strategies of social distancing and vaccination against seasonal influenza. Mathematical Biosciences Engineering, 10(5 6), 1615-1634.

[40] Sieber, J., 2006. Dynamics of delayed relay systems. Nonlinearity, **19**(11), 2489.

[41] Smith, H. L. and Thieme, H. R., Dynamical Systems and Population Persistence, Vol. 118. American Mathematical Soc., 2011.

[42] Utkin, V. I. (1978). Sliding modes and their applications in variable structure systems. Moscow: Mir.

[43] Utkin, V. I. (1992). Sliding modes in control and optimization. Berlin: Springer.

[44] Wang, A. and Xiao, Y., 2013. Sliding bifurcation and global dynamics of a Filippov epidemic model with vaccination. Int J. Bifurcat. Chaos., **23**(08), p.1350144.

[45] Wang, A., Xiao, Y. and Smith, R., 2019. Dynamics of a non-smooth epidemic model with three thresholds. Theor Biosci., pp.1-19.

[46] Wang, W., 2006. Backward bifurcation of an epidemic model with treatment. Math. Biosci. **201**(1-2), pp. 58–71.

[47] Wang, A., Xiao, Y. and Zhu, H., 2017. Dynamics of a Filippov epidemic model with limited hospital beds. Math. Biosci. Eng., **15**(3), p.739.

[48] World Health Organization, 2019. Global Influenza Strategy 2019-2030.

[49] Xiao, Y., Xu, X., Tang, S., 2012. Sliding mode control of outbreaks of emerging infectious diseases. Bulletin of mathematical biology, 74(10), 2403-2422.

[50] G. Zaman, Y. H. Kang and I. H. Jung, 2008. Stability analysis and optimal vaccination of an SIR epidemic model. *BioSystems* **93**(3), 240–249.

[51] Zhou, Y., Yang, K., Zhou, K., Liang, Y., 2014. Optimal vaccination policies for an SIR model with limited resources. Acta biotheoretica, 62(2), 171-181.

[52] Zhou, W., Xiao, Y. and Heffernan, J.M., 2019. A two-thresholds policy to interrupt transmission of West Nile Virus to birds. J. Theor. Biol., **463**, pp.22-46.